8-2013

BIOFABRICATION OF SCAFFOLDS FOR INTERVERTEBRAL DISC (IVD) TISSUE REGENERATION

Benjamin Whatley
Clemson University, bwhatle@clemson.edu

BIOFABRICATION OF SCAFFOLDS FOR INTERVERTEBRAL DISC (IVD) TISSUE REGENERATION

A Dissertation
Presented to
the Graduate School of
Clemson University

In Partial Fulfillment
of the Requirements for the Degree
Doctor of Philosophy
Bioengineering

---

by
Benjamin R. Whatley
August 2013

Accepted by:
Dr. Martine LaBerge, Committee Chair
Dr. Xuejun Wen
Dr. Ning Zhang
Dr. Hai, Yao
Dr. Mark Kindy

ABSTRACT

The ultimate goal of tissue regeneration is to replace damaged or diseased tissue with a cell-based or biomaterial-based tissue that accurately mimics the functionality, biology, mechanics, and cellular and extracellular matrix (ECM) composition of the native tissue. Specifically, the ability to control the architecture of tissue engineered constructs plays a vital role in all of these issues as scaffold architecture has an affect on function, biomechanics, and cellular behavior. Many tissue engineered scaffolds focus on the ability to mimic natural tissue by simulating the ECM due to the fact that in each distinct tissue, the ECM serves as a structural component by providing unique mechanical strength as well as regions for cellular attachment or the storage of a variety of biomolecules. Additionally, cellular behavior has the ability to be controlled based on the structure and composition of the ECM. More specifically, matrix has the ability to modulate a variety of cellular behaviors such as: adhesion, morphology, migration, proliferation, and differentiation while also controlling the ability of cells to produce and synthesize ECM with similar characteristics to that of surrounding tissue. Tissue matrix and structure plays an essential role during the process of tissue formation, remodeling, and regeneration.

The ability to mimic native tissue ECM using various biofabrication-based techniques has become an emerging concept in the realm of tissue regeneration. Biofabrication utilizes automated computer-aided-design (CAD) and computer-controlled technologies to create reproducible biomaterial and cell-based scaffolds that have the ability to imitate native tissue ECM. Of particular interest are strategies that employ

biofabrication with the aim of improving the overall control over scaffold architecture and microstructure while also providing reproducibility.

Due to their versatility, a variety of promising biofabrication strategies exist, including rapid prototyping methods such as bioprinting and additive manufacturing, which rely on the deposition or extrusion of materials. Using these methods, a multitude of materials can be easily used to fabricate scaffold structures with various morphologies. However, the potential of many biofabrication methods in tissue engineering applications is limited by the potential resolution of the structures that can be created. It was our goal to investigate a unique biofabrication strategy with the aim of fabricating 3-D scaffolds at a high resolution with morphological, biological, and mechanical properties similar to those of natural intervertebral discs (IVDs).

Initially, a CAD-based biofabrication approach was developed and systematically optimized. This method was selected to utilize a custom-designed computer interface with 3-D motion control that allowed for greater resolution and precision of the fabricated scaffold architecture. Furthermore, we incorporated a temperature controlled polymer collection stage, which proved advantageous in enhancing the resolution of the biofabrication technique. By lowering the temperature of the collecting stage below the freezing point of the polymer solution, it was discovered that the extruded polymer solution could be solidified directly as it exited the micropipette extrusion tip through an increase in viscosity. Results from initial studies provided valuable clues towards determining the relationship between motor speeds, polymer solution temperatures, micropipette size, extrusion rate, and polymer solution viscosity. These results

encouraged the investigation of the ability to use this method to precisely control scaffold spatial orientation for the fabrication of IVD scaffolds.

Since previous IVD scaffold fabrication methods have not effectively accounted for the inadequacies of spinal fusion and artificial disc replacement in the treatment of a degenerated disc, we addressed the significance of matching native tissue histology and biomechanics by using fabricated scaffolds that closely mimic natural IVD tissue. The annulus fibrosus (AF), or outer region of the IVD, was the focus of this project due to current and previous challenges in recreating its discrete tissue architecture, which is not an issue for the inner nucleus pulposus (NP) region, as it is more commonly mimicked with the use of a hydrogel-based biomaterial.

Multiple elastomeric materials, including biocompatible and biodegradable polyurethane (PU) and chitosan-gelatin (CS/GEL), were investigated to evaluate the usefulness of this biofabrication approach to create biomimetic IVD scaffolds utilizing various materials. It was determined that the biofabrication method enabled the use of multiple materials and that the fabricated scaffolds were able to mimic the kidney shaped structure of the IVD. Additionally, the scaffolds exhibited ideal concentric lamellar thickness and spacing, accurately mimicking the native structure of the AF in the human IVD. To the best of our knowledge, these accomplishments in recreating the native AF histological architecture within tissue engineered constructs have not been achieved elsewhere. Cells attached and aligned on the scaffolds in the direction of the concentric lamellar structure, emulating cell behavior comparable to the native AF. These 3-D scaffolds exhibited ideal elastic properties and did not experience permanent deformation

under dynamic loading. Additionally, the scaffold mechanical properties showed no significant differences when compared with native human IVD tissue. The scaffolding promoted chondrocyte cell attachment and proliferation in alignment with the concentric lamellae, proving this method improves upon current IVD scaffold fabrication approaches, as it takes into account native tissue structure and cell response.

To expand upon these findings, the biomimetic IVD scaffolds were investigated to analyze the formation of 3-D cellularized tissue. 3-D multicellular spheroids formed from chondrocytes were incorporated within the scaffold to fully cellularize the void spacing within the IVD scaffold lamellae. The ability of this 3-D cellularized structure to emulate native IVD tissue was then further analyzed by evaluating the ability of the scaffolds to synthesize matrix that was structurally and compositionally similar to that of native tissue. Our studies indicate that the 3-D cellularized IVD constructs accurately mimic native IVD tissue and provide not only a scaffold, but a cellularized platform to promote tissue regeneration. Future studies will assess the biofabricted IVD structures for tissue regeneration and biostability using *in vivo* rodent subcutaneous animal models.

DEDICATION

This thesis is dedicated to my dad, mom, and sister. You have provided me with amazing opportunities throughout my life, and words cannot express the gratitude I have for that. I will never be able to repay you for all of the support, inspiration, and love you have shown me. Additionally, I would like to dedicate this to all of my friends who I have become close to throughout the years. You have all provided great experiences that have shaped who I am today, and I am lucky to have you in my life.

ACKNOWLEDGEMENTS

Throughout my experiences as a PhD student, I have had the gratitude to meet a number of people who played an influential role in shaping the person that I have developed into, both academically and personally. First, I would like to thank my research advisor Dr. Xuejun Wen, who welcomed me into his laboratory 6 years ago. Dr. Wen provided in-depth insight into my projects and ensured that I had all of the necessary resources and knowledge to aid in my research and ensure I was successful. Without Dr. Wen's guidance and supervision, I would have been lost. His intense enthusiasm for my success was highly apparent, for which I am extremely grateful. Additionally, I would like to thank Dr. Martine LaBerge, my committee chair, who helped me overcome significant setbacks and hurdles during my studies. I would also like to thank my other committee members: Dr. Ning Zhang and Dr. Hai Yao, who provided invaluable insight and professional guidance relating to my project.

I'd like to give special thanks to the Clemson-MUSC bioengineering program and the entire Wen Lab for Regenerative Medicine, which was paramount in helping advance my studies. I would like to especially thank those that provided significant contributions, including: Brooke Damon, Vince Beachley, Xiaowei Li, Xiaoyan Liu, Jon Kuo, Bo Xue, Wendy Vanden Berg-Foels, and Yongzhi Qiu.

I would like to give a huge "thank you" to my girlfriend, Eleni, for not only providing significant contributions to my work, but for putting up with me and providing a loving and supportive force in my life. I could not have done this without you.

Lastly, I am grateful for support from an NIH predoctoral fellowship (NIH F31AG040929).

TABLE OF CONTENTS

Page

Table of Contents (Continued)

Page

Table of Contents (Continued)

Page

LIST OF FIGURES

Figure **Page**

List of Figures (Continued)

Figure **Page**

List of Figures (Continued)

Figure **Page**

List of Figures (Continued)

Figure **Page**

List of Figures (Continued)

Figure **Page**

LIST OF TABLES

Table **Page**

CHAPTER 1

1. INTRODUCTION

1.1 Intervertebral disc (IVD) Degeneration

Intervertebral disc (IVD) degeneration is characterized by the deterioration of the disc tissue. This deterioration is characterized by unique disorganization of extracellular matrix (ECM) within each portion of the IVD. In the inner region of the disc, the nucleus pulposus (NP), proteoglycan (PG) content decreases. In the outer disc region, the annulus fibrosus (AF), the organized lamellar collagenous structure begins to weaken. With a decrease in PG content, the inherent water content of the disc reduces. This dehydration within the NP is accompanied by a loss in disc height, and a subsequent decrease in swelling pressure. Further, as the organized AF structure deteriorates, it becomes less stable and begins to tear. This tearing within the AF prevents the annulus from containing the swelling pressure from the NP. The combination of a loss in PG content in the NP and a tearing of the collagenous lamellae in the AF, the disc degenerates and begins to fail in its duty to support spinal loading. This degeneration is accompanied by a loss in disc height, resulting in compression of the spinal nerves, which causes intense back pain for patients, and is oftentimes the underlying cause for patients to seek medical intervention.

1.2 Clinical Intervention Strategies

Initially, patients with a degenerated IVD are treated with rest, therapy, and medication. Usually, these therapeutic remedies ameliorate the pain and other issues such as resulting disabilities. However, when these therapies prove ineffective, surgical intervention is necessary. Discectomy, or removal of the degenerated portion of the IVD, is often the first step towards relieving a patients symptoms. Alternatively, patients can undergo spinal fusion to immobilize the degenerated region of the spine, which helps to temporarily relieve pain. However, fusion does not restore disc function or patient mobility and prevents natural biomechanical forces on the spine, possibly leading to further disc degeneration.

Recently, patients have also been given the option of replacing the IVD with a artificial disc replacement, which have been used in Europe for over a decade and are recently gaining interest and clinical approval in the United States. However, there are some downfalls to these current disc replacements. Though they aid in the preservation of motion as well as disc height, they do not replicate physiologic motion or absorb compressive forces as their composition is mostly rigid polymeric and metallic materials. Due to this composition, these implants may also produce wear particles and cause osteolysis. Furthermore, current implants exhibit significant differences in compliance from that of the native tissue, which may cause stress shielding and subsequent implant migration into the vertebral bodies. Although these current clinical interventions alleviate some symptoms of disc degeneration, they do nothing to address the underlying cause of the degenerated disc tissue itself, and often lead to further disc degeneration at adjacent

vertebrae levels. Due to the problems associated with these conventional approaches for IVD degeneration, tissue engineered constructs are now being investigated, as they offer exceptional opportunities to improve overall patient satisfaction and well being by promoting tissue repair.

1.3 IVD Tissue Regeneration

Tissue engineering, which is oftentimes referred to as regenerative medicine, is an interdisciplinary field that incorporates ideas from: biology, chemistry, materials science, engineering, and medicine. Using a combination of these disciplines, therapeutic methods to promote regeneration of many tissues of the body, including the IVD, are being investigated by researchers worldwide, including cell-based therapies, signaling molecule therapies, and biomaterial-based therapies. These approaches are often used in combination, as biomolecule and cell-based therapies alone may prove ineffective in supporting spinal loading. A biomaterial structure is likely necessary to provide mechanical stability and support loading throughout the IVD regeneration process, as well as provide guidance for cell growth and new ECM organization. For these reasons, biomaterial scaffolds should have similar overall structures and mechanics to that of the native tissue. Additionally, scaffolding constructs provide the ability to incorporate and deliver signaling molecules which often enhance the success of the regenerated construct.

A major goal of tissue engineered constructs is to mimic the targeted tissue's ECM structure and composition with a biomaterial scaffold. Through mimicry of ECM, a biomaterial scaffold provides a platform for the guidance of cellular orientation. As scaffolds with a defined structure can control cell morphology, they subsequently control

ECM deposition, including both the type and organization of the synthesized matrix. Further, desirable mechanical properties similar to that of native tissue can be achieved by controlling ECM composition and orientation on a tissue scaffold.

1.4 Limitations

Tissue engineering serves as a promising alternative to the current treatment options available for patients requiring surgical intervention due to a degenerated spinal disc. Tissue engineered IVDs may offer the advantage of motion preservation and disc space restoration. However, to date, researchers have not created an IVD tissue scaffold that accurately mimics the native tissue histology in combination with similar biomechanics of the natural IVD tissue. In order to engineer a normal IVD structure, the materials and structures to be used for IVD tissue regeneration must mimic the 3-D histological architecture of the native IVD, which will promote the formation of organized cellular and extracellular structures similar to that of native IVD tissues. The close correlation between the biological functions and the molecular compositions of the disc structures strongly suggests that a major task of IVD regeneration is to create scaffolds that precisely reproduce the structural, biological, and mechanical functions of the disc structure and organize them in a spatial manner similar to that of the native disc. Many researchers have attempted to recreate the IVD, but the discrete tissue architectures of the NP and AF have posed great challenges. Furthermore, the biological functions, microstructures, and mechanical properties of current scaffolds are far from satisfactory, perhaps due to the poor ability to control scaffold architecture during fabrication. Although current approaches focused on IVD tissue regeneration are far from

satisfactory, the results from these studies help to provide a platform towards the creation of a successful and clinically-relevant approach to regenerate IVD tissue. Based on the previous successes and failures in tissue engineering IVD scaffolds, we have developed a unique strategy attempting to further advance IVD tissue engineering.

1.5 Project Objective, Significance, and Innovation

The ***objectives*** of this research were to use bioengineering strategies to pursue the development of materials and methods to imitate the IVD and facilitate tissue regeneration. To this end, our aims were to use a biofabrication technology to create reproducible scaffolds that mimicked the lamellar microstructure of the AF in native IVD tissues. We believe that this biomimetic approach will promote the formation and synthesis of ECM more similar in composition, organization, and mechanics to that of native tissue, therefore providing a more feasible approach towards regenerating IVD tissue.

The degenerated spinal disc is one of the most expensive medical issues currently encountered, as it results in the disability of many people within the aging population. This project has the potential to ***significantly impact*** worldwide healthcare goals involving the restoration of native IVD tissue by decreasing its economic burden and impact on society. The ultimate goal in tissue engineering an IVD is to replace the degenerated disc tissue with a functional scaffold that will promote the growth of new tissue while also maintaining natural motion and load bearing abilities. More specifically, the strategies described in this work may aid in the promotion of native tissue formation to ultimately treat the problems associated with IVD degeneration rather

than conventional clinical approaches, which focus only on relieving the symptoms. The aims proposed within this project will generate conceptual advances in understanding IVD biomaterial and scaffold implant design criteria, leading to increased technical knowledge for the development of a new clinically relevant IVD replacement.

1.6 Specific Aims and Rationale

Aim 1: To develop a biofabrication approach that would allow for the creation of IVD scaffolds with precise control of scaffold structure.

Rationale: Current methods focused on creating IVD scaffolds are limited in their ability to accurately mimic native IVD structure. To this end, we believe that utilizing a computer-controlled polymeric extrusion-based biofabrication approach will enable IVD scaffolds to be created with distinct architectures. Our hypothesis is that this type of device, along with the incorporation of a temperature-controlled collection mechanism, would allow for the increase of the viscosity of the polymer solution in order to solidify precise structures directly upon deposition.

Aim 2: To fabricate tissue engineered scaffolds with structural and mechanical properties highly similar to native IVD tissue.

Rationale: We hope to use our biofabrication approach to create IVD scaffolds with the precise characteristics of the native IVD tissue. Specifically, we want to mimic the IVD shape, concentric lamellar structure, lamellar spacing, and its biomechanical properties. It is our hypothesis that our unique biofabrication approach will facilitate in the

fabrication of complex scaffolds with highly similar biomimetic characteristics of the native IVD tissue.

Aim 3: Evaluate the tissue regeneration capabilities of the biofabricated IVD tissue engineered scaffolds *in vitro*.

Rationale: Elastic lamellar-based scaffolds will be assessed for their potential as suitable structures for IVD tissue regeneration. It is our hypothesis that our constructs will exhibit desirable characteristics while demonstrating potential as functional IVD scaffolds for tissue regeneration.

1.7 Organization of Dissertation

The following manuscript is arranged into different chapters that showcase individual studies relating to the overall aims of the project. In Chapter 2, a comprehensive literature review is presented. This chapter focuses on the specifics of the IVD structure, the causes and results of disc degeneration, current methods available to repair a degenerated disc, and lastly, different methods and techniques that have been explored for tissue regeneration of the IVD. Emerging tissue engineered scaffolds and techniques for IVD regeneration are discussed in detail. Overall assessments of these current strategies to enhance IVD tissue regeneration are provided, specifically focusing on *in vitro* and *in vivo* analyses. Chapter 3 provides the results from the first investigation into our unique biofabrication strategy, which was aimed at creating biomimetic IVD scaffold structures. The results of this experiment proved the ability of

the biofabrication method to precisely control polymer extrusion at a high resolution while also providing the initial platform towards mimicking IVD shape and structure. Mechanical properties of the scaffolds were also investigated to ensure elasticity of the constructs. In Chapter 4, the previous findings are further elaborated upon, showing that this novel IVD biofabrication method can utilize multiple polymeric biomaterials in the creation of IVD scaffolds. The ability of the scaffolds to mimic lamellar and interlamellar spacing as well as the scaffolds' ability to control cellular morphology similarly to native tissue is discussed. Finally, it was demonstrated that the biomimetic scaffolds have similar mechanical properties when compared to native IVD tissue. In Chapter 5, a 3-D cellularized version of the scaffold discussed in previous chapters was fabricated. It was demonstrated that IVD constructs could be cellularized within the voids of their lamellar structure using multicellular spheroids. Additionally, cellular morphology, as well as ECM synthesis were analyzed and compared to native IVD tissue. Chapter 6 summarizes overall conclusions drawn from the body of work and discusses challenges and future directions related to the progress of the presented research.

CHAPTER 2

2. INTERVERTEBRAL DISC (IVD): STRUCTURE, DEGENERATION, REPAIR, AND REGENERATION

2.1 Introduction

Over 80% of the adult population experiences low back pain at some point in their lives, resulting in $90 billion in annual costs to alleviate and treat this pain [1-4]. The degeneration of the intervertebral disc (IVD) is thought to be the primary cause of low back pain, causing compression of the spinal nerves and adjacent vertebrae. It is difficult to pinpoint the exact cause of degeneration, but it is thought that many confounding factors may play a significant role in the degenerative process.

The IVD is a tough tissue structure sandwiched between the vertebral bodies (Figure 2.1). It has three functions including: 1) acting as a ligament to hold the vertebrae of the spine together; 2) a shock absorber; and 3) a "pivot point" that allows the spine to bend, rotate, and twist. There are three distinct structures in the IVD: the nucleus pulposus (NP), the water-rich gelatinous center that primarily bears the pressure; the annulus fibrosus (AF), the collagen-rich fibrous structure of ~15-25 concentric sheets of collagen (lamellae) that confines the pressurized NP; and the vertebral end-plates (VEP), which are cartilaginous plates that are interwoven into the AF at the disc-vertebrae interface and supply nutrients to the disc. All three of the IVD structures contain chondrocyte-like disc cells. The NP contains large concentrations of negatively charged proteoglycans (PGs), which cause the NP to retain water and maintain its swelling

pressure [5,6]. PGs help to maintain water content and swelling pressure in the IVD and intertwine in a lose network of collagen type II fibers [5,7,8]. The AF has a lamellar structure composed of collagen type I and II fibers. This lamellar architecture helps maintain the tensile properties of the disc while providing structural support for PG synthesis [9].

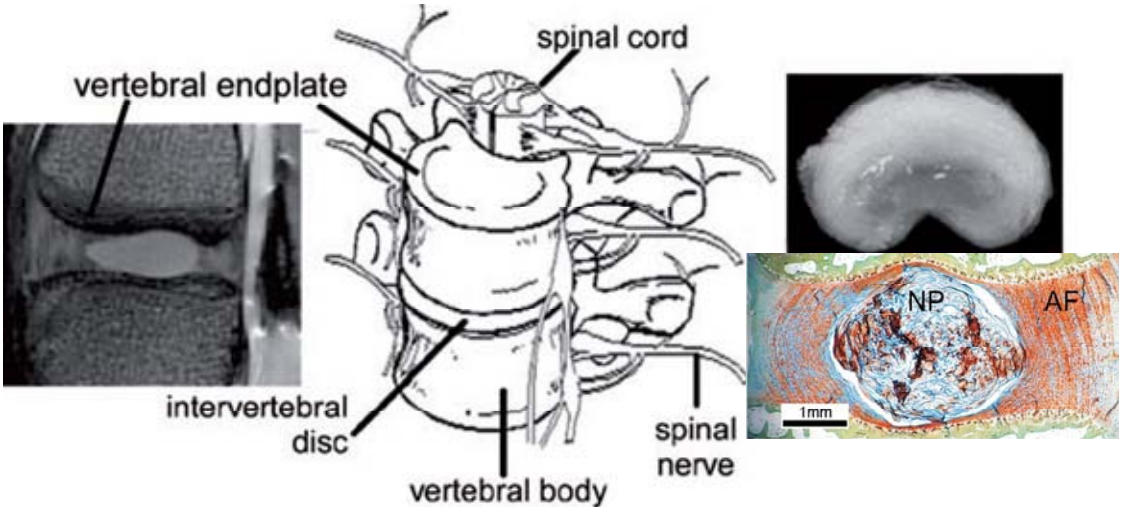

Figure 2. 1: MRI of IVD showing NP and AF in distinct regions (left). Schematic of spinal column (middle). Anatomy of normal disc with histological stain (right) [10-12].

Current treatments to help alleviate low back pain due to IVD degeneration include rest and medication. However, when these methods do not suffice, patients must undergo procedures for a spinal fusion or an artificial disc replacement. Spinal fusion helps to temporarily relieve pain, but does not restore disc function and prevents natural biomechanical forces on the spine. This possibly leads to further degeneration at adjacent levels [13]. Therefore, fusion is not ideal as it sacrifices natural motion and may exacerbate the problem of further degeneration down the road. An alternative to spinal fusion is an

artificial disc replacement, which has been used in Europe for over a decade and is recently gaining interest and clinical approval in the United States [14,15]. Current disc replacements aid in the preservation of some natural motion as well as disc height, but they do not absorb compressive forces as their composition is mostly rigid metallic materials. Also, these implants produce wear particles and may cause osteolysis [16]. In addition, current implants exhibit significant differences in compliance from that of native tissue, which may cause stress shielding and subsequent implant migration into the vertebral bodies. Because of the problems associated with these conventional approaches, tissue engineered constructs may help promote integration of natural tissue while preserving natural kinematics, disc height, and the ability to absorb compressive forces.

Successfully tissue-engineered IVD tissue must have the native IVD histological and macro structures. Therefore, in order to engineer normal IVD structure, the materials and structures to be used for IVD tissue engineering must mimic the 3-D architecture of native IVD to promote the formation of organized cellular and extracellular structures similar to that of native IVD tissues. The scaffolds must allow the infiltration of nutrients and removal of wastes to maintain cell viability. The close correlation between the biological functions and the molecular compositions of the disc structures strongly suggests that a major task of IVD regeneration is to create scaffolds that precisely reproduce the structural and biological functions of disc structure and organize them in a spatial manner similar to that of native disc. Many researchers have attempted to recreate the IVD, but the unique composition and structure of the disc has posed great challenges. Furthermore, the biological functions, microstructures, and mechanical properties of

current scaffolds are far from satisfactory. The ultimate goal in tissue engineering an IVD is to replace the degenerated disc tissue with a functional scaffold that will promote the growth of new, healthy tissue while also maintaining the motion and load bearing abilities and preventing adjacent disc degeneration.

2.2 IVD Structure

The IVD is a complex joint which permits flexible motion within the spine while serving as a shock absorber. The purpose of the disc is to allow 3-D motion, but also to prevent excessive motion and maintain mechanical stability. There are 3 main components within the IVD: the NP, AF, and VEP. The NP consists of the soft center within the spinal disc, while the outer portion of the disc which surrounds the NP is referred to as the AF. The VEP is composed of fibrocartilage and surrounds the disc on the top and bottom and separates the IVD from the spinal vertebrae.

IVDs are composed of cartilage, making regeneration difficult because it is an avascular tissue. Due to its avascular nature, nutrient transport and waste removal is a much more complicated process relying solely on diffusion across the VEP and within the disc matrix [17-19]. The IVD is the largest avascular tissue in the human body, with only the peripheral portion of the tissue containing a blood supply. Similarly, there is a lack of nerves as well. Some nerve extensions innervate the periphery of the spinal disc, but the majority of the disc is not innervated. It is thought that compression of the nerves on the periphery of the disc is responsible for a patient's perceived pain as the disc degenerates. A large problem in nutrient and solute transport is the calcification of vertebral endplates which occurs as the disc degenerates. If nutrients are not provided to disc cells and waste

products are also not removed, then these waste products linger in the matrix of the disc preventing the maintenance of healthy IVD chondrocytes. Decreased nutrition accompanied with a loss in PG and water content significantly depletes the ability of IVD cells to function properly. Subsequently, disc degeneration occurs if nutrition is depleted or impeded. Oxygen concentration gradients change across the cross section of the disc, decreasing towards the center as the peripheral cells use the oxygen first [20]. Opposite the oxygen gradient is the lactate gradient, which is greater in the disc center [20]. The low oxygen and high lactate concentrations in the NP create an acidic environment where the amount of PG may be subsequently decreased [21]. Because the IVD is in a nutrient deficient environment, only a small amount of cells can survive. By tissue standards, the IVD contains a low cell density, with most of the tissue composed predominately of ECM molecules. The main function of cells within the IVD is to constantly secrete ECM in order to maintain a stable tissue. As matrix is constantly synthesized, it is also being degraded which ensures that the ECM remains a structured environment. This ECM consists mostly of PGs, highly concentrated and negatively charged molecules that increase the water content, as well as a variety of different collagen molecules which promote the strength of the AF [5]. The most prevalent types of collagen are collagen types I and II, which make up 80% of the collagen composition within the disc. However, collagen types III, V, VI, IX, and XI are also present to help organize the disc into its lamellar structure [22].

2.2.1 Nucleus Pulposus (NP)

The NP is a gelatinous structure consisting of a large amount of PGs or aggrecans with sparsely arranged collagen fibrils serving as supporting matrix (Figure 2.2). PGs, a major matrix component, are glycoproteins containing a protein core and at least 1 glycosaminoglycan (GAG) chain [22]. The PGs are similar to articular cartilage, also containing hyaluronan (HA) [23]. Because PGs, and more specifically GAGs, are hydrophilic, they maintain a large quantity of water in the IVD. The high concentration of GAGs increases the osmotic pressure of the NP and allows it to swell and resist large compressive loads [24-26]. It is believed that decreasing the amount of GAGs will decrease the disc height and cause disc degeneration as the NP becomes more fibrous. Normal, healthy discs represent a changing profile of inhomogeneous material across the disc with GAG and water content increasing towards the disc center [27]. The purpose of the NP is to resist compressive forces and evenly redistribute the forces within the spine. While PGs make up roughly 50% dry weight of the NP, the NP is also composed of 25% collagen [22,28,29]. Collagen type II is highly prevalent in the NP as its concentration decreases towards the peripheral AF [22]. Each of these molecules aid in the regulation of growth factors, therefore controlling cellular metabolism.

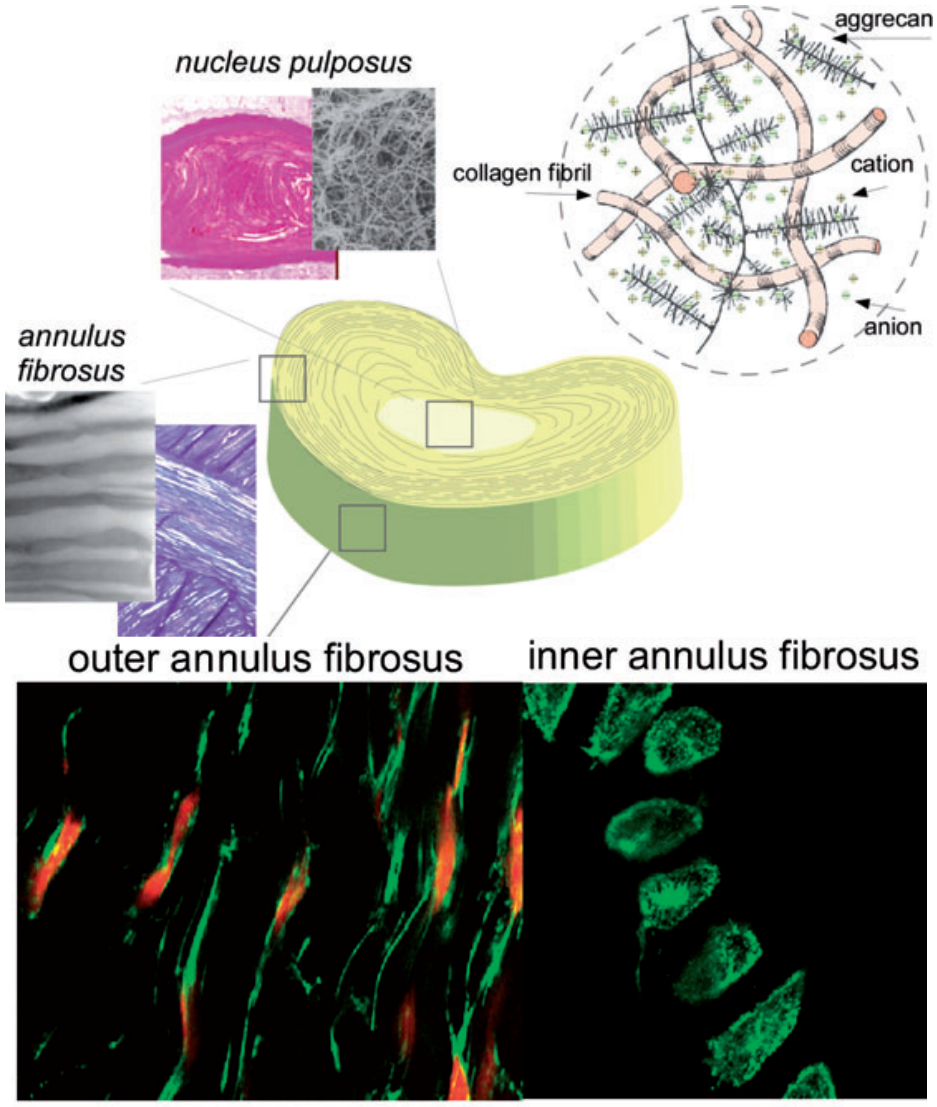

Figure 2. 2: Schematic showing different regions of the IVD and their composition and structure (top). Fluorescent imaging showing different cell morphology in different disc regions (bottom) [11].

Though the ECM is the main component of the NP, it also contains around $4x10^6$ cells/ml [22]. The cells are mostly chondrocytes and are more rounded as compared to cells in the AF (Figure 2.2) [30]. NP cells also develop a larger cytoplasm and a more complex structure than AF cells [31]. Characteristic markers for chondrogenic expression of NPs include collagen types II and IX, aggrecan, and SOX9 [32-35].

2.2.2 Annulus Fibrosus (AF)

The IVD is largely heterogeneous and exemplifies great differences between the NP and the AF (Table 2.1). The AF and NP are separated by what is called the transition zone [36]. The AF is present to withstand the tension created during NP deformation. The AF is composed of more than 2/3 collagen, where PGs make up only a small percentage of its composition [22,28,37]. The AF can be separated into the inner AF and the outer AF. The outer AF contains an oriented lamellar array of densely packed collagen fibers, while the inner AF is similar to the outer portions except it is not as dense and the oriented lamellae are not as organized [22]. Collagen type I is highly prevalent in the outer AF, while its concentration decreases towards the NP [22]. The AF has a multilayered, oriented lamellar structure with concentric layers creating a regular pattern of collagen type I fibers (Figure 2.2) [38]. The collagen fibrils are oriented concentrically with each subsequent layer oriented 60° to the spinal column. As the outer AF moves inward and approaches the NP, the orientation of the concentric lamellae gradually changes from angles of 62° to 45° [39].

The AF contains roughly $9x10^6$ cells/ml. Cells within the AF resemble fibroblasts, showing a thin elongated structure oriented parallel to the collagen fibers within the

concentric lamellae (Figure 2.2). The NP and inner AF contain only chondrocytes, while the outer AF contains mostly fibrochondrocytes [40].

Table 2. 1: Difference in IVD composition and mechanical properties between the annulus fibrosus and nucleus pulposus [41-50].

	Outer AF	**Inner AF**	**NP**
Water (per weight)	65-75%	75-80%	75-90%
Collagen (per dry weight)	75-90%	40-75%	25%
Proteoglycans (per dry weight)	10%	20-35%	20-60%
Other Proteins (per dry weight)	5-15%	5-40%	15-55%
	AF		**NP**
Compressive Modulus (MPa)	0.116-2.3		0.003-.031
Tensile Modulus (MPa)	0.2-136		N/A

As the majority of artificial disc replacements are performed on the lumbar spine, this review will focus on that region. Although, spinal disc composition does not seem to be significantly affected by the discs level within the spine, the size of the IVD increases inferiorly down the spine [51]. IVDs in the lumbar spine are the largest with a height of around 1 cm and a diameter of 4 cm [52]. For this reason, the lower back is the most common area for disc degeneration, since diffusion of nutrients to the cells is much more difficult and takes longer to occur.

2.3 Disc Degeneration

As we age, the disc degenerates. The incidence of low back pain increases with age, creating a relationship between age related disc degeneration and the frequency of low back pain [22,53]. What is less understood are the mechanisms causing this degeneration

and the process through which the degeneration occurs. Many researchers believe that the degeneration of the spinal disc is a natural aging process. IVD degeneration involves tissue loss or destruction over time, which decreases disc height and ultimately sacrifices mechanical function of the vertebral body. However, evidence suggests other factors are involved with increasing disc degeneration such as cell nutrition and transport, the presence of degradative enzymes, mechanical loading, smoking, and exposure to intense vibrations [54-56]. Although many of these factors may contribute to the aging process, they cannot be ignored, leading to the term degenerative disc disease (DDD) which encompasses all of the degenerative effects of aging.

Presumably, it is difficult to characterize the morphology of the degenerated disc. Many researchers have developed ways to grade disc degeneration, however, these methods do not deal with the entire disc and do not completely characterize all the levels of degeneration causing some ambiguity [57]. Clinically, disc degeneration and disc height are evaluated using magnetic resonance imaging (MRI). MRI enables each portion of the IVD to be investigated and allows changes in the disc to be analyzed [58,59]. MRI is the most clinically effective way to analyze disc degeneration by comparing disc water content and height, and looking for tears or irregularities within the tissue [60]. When the disc loses height due to tears in the AF or the NP bursting, the compressed vertebrae may pinch spinal nerves or rub together, causing intense pain. Some pain from the IVD is thought to arise from nerve fiber growth into the degenerated disc [61].

Disc degeneration may be influenced by calcification with calcium phosphate crystalline deposits, as the presence of these deposits increase as the disc ages, hindering

nutrient diffusion [62]. Also, the amount and size of PGs within the NP significantly decreases with as the disc degenerates [41,63-65]. Decreases in PG content are correlated with dehydration as these molecules are major contributors to the higher water content in the IVD [22]. At early stages of disc degeneration, the NP dehydrates and becomes more fibrous [66-68]. Desiccation of the NP is followed by tearing within the AF (Figure 2.3). These events may result in further disc matrix degradation, loss of hydration, and subsequently a decrease in disc height. Each of these events decreases the discs ability to properly function.

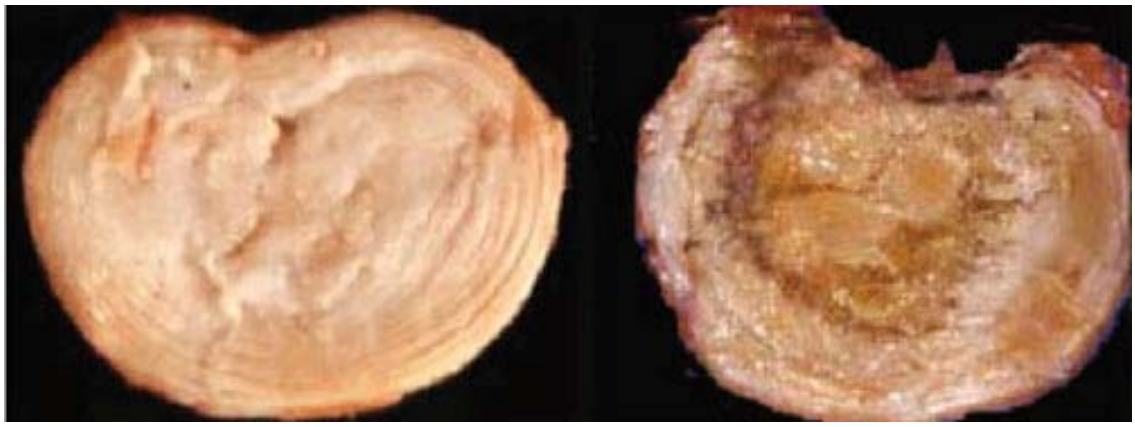

Figure 2. 3: Picture of normal disc (left) and degenerated disc (right) where the degenerated disc is more disorganized and has a more fibrous appearance [69].

As disc degeneration progresses, there is a significant loss in PGs, water, and collagen type II. Cellular microstructure may also be compromised during disc degeneration. An alteration from a differentiated chondrocyte phenotype to a more fibrotic phenotype in the NP occurs [70]. IVD shape and size are altered by changes in water content which lead to a hindrance in the discs ability to absorb loads.

Matrix turnover is common within the healthy IVD. During disc degeneration, matrix is both degraded and altered through a variety of biochemical processes. PGs and other ECM proteins are degraded by serine proteinases and matrix metalloproteinases (MMPs), cytokines (specifically IL-1 & IL-6), nitric oxide (NO), and prostaglandin E_2 (PGE_2) [22,71,72]. MMPs are catabolic enzymes which encourage matrix degradation and studies have shown degenerated discs to contain greater levels of MMPs. One goal to stop disc degeneration is to create an environment in which the disc is in a more anabolic state in order to increase matrix synthesis and decrease matrix degradation. A normal healthy disc inhibits MMPs by using tissue inhibitors of MMPs (TIMPs). TIMP-1 can increase the amount of PG and matrix production. MMPs 1,2,3,7,8 and 13 have all been found in the IVD, with the majority of these proven to be more active in the degenerated disc [73,74]. MMP-1 (collagenase), MMP-2 (gelatinase), and MMP-3 (stromelysin) have all been directly implicated in aggrecan and matrix protein degradation [75]. MMPs 1-3 have shown to degrade aggrecan, collagen types I and II, and collagen types IV and V, respectively [22]. Interleukin 1 (IL-1) and tumor necrosis factor α (TNF-α) may also affect the disc metabolism. IL-1 may increase the rate of matrix degradation through the release of MMPs and may also decrease PG production [76-78].

The collagens' organized lamellar structure deteriorates, as well, and the degraded matrix molecules become granular and evident within the NP [29,79]. Throughout the aging process, the presence of collagen remains the same [5]. However, the different collagen types and their ratios appear to change [80,81]. Collagen crosslinking is also altered during degeneration, decreasing the ability of the disc to support mechanical loads [82]. The

increase of disorganized collagen type I with the corresponding loss of collagen type II and PGs in the disc matrix has been identified as a reason degenerated discs have inferior mechanical properties [83].

Due to matrix degradation by enzymatic and structural changes, the disc and matrix undergo mechanical changes as well. It has been observed that degenerated discs have less height and are less stiff than normal discs [84]. Structural changes are thought to contribute to disc degeneration, in turn altering the ability of the disc to support mechanical loading. During degeneration, the disc becomes less elastic, preventing its ability to absorb and dissipate spinal forces [22,85]. As the IVD is loaded, it loses water content. Studies have shown that excessive water movement caused by mechanical loading decreases the synthesis of ECM [86]. Biomechanical changes in the disc likely aid in degeneration. IVD degeneration is identified by altered material properties, ECM, and morphology [87,88]. The lamellar morphology of the AF is highly disorganized in degenerated discs, while overall disc structure is also modified. A degenerated disc has distorted architecture, responding to stresses differently and possibly causing patients perceived pain.

Cartilage does not maintain the inherent ability to regenerate. As the disc degenerates and ages, there is a decrease in the number of viable cells [29,79]. This decrease along with a decrease in nutrient delivery have been implicated as important factors causing disc degeneration [89]. It is not well understood, but a decrease in cell viability may be due to apoptosis of the disc cells caused by mechanical loading of the AF. However, many cellular factors must be considered when determining causes of disc

degeneration. Degeneration of the IVD causes a significant structural alteration in both regions of the disc, leading to a decrease in height, and ultimately resulting in pain. During normal daily life, patients with degenerated discs experience excrutiating pain, leading to a decline in their quality of life. The progression of disc degeneration leads to further instability in adjacent vertebral levels [90].

2.4 Clinical Solutions to Disc Repair

2.4.1 Discectomy/ Fusion

Currently, it has proven difficult for clinicians to manage the low back pain implicated by a degenerated IVD. The majority of patients are treated with rest, exercise and/or medications [91]. When these therapies are ineffective, surgery is required. The two most common surgical procedures for patients with degenerated spinal discs are discectomy and arthrodesis. Discectomy is a process in which the degenerated portion of the IVD is excised or removed. Arthrodesis is a process of fusing two adjacent vertebral bodies together and is often referred to as spinal fusion [92].

Although removal of degenerated or damaged disc tissue is common, it typically leads to a loss in height of the IVD correlated with negative biomechanical changes and anatomical problems. Some patients benefit from a discectomy as it may offer temporary pain relief. However, postoperatively, the disc structure is highly compromised, leading to further degeneration and instability [87]. After a discectomy, no regeneration of IVD tissue takes place, making further disc degeneration likely [93].

Due to the disadvantages and limited success of a discectomy, clinicians often turn to spinal fusion to aid in patient comfort and further stabilize the spine. However, the rates of clinical success for spinal fusion are also low [94]. The main purpose of spinal fusion is to prevent motion within the diseased spine segment. In turn, this loss in mobility should decrease a patient's perceived pain [95]. Problems with spinal fusion, however, include possible degeneration of adjacent segments and failure to completely immobilize the degenerated region of the spine [95]. Spinal fusion has proven to increase stress concentrations on adjacent motion segments within the spine after analysis using biomechanical studies and finite element analysis [96,97]. Because discectomy and spinal fusion result in a loss of function and may promote adjacent disc degeneration, new studies are being investigated to help alleviate a patients perceived back pain [98].

2.4.2 Replacement

Discectomy and spinal fusion are only short term solutions to recurring low back pain or a degenerative IVD. A total IVD replacement, or arthroplasty, has advantages over fusion, eliminating pain while increasing patient mobility [60,95]. A primary advantage of a disc replacement over spinal fusion is the preservation of some spinal motion [99]. Implants for disc replacements should be biocompatible, durable, and easily implantable. Disc replacements remove diseased tissue and reduce pain by restoring disc height. There are different types of disc replacements including a NP replacement and total disc replacements.

NP replacements are less invasive and promote natural forces on the spine [100]. NP implants often have high water contents and promote fluid movement during loading to enable nutrient delivery and mimic the native tissue environment. The prosthetic disc nucleus (PDN) is a NP replacement consisting of a hydrogel core constrained by a biodegradable woven fiber mesh to prevent excessive hydrogel swelling (Figure 2.4) [101]. The PDN has passed FDA guidelines pertaining to cytotoxicity tests and biomechanical fatigue tests [102]. PDN is implanted in a dried form and absorbs fluid after implantation. Currently, NP replacements must be implanted through incisions in the AF. This surgical trauma, however, may compromise the integrity of the operated disc, resulting in an inflammatory response that may ultimately promote the degenerative process. The use of a NP replacement is not as widespread as the use of total disc replacement.

A total disc replacement is used when the integrity of the native AF has been compromised or indicated as a cause of pain. Total artificial spinal discs also help re-establish flexibility of the spine. There are a few commercially available artificial spinal discs that have been approved by the FDA. The SB Charitè® and ProDisc® are FDA approved in the US with another, the Maverick®, undergoing clinical trials (Figure 2.4) [15,103-105]. The SB Charitè® and ProDisc® have both been used for more than a decade in studies done mostly in Europe, and both disc replacements have shown a decrease in operative time, blood loss, and length of hospitalization as compared with spinal fusion [106]. Patients implanted with the ProDisc® and the SB Charitè® reported significantly less pain than spinal fusion patients, indicating that the recovery time may be shorter [99,107].

Other studies have confirmed the findings that artificial replacements have proven to increase patient satisfaction compared with spinal fusion [108,109].

The SB Charitè® consists of 2 cobalt chromium alloy endplates and a biconvex polyethylene (PE) spacer allowing for unlimited axial rotation, but only 20° flexion [100,110]. The endplates are coated with titanium and hydroxyapatite to promote osteointegration into the adjacent vertebrae. On the other hand, the ProDisc® consists of endplates composed of cobalt chrome molybdenum alloy with a fixed ultra-high-molecular-weight PE (UHMWPE) bearing surface that articulates on the metal [111]. The metal implants contain porous coatings or screws to promote bone ingrowth [100]. The Maverick® is an all metal disc implant containing a ball and socket that offers high fatigue strength [112].

Figure 2. 4: Current Food and Drug Administration approved implants: PDN, SB Charitè®, ProDisc® (left- right) [102,113,114].

The use and necessesity of total disc replacements is debatable and comparison between different available implants is understudied. However, although there are improvements to conventional treatments with artificial discs, there are also drawbacks. Problems with current prosthetic devices include extrusion, infection, loosening, and cytotoxicity [115-117]. Long term survival and integrity of these implants is unknown

because the devices are quite new in clinical use. Problems with a metal on metal approach are a large compliance mismatch and the creation of toxic wear debris [100]. This microscopic wear debris can cause foreign body reaction in the body, and possibly destruction of the tissue implant interface [100]. As the implants are secured in the vertebral bodies, the metal endplates may dislocate or migrate out of the bone. Loosening and wear of the PE may occur in the SB Charitè® and ProDisc®, while the PE may also experience creep, or even fracture [118-120]. Because there are problems with current disc replacements, and because they may fail, a revision may be required. Typically, revision operations require a removal of the artificial disc followed by spinal fusion to immobilize the affected tissue. Revision operations for artificial disc replacements are risky and dangerous as scar tissue makes it difficult for the surgeon to navigate the large vessels near the spine [121]. Therefore, longevity studies analyzing the long term effectiveness of current implants are necessary.

Disc replacements allow some motion, but restrict certain movements and do not replicate physiologic spinal motion or stability [118]. Total disc replacement procedures do not provide an effective treatment method for all patients, as the results are not consistently reproducible [95]. Other problems involving current disc replacement strategies include altered loading and compliance mismatch between the metal/polymer based implants and the native tissue [122]. Often, current disc replacements do not absorb compressive forces. During procedures for discectomy, spinal fusion, and disc replacement, degeneration at other disc levels may be increased [123]. Although implants

for disc replacement currently exist, no methodology has proven completely successful in improving the ability of native disc tissue to regenerate.

2.5 IVD Regeneration

An apparent need for an alternative to conventional IVD replacement or spinal fusion is obvious. Current artificial discs do not promote tissue remodeling. Tissue engineering offers an attractive method to design a biomaterial that will aid in the regeneration of natural IVD tissue. As current surgical procedures only focus on symptoms related to IVD degeneration, IVD tissue engineering offers multiple strategies to prevent and possibly cure degenerated discs by encouraging tissue repair. Tissue engineering promotes tissue regeneration by encompassing the use of biomaterial scaffolds, stem cells, and growth factors.

Therapeutic strategies for tissue engineering are advantageous because they can be implanted simultaneously with a discectomy. Once removed, appropriate biomaterials that have been designed to possess the desired biological, chemical, physical and mechanical properties can then replace degenerated tissue. These biomaterial structures should not illicit an immune response, have a structure similar to native tissue, be biocompatible and biodegradable, and exhibit similar mechanical properties to those of the natural tissue after successful regeneration. Many biomaterials currently exist which have proven their biocompatibility, but newly developed materials must pass this requirement first and foremost [124]. However, not all materials are suitable for every application, and when choosing materials for the IVD many factors should be considered.

An ideal scaffold would be porous to provide cell attachment and tissue ingrowth, while also allowing the diffusion of nutrients and waste. The porous structure should allow room for ECM to be secreted and ultimately form the tissue similar to normal native IVD tissue.

Though biomaterial-free approaches do exist, in the spine, it may be necessary to use biomaterials, as they serve as a load bearing structure to support biomechanical forces while cells proliferate and create their own matrix. Biomaterials are important to provide a stable environment for disc tissue regeneration [125]. Because the native disc has a low density of cells, there is great concern that without a biomaterial carrier the implanted or recruited therapeutic cells will have trouble synthesizing functional matrix to support IVD biomechanics. Biomaterial carriers or scaffolds are important because biomaterials offer cells a 3-D environment to guide cell behavior. Biomaterials can guide cell attachment and growth along a defined micro and macrostructure to better mimic native tissue structure. However, for tissue engineering purposes, it is important to note that seeding cells at a high density is not attractive due to the unique IVD environment, which is not conducive to maintain the viability of a large population of cells [11].

A biomaterial structure or therapy for disc regeneration should be able to handle normal physiologic stresses on the IVD, which have been measured at around 1 MPa [47]. Biomaterial supporting structures should also be able to handle continuous dynamic loading over time while proving fatigue resistant. Also, for tissue engineering, it is important for the biomaterial to degrade over time and allow natural cell and ECM based tissue to take its place. When designing biodegradable materials, it is important to control

the degradation time and alter it in order to allow for new tissue infiltration. It is also important to evaluate the degraded material and verify it to be non-toxic to prevent an adverse immune response. Many materials offer the advantage of being able to have their mechanical properties and degradation times specifically tailored by creating copolymers, varying molecular weights, and altering crosslinking density. These materials include both synthetic and natural biomaterials, with many of these polymers showing superb biocompatible properties. Natural materials offer an advantage of promoting cell attachment and cellular recognition of the material. However, it is much easier to tailor the mechanical and physical properties of synthetic materials. Each of these material types show promise for IVD tissue regeneration.

One major hurdle in the development of a scaffold for IVD tissue engineering is the ability of researchers to mimic the lamellar organization of the AF [11]. The native disc histology and dynamics should be mimicked in biomaterial structures for IVD regeneration. In this regard, the ability of a biomaterial structure to enable natural motion may help prevent tissue degeneration at adjacent disc levels while encouraging natural tissue regeneration.

Tissue engineering techniques are mainly evaluated on the ability to increase ECM synthesis and restore disc height. When evaluating a biomaterial structure, cells in the NP region should be more morphologically rounded as this morphology has proven to synthesize more collagen type II, while cells in the AF region should be more elongated, as this morphology has proven to synthesize more collagen type I [11]. The majority of successes with tissue engineering approaches for IVD regeneration have focused on the

production of ECM and PGs which increase water content and mechanical stability. Qualitative studies such as staining with H&E, Alcian Blue, and Safranin-O are useful in evaluating specific cell behavior and matrix synthesis on scaffolds.

2.5.1 Cell Based Therapy

A large focus in the field of IVD tissue engineering is currently supported by cell based transplantation therapies. Mesenchymal stem cells (MSCs) are thought to halt IVD degeneration and possibly regenerate some tissue despite the degree of degeneration [126]. MSCs can be found in bone marrow, adipose tissue and many other connective tissues and are a multipotent type of adult stem cell that are less susceptible to tumor formation than embryonic stem cells [126,127]. Stem cells can be differentiated down a chondrogenic pathway and may have the ability to express IVD cell phenotypes. Because MSCs lack HLA class II antigen expression, they may have the ability to be used for allogenic transplantations [128]. The delivery method of cell based therapies would be primarily through injection into the IVD.

MSCs in hypoxic situations (2% O_2) exhibit a tendency to differentiate towards a phenotype similar to that of NP cells [4]. Under hypoxic conditions MSCs increased the amount of surface receptors for matrix and integrins, specifically β1, β3, and α2 integrins while maintaining desired levels of CD44 (hyaluronan receptor), CD105, CD166 (ALCAM) [4]. When injected into the degenerated disc tissues, stem cells may naturally differentiate towards a chondrocyte phenotype based on the environmental cues. MSC transplantation has shown to restore native disc height, cellularity, and structure in animal

models (Figures 2.5 & 2.6) [123]. Transplantation of human chondrocytes has proved effective in the therapeutic treatment of lesions within cartilage tissue [129]. However, chondrocytes are difficult to obtain for cell culture due to their limited availability in the adult human body.

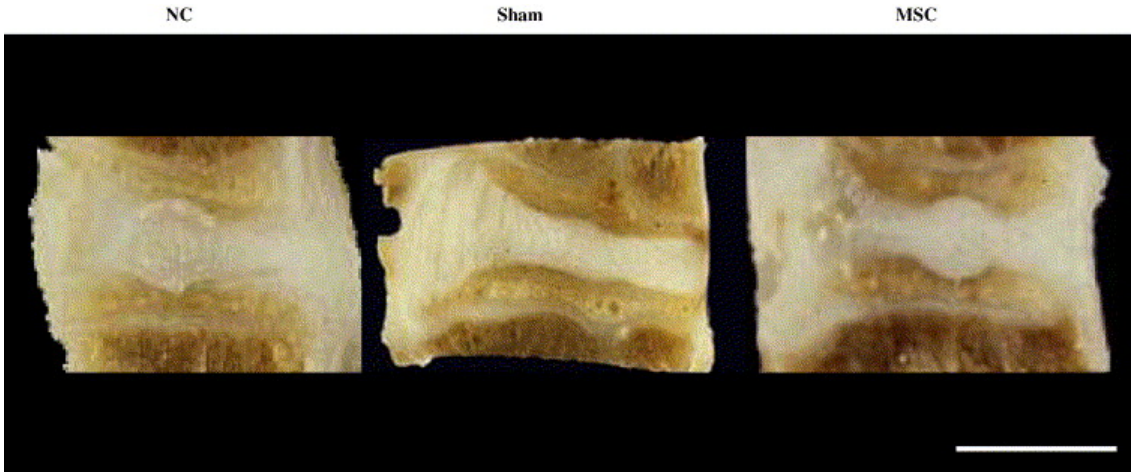

Figure 2. 5: Normal rabbit IVD, sham operated disc, MSC transplanted disc(left-right) [123].

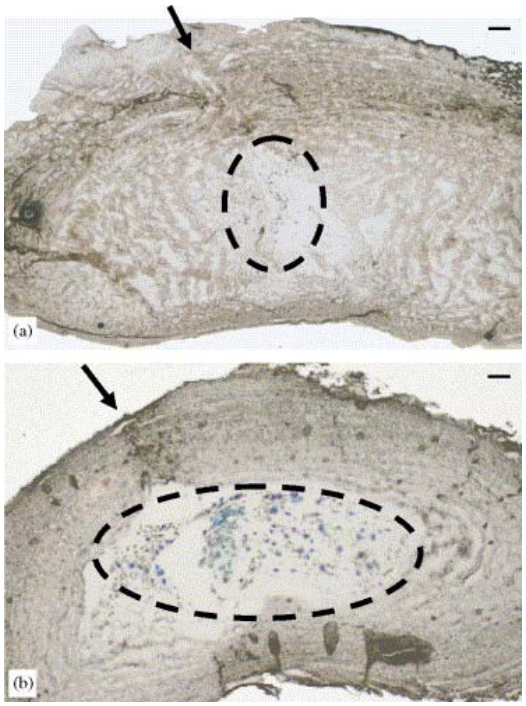

Figure 2. 6: MSCs transplanted (arrow shows injection site) into the NP region at 2 weeks (a), and at 24 weeks (b) with circled region showing increased cell viability and expansion at 24 weeks [123].

Autologous cells would likely be approved clinically as immune rejection would not pose a threat. Recent success has been shown in this field as injected autologous cells have reduced pain and maintained disc height [130]. Autologous disc chondrocyte transplantation (ADCT) is a procedure where patients' own cells are transplanted into the disc region 12 weeks after a discectomy [130]. A large scale, multicentered, randomized clinical trial called *EuroDisc* evaluated the effectiveness of ADCT [130]. Two years after ADCT, patients showed a decrease in pain, with a significant increase in PG and fluid content as compared to patients who underwent discectomy alone [130]. The study was considered a success as one of the primary goals for IVD tissue engineering is to eliminate patient pain.

Cell therapy and injection based methods may have limitations because cell leakage could occur after injection [131]. Also, injected cells must be able to remain viable *in vivo* under high pressure and also must produce ECM to help increase disc height. This may prove very difficult without the use of a biomaterial carrier for initial mechanical support [132]. Another disadvantage for biomaterial-free methods is the inability to support *in vivo* biomechanical forces during tissue regeneration [125]. Autologous cell based approaches are not efficient as they require multiple operations to retrieve the cells and then implant the expanded cells back. The use of autologous cells also appears to be an expensive and time costly procedure. Using allogenic transplantations may allow stem cells to be expanded *in vitro* to create a steady supply of on demand cells for therapy. Stem cell lines may also be readily accessible, but their future use clinically remains in doubt due to a lack of understanding and possibility of tumor growth.

2.5.2 Signaling Molecule Based Therapy

Different signaling molecules are also being investigated as therapeutic strategies for the treatment of disc degeneration. Molecular therapy offers a way to reduce disc degeneration and possibly prevent or reverse the entire process of degeneration. If signaling molecules were to be used alone, they would have to be injected into the degenerated portion of the disc using a needle. Using multiple molecules to signal more than one cell activity may be more effective than using a single signaling molecule [70], as each of these molecules may play a specific role in allowing the IVD to regenerate [70]. Table 2.2 summarizes signaling molecules, and whether they function as mitogens or

chondrogenic morphogens. Certain signaling molecules can decrease the inflammatory response and therefore protect the disc from further degeneration. Signaling molecule therapy to regenerate the IVD may prove to be an especially important therapy in early stages of disc degeneration, where disc structure has not yet been compromised.

Table 2. 2: Different categories of therapeutic molecules for the IVD. [70]

Category	Molecule
Mitogens	IGF-1, PDGF, EGF, FGF
Chondrogenic Morphogens	TGF-β, BMP-2, BMP-7 (OP-1), BMP-13 (GDF-6, CDMP-2), GDF-5 (CDMP-1)

Signaling molecules and their expression patterns in the normal IVD are essential to understand the differentiation of IVD cells. Signaling molecules bind to specific receptors, activating signaling responses to control cell behavior [133]. Signaling molecule therapy explores the idea that different signaling molecules may work together to allow tissue remodeling. In addition to the use of signaling molecules, matrix is continuously synthesized and degraded in the IVD, which provides the opportunity to use enzymes and inhibitors to increase matrix synthesis or slow degradation.

Signaling molecule therapy may be a viable strategy for promoting the restoration of native disc matrix. Mitogens are molecules that help cells proliferate or increase the rate of mitosis. It has been shown that mitogens, such as insulin-like growth factor-1 (IGF-1), epidermal growth factor (EGF), and fibroblast growth factor (FGF), increase the rates of disc cell mitosis [70]. It also demonstrated that some mitogens, such as IGF-1 and PDGF, also upregulate PG synthesis [134]. Further, some mitogens such as PDGF and IGF-

1 have proven to help preventing the apoptosis of AF cells [135,136]. Chondrogenic morphogens can differentiate cells to express a chondrocytic phenotype instead of a fibrotic phenotype. Transforming growth factor-β (TGF-β), bone morphogenic proteins (BMPs), and growth and differentiation factors (GDFs) are molecules characterized as chondrogenic morphogens. The synthesis of type II collagen, Sox9, aggrecan, and GAGs is associated with chondrogenic morphogens as well [70]. Of these molecules, TGF- β1 was found to best maintain IVD chondrocyte viability [137]. Some chondrogenic morphogens, such as TGF- β1, are able to increase disc cell proliferation and PG synthesis [138], and in the meantime to decrease the activity of MMP-2, which slows disc degeneration [138,139]. Some chondrogenic morphogens, such as bone morphogenic protein (BMP-7), also called osteogenic protein-1 (OP-1), can increase the synthesis of multiple disc matrix proteins, such as PG, aggrecan, and type II collagen [140-142]. Figure 2.7 demonstrates that OP-1 significantly increased the production of PGs [142]. Because that, BMP-7 has the therapeutic role to aid the regeneration of the NP after injection and increase disc height [143,144]. Interleukin-1 (IL-1) and MMPs have been found in degenerated discs, all of which increase matrix degradation [60,71,72,75,145]. Therefore, activities of IL-1 and some MMPs should be inhibited to stop disc degeneration [146,147]. BMP-7 inhibits the inflammatory cytokine IL-1 and prevents the matrix degradation while increasing matrix synthesis [148].

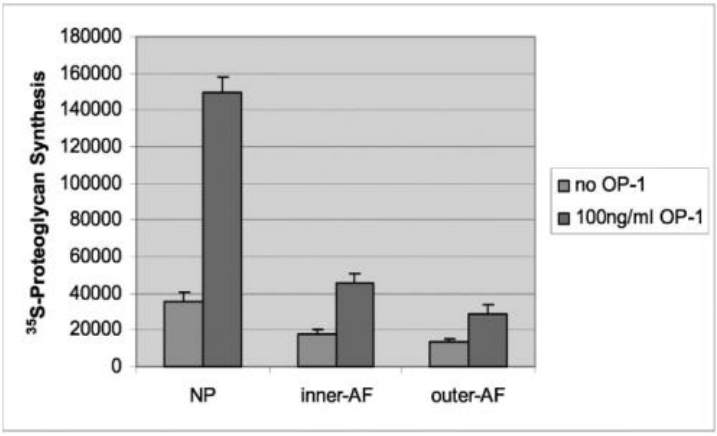

Figure 2. 7: PG content in the NP was significantly greater than the other IVD regions when treated with BMP-7. All regions showed significant difference in PG content when treated with BMP-7 when compared to controls [142].

Many different signaling molecules have been implicated in IVD regeneration. BMP-2 provides evidence of a natural affinity to increase cellular differentiation towards a chondrocytic phenotype because it increases the expression of aggrecan, a PG, and type II collagen. BMP-13, also called GDF-6 or cartilage-derived morphogenetic protein-2 (CDMP-2), has also proven to increase PG synthesis, though less effective than BMP-2. GDF-5, also called CDMP-1, which has been found in precartilaginous development of long bone formation, has worked better than TGF- β1, IGF-1, and FGF in restoring disc height in experiments. Similarly, FGF has shown to increase matrix production throughout the disc [70,138,149]. Walsh et al. have also analyzed the efficacy of different signaling molecules, including GDF-5, IGF-1, FGF, and TGF-β1, for IVD regeneration [150]. Cell population increased in the NP and inner AF in response to GDF-5 while the NP of TGF-β1 treated discs also showed evidence of cell aggregates, suggesting that GDF-5 and TGF-β1 promote disc regeneration [150]. As many signaling molecule based studies

have not provided concrete evidence, more thorough examination on the effects of each biomolecule is needed.

Cell and biomolecule based therapies will likely only be successful at the beginning stages of disc degeneration, before the disc composition and morphology have changed dramatically [126]. Drawbacks to growth factor therapy are that the degenerated portion of the disc cannot be removed and the disc height is not increased initially. Another major downfall is the biomolecules' short half-life [151]. If signaling biomolecule based therapy is to be successful, it should be coupled with a biomaterial carrier in order to avoid biomolecule denaturation. These biomolecule should have a temporal release profile in order to control the release amount. The ideal biomaterial could release desirable biomolecules into the IVD to promote successful tissue regeneration while also increasing the disc height and mechanical stability. One example using biomaterial to assist biomolecule based strategy is incorporating platelet-rich plasma (PRP) into gelatin microspheres, which allows injection of the material into the NP [152]. PRP contains many signaling molecules that have been implicated to promote IVD tissue regeneration, while improving PG synthesis in the IVD (Figure 2.8) [152,153]. These gelatin microspheres served as a delivery vehicle to enable the sustained release of growth factors from the PRP to promote tissue regeneration as the gelatin degrades [152].

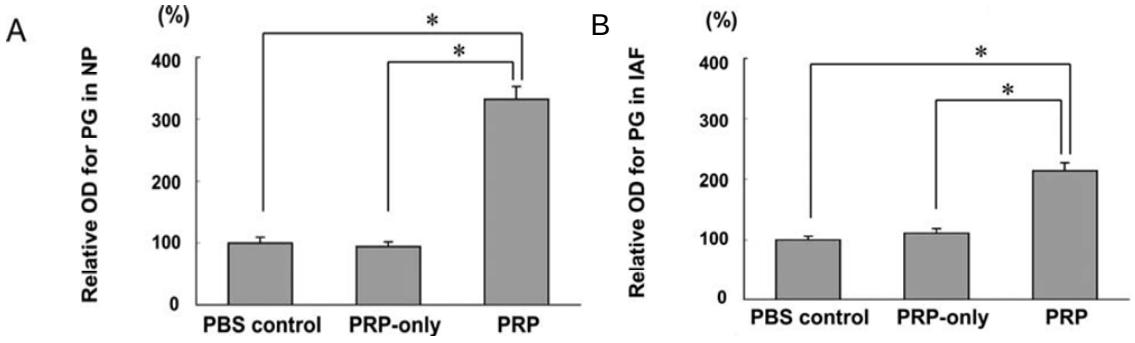

Figure 2. 8: Optical density of PGs in the NP (A), and AF (B) showing that discs treated with PRP loaded gelatin microspheres showed a much higher presence of PGs in the NP and AF as compared to control groups and PRP-only groups [152].

2.5.3 Hydrogels

Biomaterials that crosslink and gel upon injection into the desired site may show promise in the application of IVD regeneration. Injectable biomaterials are important because they are less invasive than most conventional surgical techniques. Hydrogels, which are in this class of injectable biomaterials, absorb large quantities of water and will facilitate disc regeneration by acting as a temporary scaffold and increasing hydration while aiding nutrient transport. They can also serve as a carrier or delivery vehicle for cells and signaling molecules. These materials, however, may only aid in the regeneration of the NP as the materials are physically and mechanically most similar to this portion of the tissue. IVD cells in some hydrogels will take on a natural rounded morphology, similar to that in the NP. Replacing the degenerated NP with hydrogels is an attractive method for NP regeneration. As recently as 2005, the FDA has proposed the use of more non-invasive therapeutic strategies to prevent disc degeneration, such as hydrogel injection into the NP [154,155]. Most of the hydrogels currently under investigation are

liquids at the time of injection, and undergo a gelation process after injection [123]. Many hydrogel materials may be used for IVD tissue engineering.

Different hydrogel materials have been developed to mimic the NP of the natural IVD [11]. Baer et al. used an alginate hydrogel to preserve the IVD cell phenotype. The IVD cells seeded in alginate demonstrated enhanced production of PGs, collagen types I & II, keratin sulfate, and chondroitin sulfate, all of which are constituents of the native disc [27]. However, the alginates anionic traits may prevent the formation of collagen into its natural fibrillar structure. Chondrocytes cultured in agarose gel maintained a collagen and PG structure comparable to that of natural cartilage [27].

Collagen hydrogels are attractive as they are constituents of native disc tissue. NP replacement with collagen gels has proven to restore disc height with advantageous mechanical properties in bovine animal models [156]. Also, collagen type I gels have proven to promote IVD cell proliferation while also expressing both anabolic and catabolic genes, signifying matrix synthesis and degradation, respectively [125]. These 3-D gels were used to determine how cyclic strain and hydrostatic pressure affected cell behavior [125]. Cyclic strain at a physiologic frequency of 1 Hz increased anabolic expression of collagen type II and aggrecan while also decreasing catabolic expression of MMP-3 [125]. Hydrostatic pressure increased expression of collagen I and aggrecan while it decreased expression of MMP-2&3 [125]. Therefore, moderate mechanical loading may aid in matrix synthesis while also decreasing matrix degradation [125]. Collagen hydrogel has already been used to regenerate cartilage clinically [157]. Collagen gel promotes IVD cell viability and the production of native matrix to prevent a significant loss in disc

height [158]. Furthermore, collagen hydrogels loaded with MSCs helped preserve the NP and the structure of the AF in animal models, allowing for enhanced disc regeneration as compared to collagen alone [123]. Some researchers are also investigating type II collagen hydrogel for IVD regeneration. Type II collagen is the dominant collagen type in native NP tissue and support NP cells very well. However, type II collagen degrades rapidly and only last for 2-3 weeks, which is not sufficient time to allow functional matrix to be synthesized to support physiologic loading [123,154]. Most current studies on collagen gel are only focus on the regeneration of one region of IVD tissue [158]. A better strategy would be using heterogeneous hydrogel for the regeneration of different regions of IVD tissues.

Hyaluronan (HA) gel is another material often used in IVD regeneration because it is a natural component of the native disc matrix, as well as because it increases the water content within the scaffold to enhance the discs load bearing capacity [93,159,160]. Injectable HA hydrogels have proven to prevent fibrotic tissue formation after removal of the NP in pig animal models [161]. In one study, viscous HA hydrogels were used as biomaterial carriers for the delivery of MSCs into rat coccygeal discs [91]. Four weeks after injection, cell viability increased [91]. However, after 4 weeks, the discs treated with the MSC therapy did not show a significant difference from the sham operated animals [91]. This may be because sufficient matrix was not produced.

Chitosan hydrogel has been proposed to serve as a NP replacement [162]. Chitosan is especially attractive for IVD regeneration as it has shown to promote chondrocyte attachment and proliferation while having similar properties to extracellular matrix

(ECM) in native cartilage [163-166]. Chitosan has the ability to self associate or form covalent cross links, which enables a more complete hydrogel network. This type of crosslinked hydrogel allows time for cells to manufacture ECM since polymer degradation time is increased. Chitosan hydrogels can enhance the viability of chondrocytes and aid in an increase of aggrecan synthesis [52]. Cationic chitosan may be an ideal biomaterial hydrogel to use as a replacement for the NP portion of the IVD because it may aid in the attraction of anionic aggrecan molecules [52]. This attraction would allow for the possible accumulation of PGs and subsequently an increase tissue hydration. In one particular study, lower molecular weight chitosan (2.5% Protasan UP G213) exhibited superior cell viability compared to higher molecular weights [162]. Using 1% to 1.5% cationic chitosan hydrogels seeded with NP cells, roughly 80% of the synthesized PG content was retained in the hydrogels [52].

Synthetic hydrogels can be manipulated to provide different mechanical properties depending on their application. Some of the synthetic hydrogels used in IVD regeneration include polyethylene glycol (PEG), polyvinyl alcohol (PVA), polyvinyl pyrrolidone (PVP), and polyethylene oxide (PEO)-polypropylene oxide (PPO). PEG hydrogels have been used as biomaterial carriers to deliver MSCs into the NP in rat spines while maintaining cell viability [167]. PVA/PVP hydrogels have also been developed to serve as minimally invasive, injectable NP replacements [168]. However, no evidence was provided proving the ability of a PEG hydrogel to withstand loading or aid in matrix retention while the PVA/PVP materials have not been proven to produce cell morphology similar to the native NP [167,168]. Pluronic F-127 , a PEO/PPO copolymer hydrogel allowed

the synthesis of cartilage tissue, however, it cannot retain its initial shape and is unsuitable for mechanical loading.[169] Although few synthetic hydrogels are currently investigated for NP applications within the IVD, many synthetic biomaterials are being developed to mimic the AF structure which will be discussed later.

Currently, most studies on hydrogels for IVD applications are focusing on natural based materials. Although synthetic materials and their properties are easier to control, natural hydrogels provide a better environment to mimic the NP of a disc implant. One issue with injectable hydrogels is their propensity to leak out of the injection site before completely curing/gelling. Because hydrogels are mostly used to mimic the NP, other biomaterial structures are investigated to better recreate the overall structure of the AF and the native disc as a whole.

2.5.4 Biomaterial Scaffolding

A variety of solid biomaterial scaffolds have been investigated for IVD tissue regeneration. Because fibrochondrocytes may require chemical and mechanical signals in order to function and regenerate normal IVD tissue, scaffolding that has the ability to support physiologic loading is desirable [170]. Given the unique structures of IVD tissue at different regions, it is important for scaffolding constructs to accurately address the structure and composition characteristics of each region. More specifically, the NP and AF structures need to be better mimicked to provide direction and guidance for cell alignment and matrix deposition.

Annulus Fibrosus Scaffolding

Many different polymeric biomaterials have been used in attempts to regenerate the AF. PLA, PGA, and the copolymer PLGA appear attractive for tissue scaffolds because suture products based on these materials have been approved by the FDA for human use [171]. However, PLA and PGA alone are problematic for IVD applications because they are hydrophobic and do not promote cell adhesion [172]. Therefore, they are often combined with other materials to enhance cell responses. Examples of these types of materials include small intestine submucosa (SIS), demineralized bone matrix (DBM), and gelatin, which have been combined with PLGA to improve cell attachment and growth [171,173]. Another downside to the use of PLA, PGA or its copolymers is that their acidic degradation products elicit an inflammatory response [171].

SIS is an acellular material containing 80-90% oriented collagen fibers, GAGs, and growth factors, including bFGF, VEGF, and TGF-β [174,175]. Biodegradable SIS scaffolds improve PLGA materials for IVD applications as they allow incorporation of growth factors to increase metabolic activity and matrix production of cells [176]. Further, positive gene expression proved that acellular SIS materials promoted ECM and GAG production (Figure 2.9) while improving cell migration into the material after 1 month [176,177]. Also, SIS resorbs in 3 months, which is beneficial for IVD tissue regeneration as it allows time for the synthesis of ECM while supporting biomechanical loadings. However, a downside to SIS is that it has a rough and smooth side, and cells cannot attach to the smooth side [178].

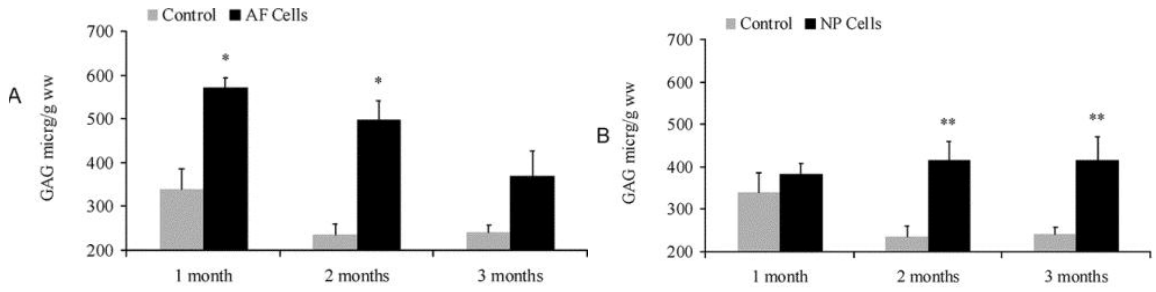

Figure 2. 9: SIS cell seeded scaffolds show significant increase in GAG content in AF (A), and NP (B), as compared to non seeded scaffolds in vitro. *p< 0.001, **p< 0.01.[176]

Studies investigating cell attachment for IVD scaffolds have proven the ability of DBM and gelatin to promote cell attachment as compared to PLA alone (Figure 2.10) [173]. Materials similar to DBM, such as Bioglass®, were also incorporated into an IVD scaffold. 3-D PLA foams composed of 0, 5, and 30 wt% Bioglass® particles were tested to determine the constructs ability to satisfy the requirements for a tissue engineered IVD [179]. The 30% Bioglass®/PLA composites increased cell proliferation and exhibited significantly higher GAG and collagen production as compared to PLA alone [179]. One downside to the use of DBM and Bioglass® materials, though, are the materials compliance and rigidity. This becomes an issue as the scaffold may not have the ability to absorb loads *in vivo*. Also, these biomaterials may not be able to be easily implanted, since they are not elastic enough to be press-fitted into the void disc space.

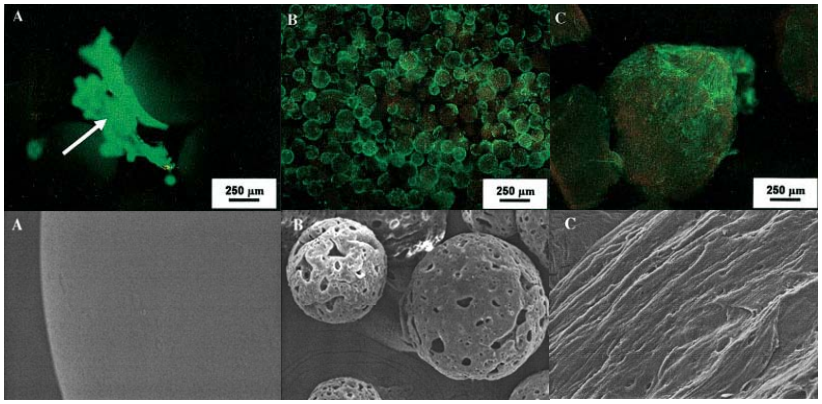

Figure 2. 10: <u>Top</u>: LIVE/DEAD imaging of cells on PLA (A), gelatin (B), and DBM (C) scaffolding with diameters of 0.7-1.1 mm, 100-150 µm, and 1-2 mm, respectively. <u>Bottom</u>: SEM after 1 month of culture showed that PLA was smooth (A), gelatin had interconnected pores (B), while the DBM consisted of an oriented structure (C) [173].

Other degradable polyesters besides PLA and PGA, such as polycaprolactone (PCL), have also been combined with DBM to increase cell attachment. A scaffold with an outer DBM region and oriented layers of PCL in the inner region was used to recreate the AF structure (Figure 2.11) [180]. The use of DBM improved the compressive and tensile strength of the scaffold [180]. However, this scaffold only mimics the AF region, and does not attempt to incorporate an integration within the scaffold for a NP region. Although cells infiltrated the scaffold and produced matrix, they did not elongate and align in an organized fashion like the native tissue (Figure 2.12) [180]. Also, as seen in previous studies, the biomechanical properties of the scaffolding construct are not elastic and do not match those of the native tissue.[180]

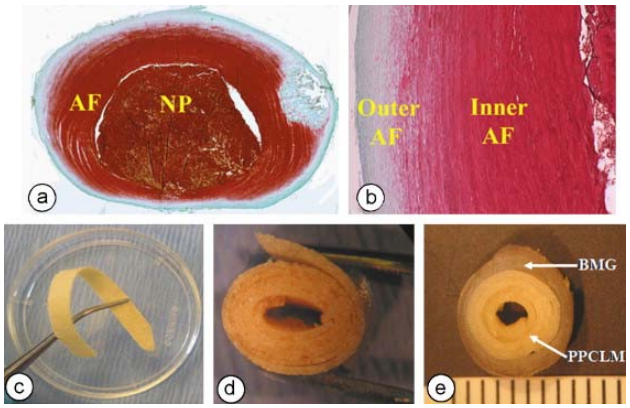

Figure 2. 11: Safranin-O staining of normal rabbit IVD (a,b). PCL scaffold fabrication technique showing concentric layers of scaffolding [180].

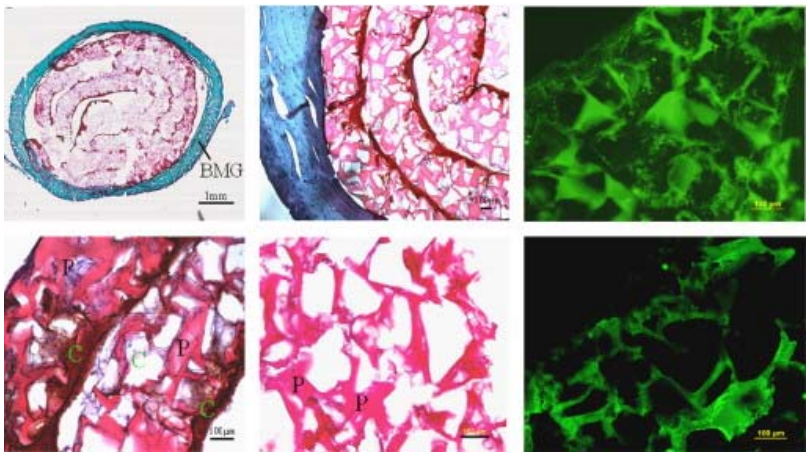

Figure 2. 12: Scaffolding at different magnifications using safranin-O staining (P: PCL, C: Chondrocytes), and collagen type II fluorescent staining (right top: cells/scaffold, right bottom: control scaffold) after 4 weeks culture [180].

PCL alone has also shown success in emulating the organized collagen fibers in the native AF. For instance aligned PCL nanofibers have been bundled together in order to create a single lamella with 1 mm thickness [181]. AF cells seeded onto these PCL bundles oriented in alignment with the fibers and synthesized matrix [181]. Though this scaffold provided accurate 3-D microstructure of a single lamellae, this technique needs

to be improved by fabricating multiple lamellae within the same scaffold to accurately mimic the native tissue architecture [181].

As can be seen, there have been many materials and structures that have been investigated for AF tissue regeneration, yet there has been little evidence of how these materials will integrate with the vertebrae. Takahata et al developed a 3-D polymer fabric (3-DF), mimicking the shape of the IVD, which was composed of UHMWPE and coated the top and bottom surfaces with hydroxyapatite bioceramic granules in hopes of promoting vertebral body ingrowth. Animal studies using this 3-DF have demonstrated bone growth into the construct, as well as firm fixation to the vertebral body [182]. 3-DF/UHMWPE discs resisted fatigue and their mechanical properties remained constant after 2 million cycles of dynamic loading, proving the materials durability [183]. One problem with this scaffold design, though, is that it was too rigid and did not accurately replicate a biphasic NP and AF region.

Nucleus Pulposus Scaffolding

As mentioned above, many materials have been extensively used for AF tissue engineering applications. Some of these same materials have also been used as NP scaffolding materials. For example, PLGA (70:30) scaffolds were used to regenerate the NP tissue using a canine animal model [83]. Evidence of tissue regeneration by chondrocyte type cells and increased ECM was observed after scaffolds completely degraded at 4 weeks [83]. Similarly, a NP replacement composed of biocompatible and incompressible polycarbonate urethane has shown to sustain biomechanical loading to maintain disc

height after a discectomy [184]. The material consists of a memory coiling spiral which can roll into shape after being implanted into the region of the removed NP (Figure 2.13) [184]. A drawback to the use of polycarbonate urethane is that the AF must be intact and healthy to support spinal loads [184]. However, because these materials are not injectable, they may damage the AF, which may lead to further disc degeneration. Therefore, a material for NP regeneration combined with other scaffolding materials used in AF tissue engineering is a more attractive idea to mimic the biphasic IVD composition.

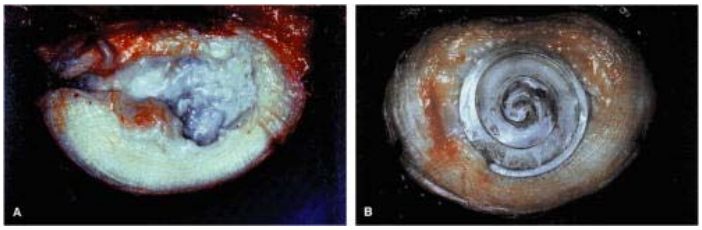

Figure 2. 13: Human cadaveric IVD after NP removal (A), and after implantion of memory coiling spiral in the NP (B) [184].

<u>Biphasic IVD Scaffolding</u>

It has been shown that a variety of materials have been used to emulate one region of the IVD. However, these materials can be used in conjunction in order to create composite structures that mimic the biphasic structure of the natural IVD and simultaneously reproduce NP and AF tissue. Composites that use polymers such as PGA or PLGA to mimic the AF, and alginate to mimic the NP have been developed [185,186]. In one design, a radically oriented PGA mesh combined with an alginate hydrogel has been formed into a composite to emulate the AF and NP, respectively. Each of these materials maintained their distinct regions after 4 months implantation (Figure 2.14) [185]. Also, this scaffold allowed for newly formed NP and AF tissue, which possessed a high intensity

safranin-O staining after 12 weeks *in vivo*, proving the formation of cartilage tissue [186]. Further, the GAG content and compressive modulus of the PGA-alginate scaffolds increased to values similar to native mice IVD levels (Figure 2.15) [185]. In another study, PLGA and alginate scaffolds had similar morphology and composition, as well as the structure of newly formed tissue, to that of the native tissue [186]. One limitation of these particular scaffolds, however, is that the AF region of these materials was not as lamellar and organized as the native tissue [186]. Another downside to the use of PLGA or PGA with alginate is that the mechanical properties are not as similar to human IVD tissue, which is necessary for IVD tissue engineering [185].

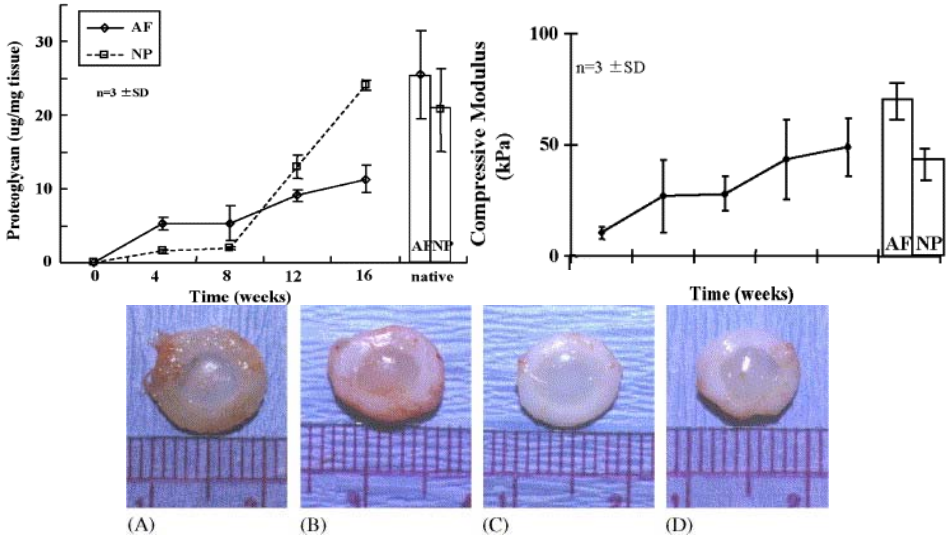

Figure 2. 14: Top: Both regions of the scaffold encouraged GAG synthesis similar to native tissue in mice (left), while the modulus of the scaffolds also increased over time to reach values similar to native tissue. Bottom: PLA/PGA and alginate scaffolding before implantation (A), and implanted for 4 weeks (B), 8 weeks (C), and 16 weeks (D) showing two distinct IVD regions.[185]

Like alginate, hyaluronan (HA) hydrogels have also been combined with PGA scaffolds. Absorbable PGA scaffolds have been combined with fibrin-HA solutions,

containing expanded human IVD chondrocytes, and formed IVD-like tissue after 2 weeks in culture [160]. *In vitro*, IVD cells assembled in 3-D on these scaffolds, while passing necessary biocompatibility requirements and showing no decrease in cell viability as observed by LIVE/DEAD staining (Figure 2.15) [160]. Also, collagens and GAGs were produced in 3-D culture, on the PGA fibrin-HA materials, however, a more fibrous tissue was formed, as collagen type I expression was greater than collagen type II expression [160]. This response was unwanted as collagen type II is more desired in a healthy disc regeneration. To expand on the use of PGA and HA, certain groups have used cell free nonwoven PGA-HA resorbable scaffolds and immersed them in serum containing growth factors in order to attract cells and induce IVD regeneration in rabbit models [159,187]. After 12 months of implantation, the animals with the scaffold treated discs exhibited extensive infiltration of ECM proteins, such as PGs and collagen type II, allowing for an enhanced disc height as compared to the controls. This study proved that long term success of PGA-HA materials is possible as chondrogenesis was observed, with an increase in PG and water content (Figure 2.16) [159,187]. Also, the ECM synthesized had a similar composition to native tissue and were resorbed completely between 40 and 60 days with a 50% loss of mechanical integrity after 7 days [159,187].

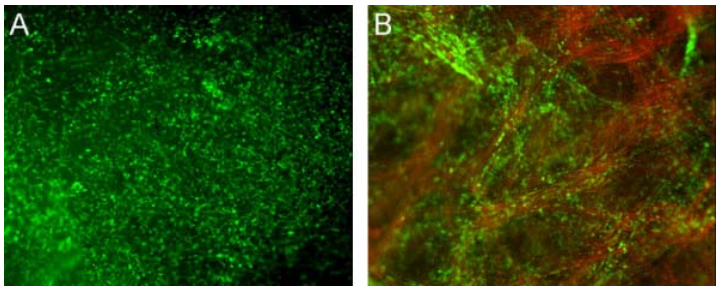

Figure 2. 15: LIVE/DEAD staining of the cells within the PGA fibrin-HA scaffold at 1 (A) and 2 (B) weeks. It can be seen in B, that live cells migrated into a more 3-D pattern. The red seen in part B is a staining of the PGA fibers [160].

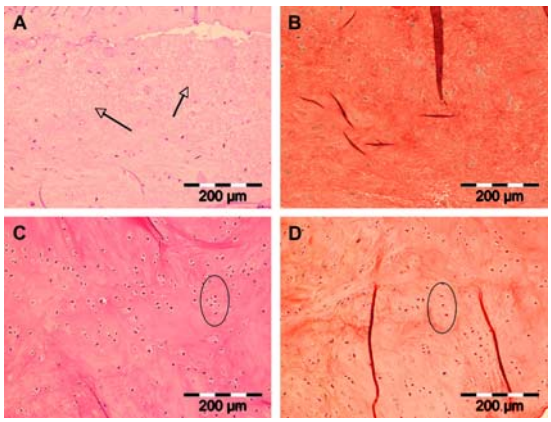

Figure 2. 16: H&E (A,C), and Safranin-O (B,D) staining 12 months after a discectomy (A,B) or PGA-HA treated materials(C,D) showing increased cellular infiltration (circles) in the implant treated discs and tissue necrosis (arrows) in the controls [187].

It has been shown that HA may be an effective hydrogel for IVD regeneration when combined with appropriate scaffolds. For this reason, biphasic biodegradable PLA nanofiber scaffolds consisting of an HA center have been tested [103]. The electrospun nanofibers resemble the native lamellar structure of the AF [103]. During culture, cells in the PLA-HA construct elongated and aligned in a concentric fashion on the nanofibers while also increasing secretion of GAGs and other ECM content, as evidenced by H&E

and alcian blue staining (Figure 2.17) [103]. PG staining with alcian blue showed no distinct organization within the NP while the AF has a more organized structure, mimicking native IVD tissue architecture (Figure 2.17) [103]. One issue with the scaffold, though, is that it does not support necessary biomechanical loads [103]. The PLA fibers should also be more aligned in the periphery of the construct to better mimic native disc tissue.

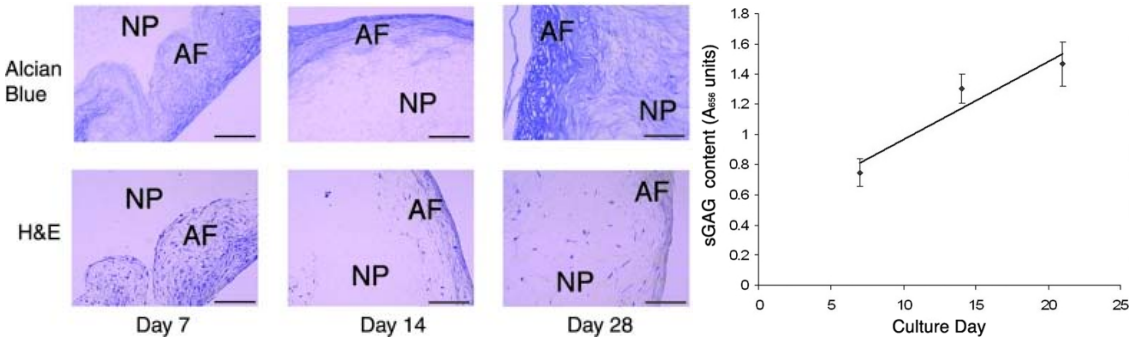

Figure 2. 17: Left: Staining of PLA/HA scaffold showing increase in cellularity and PG content in both the AF and NP over 28 days. Right: Quantitative assay showing increase in GAG synthesis over time [103].

Natural polymers, such as collagen type I have also been used in conjunction with hydrogels in order to create a biphasic IVD scaffold. In one study, a HA hydrogel surrounded by collagen type I, at a ratio of 9:1, was used to make a composite scaffolding material, which promoted growth and attachment of functional IVD cells for 60 days in culture [137]. PGs including aggrecan, decorin, biglycan, fibromodulin, and lumican as well as collagen types I & II all accumulated on the scaffold, showing that cells were synthesizing matrix similar to that of the native IVD [137]. The synthesized biomolecules, however, were not consistently retained within the scaffolds and often escaped into the

culture media [137]. For this reason, this particular biphasic construct is not effective, as the materials should retain and organize matrix molecules into functional ECM in order to properly function as an IVD scaffold.

As evidenced by previous studies, mechanical properties of IVD scaffolds are far from satisfactory. Suitable mechanical properties can be achieved, however, with the proper design and materials. One group, Gloria et al, created a scaffold with mechanical properties that were very similar to those of the natural IVD[122]. The scaffold consisted of poly (2-hydroxyethyl methacrylate)/ poly (methyl methacrylate) (PHEMA/PMMA) (80/20 w/w) hydrogel combined with poly (ethylene terephthalate) (PET) fibers [122]. The scaffolds showed a J-shaped stress-strain curve similar to most soft tissue, and did not experience signs of fatigue under dynamic loading [122]. Furthermore, acrylate materials can maintain a desirable water content of about 75wt% which is comparable to natural IVD water content [188]. Although the PHEMA/PMMA/PET construct showed superior mechanical properties as compared to other biomaterial structures, and is assumed to be biocompatible, no data was provided to prove the scaffolds ability to support cell growth and direct matrix synthesis [122]. Further evidence may show that this material construct might be ideal for IVD regeneration.

2.6 Animal Modeling

In order to evaluate the effectiveness of the strategies developed for IVD tissue repair and regeneration, it is important to use appropriate animal models. Also, because the complete process of disc degeneration is not well understood in humans, animal

models have become increasingly important. Animal models can help determine cause and effect relationships of different factors that may relate to disc degeneration. For the purpose of creating a degenerated disc, induced injury can imitate a degenerated disc [84]. Different methods have been used to simulate IVD degeneration with most models using spines and tails [84]. Results from animal studies have suggested that abnormal mechanical loading conditions lead to symptoms of a degenerated disc. Using induced degeneration in animal models, therapeutic strategies for IVD regeneration can then be evaluated for success. If successful in smaller animals, tissue engineered strategies can be further tested in larger animals that better mimic nutritional, biomechanical, and surgical applications in humans [189].

Rodent models are necessary to establish the initial success of an IVD treatment strategy. Rodent models help determine whether or not a specific regenerative therapy is promoting a desired cellular response. In order to evaluate treatment, degeneration must be induced. Research has proven that compressive forces can induce degeneration using *in vivo* mouse tail models [190]. Degeneration can also be produced by using a needle to puncture the IVD [189]. After induced degeneration, rat models have been used to test regenerative based growth factor therapy by evaluating changes in PG content and changes in disc morphology.

Small animal models, such as rabbits, are used when strategies have proven successful in rodent models. Kroeber et al used axial mechanical loading on an *in vivo* rabbit model to produce a degenerated disc (Figure 2.18) [26]. This method is the first method where disc degeneration was induced and then treatment methods were evaluated

in vivo [26]. Rabbits spines that were mechanically loaded for 14 and 28 days exhibited a significant decrease in disc height, as well as an outer AF structure that became disorganized, proving that compression simulated IVD degeneration. PGA implants were then tested in the animals with degenerated discs [26]. Abbushi et al were the first to remove the degenerated disc, using open surgery microdiscectomy, on rabbit animal models to test their implanted materials [159]. This method is advantageous over other techniques as it is a more destructive resection of tissue, better simulating the clinical environment [159].

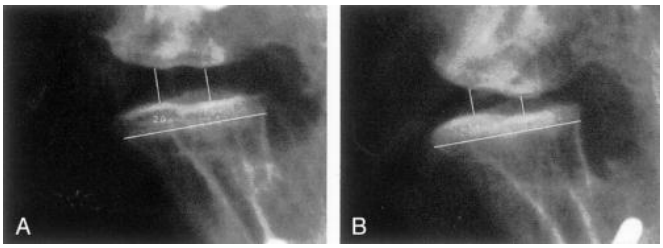

Figure 2. 18: Rabbit animal model of IVD after dynamic compressive loading for 28 days showed significantly less height (B) than normal (A) [26]

One inherent problem with modeling human IVDs is their size compared to animal models. Human IVDs are much larger than most rodents and smaller animals, and therefore transport of nutrients and wastes is much more difficult in human IVD [84]. For this reason, more expensive, larger animal models (canines, sheep, porcine, goats) are necessary for *in vivo* studies as diffusion of nutrients to cells in these larger models more accurately mimics human IVD circumstances. Canine spines under large compressive loads have been used to model disc degeneration [191]. Degeneration in sheep and goat

animal models has also shown to be advantageous for potential therapeutic strategies as their IVDs are similar in size to humans, and their tissue does not naturally repair [192,193]. Researchers have also investigated porcine models by promoting degeneration and then evaluating the effectiveness of a hydrogel containing stem cells to promote viability and differentiation towards a chondrogenic phenotype [194].

Animal modeling in its later stages needs to be geared more towards better mimicking a human spine size and biomechanics. The spines and IVD structures of primates is highly similar to humans [126]. Also, because primates are bipedal, the forces acting on their spines better mimic human loading conditions [126]. Although primates may be essential for studying IVD regeneration strategies in the future, to date most researchers have not used primates as models because of ethical issues and high costs.[189]

2.7 Mechanical Properties

Since animal studies have shown that compressive forces can induce degeneration, it seems there may be a correlation and a limit to the loads the IVD can support before experiencing degeneration. The ECM of the IVD consistently bears loads in the body, and these loads can be assumed to be primarily compressive [195]. The IVD is a viscoelastic tissue having time dependent responses to loading and experiences nonlinear, anisotropic behavior [84,181]. Therefore, static and dynamic compressive tests can be used as preliminary indicators for the behavior of devices and biomaterial structures for potential spinal disc applications.

Disc cells are influenced by a variety of mechanical factors such as mechanical stress, and osmotic pressure [27]. Mechanical influences that affect disc cell behavior include static compression, hydrostatic pressure, and tensile stretch. Each of these external stimuli changes the assembly of PGs, and collagen within the IVD. Atypical loading on a healthy disc can cause cellular alterations within the disc, which may be characteristic of a disease state [51]. Though some evidence suggests that normal compressive spinal loads may encourage PG synthesis, loading may also alter the matrix composition by decreasing the matrix production and degradation, and decreasing cell activity [51]. Extensive mechanical loads may cause cell death, decreasing the amount of cells available to synthesize and turnover stable ECM molecules [196]. During extended or abnormal loading periods, the IVD may attempt to remodel to better support the loading, usually resulting in a degenerated disc [190].

Because mechanical loading can be both implicated and compromised in a degenerated IVD, it is important for biomaterial structure to have similar mechanical properties compared to healthy, native tissue. Mechanical integrity, especially under compressive stresses, is important for IVD implants and tissue engineered IVD tissues. The compressive modulus of the IVD varies in each region. In the AF, the compressive modulus has been reported to range from 0.116-2.3 MPa, while in the NP the compressive modulus has been reported to range from 0.003-0.31 MPa. Therefore, a tissue engineered construct should be able to withstand these loads with some safety factor involved. It has been stated that the Young's compressive modulus of IVD scaffolds should range from 0.5-5 MPa and the ultimate strength should be at least 8-10

MPa [11,38,197,198]. The NP and inner AF are deformed less during compression. Because each of the IVD regions contains different matrix molecules, the disc has varied mechanical properties in each region. In this regard, IVD implants and tissue engineered IVD tissues should have distinct mechanical properties in each region. Mechanical properties of IVD constructs need to be better characterized as the mechanical properties are important for the IVD functions. Dynamic and static compression tests are recommended for IVD constructs as the forces on the spine are primarily compressive [131]. However, for IVD regeneration using biomaterials, biomaterial structures should be able to temporarily support limited amount of spinal loads while promoting matrix synthesis, as the regenerating matrix will eventually bear the full spinal loads when the implanted biomaterial structure degrades.

2.8 Conclusion

Worldwide healthcare goals involve the restoration and maintenance of native IVD tissue to decrease its economic burden and impact. The degenerated spinal disc is one of the most expensive medical problems currently encountered today as it causes disability among many people in the aging population [130]. One major hurdle in creating a regenerative therapy for the IVD is that its structure is highly unique and has multiple distinct regions. The NP is a disorganized conglomeration of collagen type II and highly anionic PGs which help attract water to maintain the disc height. On the other hand, the AF consists of highly organized collagen type I based lamellar architecture which helps prevent bulging in the NP. The distinct structure of each region of the IVD enables the

disc to withstand the everyday dynamic forces placed on the spine. Both the AF and NP structures are avascular, meaning cellular nutrition is based solely on diffusion, and also making repair of the tissue difficult, inevitably resulting in age related disc degeneration.

It is important to understand disc degeneration prior to determining an effective therapy, since a researcher must know which factors are causing the degeneration in order to stop it. All of the exact causes of disc degeneration have not been identified, although a variety of factors have been implicated, including loss of biomechanical stability, poor nutrition, genetic factors, and an increase in degradative enzymes. Disc degeneration is accompanied by a decrease in viable chondrocytes and a loss in PG content within the matrix followed by dehydration. During IVD degeneration, the disc structure of the NP and AF are highly compromised leading to a fibrous and disorganized structure. As disc degeneration progresses, the discs ability to support biomechanical forces on the spine become compromised. Eventually, the disc becomes unstable, causing an extensive perceived pain by the patient.

Clinically, the only solutions to a patient's pain resulting from a degenerated disc are therapy, rest, and medication. If these treatments are unsuccessful, a patient may require the removal of the degenerated portion of the disc, spinal fusion, or an IVD implant. Removal of the degenerated tissue does nothing to stabilize the spine and causes problems relating to the decrease in disc height which leads to increased disc degeneration. A current solution to a disc removal is spinal fusion which stabilizes and restricts motion. However, fusion creates its own problems as it increases stress concentrations on adjacent discs, causing further degeneration. Therefore, the

replacement of degenerated or damaged IVD tissue with a permanent implant is an attractive alternative to spinal fusion. Current implants help restore patient mobility and disc height. However, these implants have their own faults. Current NP replacements damage the native AF upon implantation, causing an inflammatory response that will eventually promote further tissue degeneration. Total disc replacements also have problems in that they form wear debris and have a large compliance mismatch, leading to stress shielding on adjacent vertebral levels. Another disadvantage to current disc replacements is that they do not replicate physiological motion or promote natural tissue repair.

To improve upon current solutions, tissue engineered IVD structures are being developed to regenerate the native tissue. The necessity for the development of approaches to promote IVD repair and regeneration is evident in the fact that problems still exist with current therapies to disc degeneration. Researchers are currently investigating different therapeutic methods to promote IVD regeneration, including cell based therapies, signaling molecule based therapies, and biomaterial-based regenerative therapies. Cell and molecule therapies alone are unlikely to be effective as they will not be able to support *in vivo* spinal loads. Current NP hydrogel regeneration strategies are unlikely to be successful as they may damage the AF. Once the AF is compromised, some type of scaffold support structure will be necessary to support loads. Therefore, a biphasic structure mimicking both the AF and NP is more likely to have a long term impact in IVD tissue regeneration due to the inherent mechanical stability they would provide. These tissue engineered IVD structures should have a similar structure and

mechanical properties to that of the native tissue in order to properly integrate with the tissue and resist failure. Scaffolds also have the ability to be coupled with bioactive molecules in order to promote tissue regeneration or prevent an inflammatory response, while allowing for mechanical stability [133,199,200].

Tissue engineering is the future for the treatment of IVD degeneration. Conventional treatments for IVD degeneration do not meet the requirements to restore patient satisfaction. Due to the failures of current therapies and techniques to prevent and treat IVD degeneration, new methods are needed. Novel ideas are necessary to propel IVD tissue engineering forward, starting with a basic understanding of design criteria. Using previous successes and failures in tissue engineering, the regeneration of the IVD is an achievable goal.

2.9 References

1. Luo X, Pietrobon R, Sun SX, Liu GG, Hey L. Estimates and patterns of direct health care expenditures among individuals with back pain in the United States. Spine 2004;29(1):79-86.

2. Deyo RA, Tsui-Wu YJ. Descriptive epidemiology of low-back pain and its related medical care in the United States. Spine (Phila Pa 1976) 1987;12(3):264-8.

3. Shvartzman L, Weingarten E, Sherry H, Levin S, Persaud A. Cost-effectiveness analysis of extended conservative therapy versus surgical intervention in the management of herniated lumbar intervertebral disc. Spine (Phila Pa 1976) 1992;17(2):176-82.

4. Risbud MV, Albert TJ, Guttapalli A, Vresilovic EJ, Hillibrand AS, Vaccaro AR, Shapiro IM. Differentiation of mesenchymal stem cells towards a nucleus pulposus-like phenotype in vitro: implications for cell-based transplantation therapy. Spine 2004;29(23):2627-32.

5. Urban JP, McMullin JF. Swelling pressure of the lumbar intervertebral discs: influence of age, spinal level, composition, and degeneration. Spine (Phila Pa 1976) 1988;13(2):179-87.

6. Johnstone B, Urban JP, Roberts S, Menage J. The fluid content of the human intervertebral disc. Comparison between fluid content and swelling pressure profiles of discs removed at surgery and those taken postmortem. Spine 1992;17(4):412-6.

7. Urban JP, McMullin JF. Swelling pressure of the inervertebral disc: influence of proteoglycan and collagen contents. Biorheology 1985;22(2):145-57.

8. Ohshima H, Tsuji H, Hirano N, Ishihara H, Katoh Y, Yamada H. Water diffusion pathway, swelling pressure, and biomechanical properties of the intervertebral disc during compression load. Spine 1989;14(11):1234-44.

9. Wan Y, Feng G, Shen FH, Balian G, Laurencin CT, Li X. Novel biodegradable poly(1,8-octanediol malate) for annulus fibrosus regeneration. Macromol Biosci 2007;7(11):1217-24.

10. Columbia-Presbyterian Neurosurgery.

11. Setton LA, Bonassar L, Masuda K. Regeneration and Replacement of the Intervertebral Disc: Elsevier; 2007.

12. Leung VY, Chan WC, Hung SC, Cheung KM, Chan D. Matrix remodeling during intervertebral disc growth and degeneration detected by multichromatic FAST staining. J Histochem Cytochem 2009;57(3):249-56.

13. Cowan JA, Jr., Dimick JB, Wainess R, Upchurch GR, Jr., Chandler WF, La Marca F. Changes in the utilization of spinal fusion in the United States. Neurosurgery 2006;59(1):15-20; discussion 15-20.

14. Huang RC, Girardi FP, Cammisa FP, Jr., Lim MR, Tropiano P, Marnay T. Correlation between range of motion and outcome after lumbar total disc replacement: 8.6-year follow-up. Spine 2005;30(12):1407-11.

15. McAfee PC, Cunningham B, Holsapple G, Adams K, Blumenthal S, Guyer RD, Dmietriev A, Maxwell JH, Regan JJ, Isaza J. A prospective, randomized, multicenter Food and Drug Administration investigational device exemption study of lumbar total disc replacement with the CHARITE artificial disc versus lumbar fusion: part II: evaluation of radiographic outcomes and correlation of surgical technique accuracy with clinical outcomes. Spine (Phila Pa 1976) 2005;30(14):1576-83; discussion E388-90.

16. Shuff C, An HS. Artificial disc replacement: the new solution for discogenic low back pain? Am J Orthop 2005;34(1):8-12.

17. Bibby SR, Fairbank JC, Urban MR, Urban JP. Cell viability in scoliotic discs in relation to disc deformity and nutrient levels. Spine (Phila Pa 1976) 2002;27(20):2220-8; discussion 2227-8.

18. Yao H, Gu WY. Physical signals and solute transport in human intervertebral disc during compressive stress relaxation: 3D finite element analysis. Biorheology 2006;43(3-4):323-35.

19. Yao H, Justiz MA, Flagler D, Gu WY. Effects of swelling pressure and hydraulic permeability on dynamic compressive behavior of lumbar annulus fibrosus. Ann Biomed Eng 2002;30(10):1234-41.

20. Holm S, Maroudas A, Urban JP, Selstam G, Nachemson A. Nutrition of the intervertebral disc: solute transport and metabolism. Connect Tissue Res 1981;8(2):101-19.

21. Ohshima H, Urban JP. The effect of lactate and pH on proteoglycan and protein synthesis rates in the intervertebral disc. Spine 1992;17(9):1079-82.

22. Cassinelli E, Kang J. Current Understanding of Lumbar Disc Degeneration. Operative Techniques in Orthopaedics 2000;10(4):254-262.

23. Jahnke MR, McDevitt CA. Proteoglycans of the human intervertebral disc. Electrophoretic heterogeneity of the aggregating proteoglycans of the nucleus pulposus. Biochem J 1988;251(2):347-56.

24. Buckwalter JA. Aging and degeneration of the human intervertebral disc. Spine 1995;20(11):1307-14.

25. Kraemer J. Natural course and prognosis of intervertebral disc diseases. International Society for the Study of the Lumbar Spine Seattle, Washington, June 1994. Spine (Phila Pa 1976) 1995;20(6):635-9.

26. Kroeber MW, Unglaub F, Wang H, Schmid C, Thomsen M, Nerlich A, Richter W. New in vivo animal model to create intervertebral disc degeneration and to investigate the effects of therapeutic strategies to stimulate disc regeneration. Spine (Phila Pa 1976) 2002;27(23):2684-90.

27. Baer AE, Wang JY, Kraus VB, Setton LA. Collagen gene expression and mechanical properties of intervertebral disc cell-alginate cultures. J Orthop Res 2001;19(1):2-10.

28. Maroudas A, Stockwell RA, Nachemson A, Urban J. Factors involved in the nutrition of the human lumbar intervertebral disc: cellularity and diffusion of glucose in vitro. J Anat 1975;120(Pt 1):113-30.

29. Trout JJ, Buckwalter JA, Moore KC. Ultrastructure of the human intervertebral disc: II. Cells of the nucleus pulposus. Anat Rec 1982;204(4):307-14.

30. Lee CR, Sakai D, Nakai T, Toyama K, Mochida J, Alini M, Grad S. A phenotypic comparison of intervertebral disc and articular cartilage cells in the rat. Eur Spine J 2007;16(12):2174-85.

31. Fujita N, Miyamoto T, Imai J, Hosogane N, Suzuki T, Yagi M, Morita K, Ninomiya K, Miyamoto K, Takaishi H and others. CD24 is expressed specifically in the nucleus pulposus of intervertebral discs. Biochem Biophys Res Commun 2005;338(4):1890-6.

32. Roberts S. Disc morphology in health and disease. Biochem Soc Trans 2002;30(Pt 6):864-9.

33. Sive JI, Baird P, Jeziorsk M, Watkins A, Hoyland JA, Freemont AJ. Expression of chondrocyte markers by cells of normal and degenerate intervertebral discs. Mol Pathol 2002;55(2):91-7.

34. Lefebvre V, Huang W, Harley VR, Goodfellow PN, de Crombrugghe B. SOX9 is a potent activator of the chondrocyte-specific enhancer of the pro alpha1(II) collagen gene. Mol Cell Biol 1997;17(4):2336-46.

35. Chelberg MK, Banks GM, Geiger DF, Oegema TR, Jr. Identification of heterogeneous cell populations in normal human intervertebral disc. J Anat 1995;186 (Pt 1):43-53.

36. Buckwalter JA, Pedrini-Mille A, Pedrini V, Tudisco C. Proteoglycans of human infant intervertebral disc. Electron microscopic and biochemical studies. J Bone Joint Surg Am 1985;67(2):284-94.

37. Buckwalter JA, Smith KC, Kazarien LE, Rosenberg LC, Ungar R. Articular cartilage and intervertebral disc proteoglycans differ in structure: an electron microscopic study. J Orthop Res 1989;7(1):146-51.

38. Hukins DW. Tissue engineering: a live disc. Nat Mater 2005;4(12):881-2.

39. Cassidy JJ, Hiltner A, Baer E. Hierarchical structure of the intervertebral disc. Connect Tissue Res 1989;23(1):75-88.

40. Melrose J, Smith SM, Appleyard RC, Little CB. Aggrecan, versican and type VI collagen are components of annular translamellar crossbridges in the intervertebral disc. Eur Spine J 2008;17(2):314-24.

41. Antoniou J, Steffen T, Nelson F, Winterbottom N, Hollander AP, Poole RA, Aebi M, Alini M. The human lumbar intervertebral disc: evidence for changes in the biosynthesis and denaturation of the extracellular matrix with growth, maturation, ageing, and degeneration. J Clin Invest 1996;98(4):996-1003.

42. Mow VC, Huiskes R, Stokes IA, Iatridis JC. Basic Orthopaedic Biomechanics and Mechano-Biology, Chapter 12: Biomechanics of the Spine: Lippencott, Williams & Wilkins; 2004. 543-561 p.

43. Best BA, Guilak F, Setton LA, Zhu W, Saed-Nejad F, Ratcliffe A, Weidenbaum M, Mow VC. Compressive mechanical properties of the human anulus fibrosus and their relationship to biochemical composition. Spine (Phila Pa 1976) 1994;19(2):212-21.

44. Perie D, Korda D, Iatridis JC. Confined compression experiments on bovine nucleus pulposus and annulus fibrosus: sensitivity of the experiment in the determination of compressive modulus and hydraulic permeability. J Biomech 2005;38(11):2164-71.

45. Klisch SM, Lotz JC. A special theory of biphasic mixtures and experimental results for human annulus fibrosus tested in confined compression. J Biomech Eng 2000;122(2):180-8.

46. Johannessen W, Vresilovic EJ, Wright AC, Elliott DM. Intervertebral disc mechanics are restored following cyclic loading and unloaded recovery. Ann Biomed Eng 2004;32(1):70-6.

47. Wilke HJ, Neef P, Caimi M, Hoogland T, Claes LE. New in vivo measurements of pressures in the intervertebral disc in daily life. Spine (Phila Pa 1976) 1999;24(8):755-62.

48. Ebara S, Iatridis JC, Setton LA, Foster RJ, Mow VC, Weidenbaum M. Tensile properties of nondegenerate human lumbar anulus fibrosus. Spine (Phila Pa 1976) 1996;21(4):452-61.

49. Marchand F, Ahmed AM. Investigation of the laminate structure of lumbar disc anulus fibrosus. Spine 1990;15(5):402-10.

50. Skaggs DL, Weidenbaum M, Iatridis JC, Ratcliffe A, Mow VC. Regional variation in tensile properties and biochemical composition of the human lumbar anulus fibrosus. Spine (Phila Pa 1976) 1994;19(12):1310-9.

51. Urban MR, Fairbank JC, Bibby SR, Urban JP. Intervertebral disc composition in neuromuscular scoliosis: changes in cell density and glycosaminoglycan concentration at the curve apex. Spine 2001;26(6):610-7.

52. Roughley P, Hoemann C, DesRosiers E, Mwale F, Antoniou J, Alini M. The potential of chitosan-based gels containing intervertebral disc cells for nucleus pulposus supplementation. Biomaterials 2006;27(3):388-96.

53. Miller JA, Schmatz C, Schultz AB. Lumbar disc degeneration: correlation with age, sex, and spine level in 600 autopsy specimens. Spine (Phila Pa 1976) 1988;13(2):173-8.

54. Battie MC, Videman T, Gibbons LE, Fisher LD, Manninen H, Gill K. 1995 Volvo Award in clinical sciences. Determinants of lumbar disc degeneration. A study relating lifetime exposures and magnetic resonance imaging findings in identical twins. Spine (Phila Pa 1976) 1995;20(24):2601-12.

55. Battie MC, Videman T, Gill K, Moneta GB, Nyman R, Kaprio J, Koskenvuo M. 1991 Volvo Award in clinical sciences. Smoking and lumbar intervertebral disc degeneration: an MRI study of identical twins. Spine (Phila Pa 1976) 1991;16(9):1015-21.

56. Pope MH, Magnusson M, Wilder DG. Kappa Delta Award. Low back pain and whole body vibration. Clin Orthop Relat Res 1998(354):241-8.

57. Thompson JP, Pearce RH, Schechter MT, Adams ME, Tsang IK, Bishop PB. Preliminary evaluation of a scheme for grading the gross morphology of the human intervertebral disc. Spine 1990;15(5):411-5.

58. Modic MT, Hardy RW, Jr., Weinstein MA, Duchesneau PM, Paushter DM, Boumphrey F. Nuclear magnetic resonance of the spine: clinical potential and limitation. Neurosurgery 1984;15(4):583-92.

59. Modic MT, Pavlicek W, Weinstein MA, Boumphrey F, Ngo F, Hardy R, Duchesneau PM. Magnetic resonance imaging of intervertebral disk disease. Clinical and pulse sequence considerations. Radiology 1984;152(1):103-11.

60. An HS, Anderson PA, Haughton VM, Iatridis JC, Kang JD, Lotz JC, Natarajan RN, Oegema TR, Jr., Roughley P, Setton LA and others. Introduction: disc degeneration: summary. Spine (Phila Pa 1976) 2004;29(23):2677-8.

61. Freemont AJ. The cellular pathobiology of the degenerate intervertebral disc and discogenic back pain. Rheumatology (Oxford) 2009;48(1):5-10.

62. Lee RS, Kayser MV, Ali SY. Calcium phosphate microcrystal deposition in the human intervertebral disc. J Anat 2006;208(1):13-9.

63. Lyons H, Jones E, Quinn FE, Sprunt DH. Changes in the protein-polysaccharide fractions of nucleus pulposus from human intervertebral disc with age and disc herniation. J Lab Clin Med 1966;68(6):930-9.

64. Buckwalter JA, Roughley PJ, Rosenberg LC. Age-related changes in cartilage proteoglycans: quantitative electron microscopic studies. Microsc Res Tech 1994;28(5):398-408.

65. Buckwalter JA, Woo SL, Goldberg VM, Hadley EC, Booth F, Oegema TR, Eyre DR. Soft-tissue aging and musculoskeletal function. J Bone Joint Surg Am 1993;75(10):1533-48.

66. Adams MA, Hutton WC. Prolapsed intervertebral disc. A hyperflexion injury 1981 Volvo Award in Basic Science. Spine 1982;7(3):184-91.

67. Kirkaldy-Willis WH, Wedge JH, Yong-Hing K, Reilly J. Pathology and pathogenesis of lumbar spondylosis and stenosis. Spine 1978;3(4):319-28.

68. Pearce RH, Grimmer BJ, Adams ME. Degeneration and the chemical composition of the human lumbar intervertebral disc. J Orthop Res 1987;5(2):198-205.

69. Urban JP, Roberts S. Degeneration of the intervertebral disc. Arthritis Res Ther 2003;5(3):120-30.

70. Yoon ST. Molecular therapy of the intervertebral disc. Spine J 2005;5(6 Suppl):280S-286S.

71. Kang JD, Georgescu HI, McIntyre-Larkin L, Stefanovic-Racic M, Donaldson WF, 3rd, Evans CH. Herniated lumbar intervertebral discs spontaneously produce matrix metalloproteinases, nitric oxide, interleukin-6, and prostaglandin E2. Spine 1996;21(3):271-7.

72. Kang JD, Georgescu HI, McIntyre-Larkin L, Stefanovic-Racic M, Evans CH. Herniated cervical intervertebral discs spontaneously produce matrix metalloproteinases, nitric oxide, interleukin-6, and prostaglandin E2. Spine 1995;20(22):2373-8.

73. Le Maitre CL, Freemont AJ, Hoyland JA. Localization of degradative enzymes and their inhibitors in the degenerate human intervertebral disc. J. Pathol. 2004;204(1):47-54.

74. Roberts S, Caterson B, Menage J, Evans EH, Jaffray DC, Eisenstein SM. Matrix metalloproteinases and aggrecanase: their role in disorders of the human intervertebral disc. Spine (Phila Pa 1976) 2000;25(23):3005-13.

75. Fujita K, Nakagawa T, Hirabayashi K, Nagai Y. Neutral proteinases in human intervertebral disc. Role in degeneration and probable origin. Spine (Phila Pa 1976) 1993;18(13):1766-73.

76. Kang JD, Stefanovic-Racic M, McIntyre LA, Georgescu HI, Evans CH. Toward a biochemical understanding of human intervertebral disc degeneration and herniation. Contributions of nitric oxide, interleukins, prostaglandin E2, and matrix metalloproteinases. Spine 1997;22(10):1065-73.

77. Palmer RM, Hickery MS, Charles IG, Moncada S, Bayliss MT. Induction of nitric oxide synthase in human chondrocytes. Biochem Biophys Res Commun 1993;193(1):398-405.

78. Woessner JF, Jr., Gunja-Smith Z. Role of metalloproteinases in human osteoarthritis. J Rheumatol Suppl 1991;27:99-101.

79. Trout JJ, Buckwalter JA, Moore KC, Landas SK. Ultrastructure of the human intervertebral disc. I. Changes in notochordal cells with age. Tissue Cell 1982;14(2):359-69.

80. Brickley-Parsons D, Glimcher MJ. Is the chemistry of collagen in intervertebral discs an expression of Wolff's Law? A study of the human lumbar spine. Spine (Phila Pa 1976) 1984;9(2):148-63.

81. Herbert CM, Lindberg KA, Jayson MI, Bailey AJ. Proceedings: Intervertebral disc collagen in degenerative disc disease. Ann Rheum Dis 1975;34(5):467.

82. Monnier VM, Kohn RR, Cerami A. Accelerated age-related browning of human collagen in diabetes mellitus. Proc Natl Acad Sci U S A 1984;81(2):583-7.

83. Ruan DK, Xin H, Zhang C, Wang C, Xu C, Li C, He Q. Experimental intervertebral disc regeneration with tissue-engineered composite in a canine model. Tissue Eng Part A 2010;16(7):2381-9.

84. Lotz JC. Animal models of intervertebral disc degeneration: lessons learned. Spine (Phila Pa 1976) 2004;29(23):2742-50.

85. Iatridis JC, Weidenbaum M, Setton LA, Mow VC. Is the nucleus pulposus a solid or a fluid? Mechanical behaviors of the nucleus pulposus of the human intervertebral disc. Spine (Phila Pa 1976) 1996;21(10):1174-84.

86. Ohshima H, Urban JP, Bergel DH. Effect of static load on matrix synthesis rates in the intervertebral disc measured in vitro by a new perfusion technique. J Orthop Res 1995;13(1):22-9.

87. An HS, Thonar EJ, Masuda K. Biological repair of intervertebral disc. Spine (Phila Pa 1976) 2003;28(15 Suppl):S86-92.

88. Chan D, Song Y, Sham P, Cheung KM. Genetics of disc degeneration. Eur Spine J 2006;15 Suppl 3:S317-25.

89. Urban JP, Smith S, Fairbank JC. Nutrition of the intervertebral disc. Spine (Phila Pa 1976) 2004;29(23):2700-9.

90. Libera J, Hoell T, Holzhausen HJ, Ganey T, Gerber BE, Tetzlaff EM, Bertagnoli R, Meisel HJ, Siodla V. Intervertebral Disc Regeneration: Springer; 2009. 307-315 p.

91. Crevensten G, Walsh AJ, Ananthakrishnan D, Page P, Wahba GM, Lotz JC, Berven S. Intervertebral disc cell therapy for regeneration: mesenchymal stem cell implantation in rat intervertebral discs. Ann Biomed Eng 2004;32(3):430-4.

92. Bohlman HH, Emery SE, Goodfellow DB, Jones PK. Robinson anterior cervical discectomy and arthrodesis for cervical radiculopathy. Long-term follow-up of one hundred and twenty-two patients. J Bone Joint Surg Am 1993;75(9):1298-307.

93. Lipson SJ, Muir H. 1980 Volvo award in basic science. Proteoglycans in experimental intervertebral disc degeneration. Spine (Phila Pa 1976) 1981;6(3):194-210.

94. Tibrewal SB, Pearcy MJ, Portek I, Spivey J. A prospective study of lumbar spinal movements before and after discectomy using biplanar radiography. Correlation of clinical and radiographic findings. Spine (Phila Pa 1976) 1985;10(5):455-60.

95. Rousseau MA, Bradford DS, Bertagnoli R, Hu SS, Lotz JC. Disc arthroplasty design influences intervertebral kinematics and facet forces. Spine J 2006;6(3):258-66.

96. Lee CK, Langrana NA. Lumbosacral spinal fusion. A biomechanical study. Spine (Phila Pa 1976) 1984;9(6):574-81.

97. Goto K, Tajima N, Chosa E, Totoribe K, Kubo S, Kuroki H, Arai T. Effects of lumbar spinal fusion on the other lumbar intervertebral levels (three-dimensional finite element analysis). J Orthop Sci 2003;8(4):577-84.

98. Lee CK. Accelerated degeneration of the segment adjacent to a lumbar fusion. Spine (Phila Pa 1976) 1988;13(3):375-7.

99. Delamarter RB, Fribourg DM, Kanim LE, Bae H. ProDisc artificial total lumbar disc replacement: introduction and early results from the United States clinical trial. Spine (Phila Pa 1976) 2003;28(20):S167-75.

100. McCullen GM, Yuan HA. Artificial disc: current developments in artificial disc replacements. Current Opinion in Orthopaedics 2003(14):138-143.

101. Ray CD. The PDN prosthetic disc-nucleus device. Eur Spine J 2002;11 Suppl 2:S137-42.

102. Klara PM, Ray CD. Artificial nucleus replacement: clinical experience. Spine (Phila Pa 1976) 2002;27(12):1374-7.

103. Nesti LJ, Li WJ, Shanti RM, Jiang YJ, Jackson W, Freedman BA, Kuklo TR, Giuliani JR, Tuan RS. Intervertebral disc tissue engineering using a novel hyaluronic acid-nanofibrous scaffold (HANFS) amalgam. Tissue Eng Part A 2008;14(9):1527-37.

104. Huang RC, Girardi FP, Cammisa FP, Jr., Lim MR, Tropiano P, Marnay T. Correlation between range of motion and outcome after lumbar total disc replacement: 8.6-year follow-up. Spine (Phila Pa 1976) 2005;30(12):1407-11.

105. Zigler J, Delamarter R, Spivak JM, Linovitz RJ, Danielson GO, 3rd, Haider TT, Cammisa F, Zuchermann J, Balderston R, Kitchel S and others. Results of the prospective, randomized, multicenter Food and Drug Administration investigational device exemption study of the ProDisc-L total disc replacement versus circumferential fusion for the treatment of 1-level degenerative disc disease. Spine (Phila Pa 1976) 2007;32(11):1155-62; discussion 1163.

106. Zigler JE. Clinical results with ProDisc: European experience and U.S. investigation device exemption study. Spine (Phila Pa 1976) 2003;28(20):S163-6.

107. Griffith SL, Shelokov AP, Buttner-Janz K, LeMaire JP, Zeegers WS. A multicenter retrospective study of the clinical results of the LINK SB Charite intervertebral prosthesis. The initial European experience. Spine (Phila Pa 1976) 1994;19(16):1842-9.

108. Bertagnoli R, Yue JJ, Fenk-Mayer A, Eerulkar J, Emerson JW. Treatment of symptomatic adjacent-segment degeneration after lumbar fusion with total disc arthroplasty by using the prodisc prosthesis: a prospective study with 2-year minimum follow up. J Neurosurg Spine 2006;4(2):91-7.

109. Siepe CJ, Mayer HM, Wiechert K, Korge A. Clinical results of total lumbar disc replacement with ProDisc II: three-year results for different indications. Spine (Phila Pa 1976) 2006;31(17):1923-32.

110. Buettner- Janz K, Helisch HJ, Schellnack K; Intervertebral disc endoprosthesis. US patent 4759766. 1988 July 26.

111. Marnay T; Prosthesis for intervertebral discs and instruments for implanting it. US patent 5314477. 1994 May 24.

112. Salib RM, Pettine KA; Intervertebral disc arthroplasty. US patent 5258031. 1993 November 2.

113. An HS, Juarez KK. Artificial Disc Replacement. Chicago, IL; 2010.

114. Neurosurgical Instruments. 2007.

115. Denoziere G, Ku DN. Biomechanical comparison between fusion of two vertebrae and implantation of an artificial intervertebral disc. J Biomech 2006;39(4):766-75.

116. Geisler FH, Blumenthal SL, Guyer RD, McAfee PC, Regan JJ, Johnson JP, Mullin B. Neurological complications of lumbar artificial disc replacement and comparison of clinical results with those related to lumbar arthrodesis in the literature: results of a multicenter, prospective, randomized investigational device exemption study of Charite intervertebral disc. Invited submission from the Joint Section Meeting on Disorders of the Spine and Peripheral Nerves, March 2004. J Neurosurg Spine 2004;1(2):143-54.

117. Cunningham BW. Basic scientific considerations in total disc arthroplasty. Spine J 2004;4(6 Suppl):219S-230S.

118. Ross ER. Revision in artificial disc replacement. Spine J 2009;9(9):773-5.

119. van Ooij A, Oner FC, Verbout AJ. Complications of artificial disc replacement: a report of 27 patients with the SB Charite disc. J Spinal Disord Tech 2003;16(4):369-83.

120. Rawlinson JJ, Punga KP, Gunsallus KL, Bartel DL, Wright TM. Wear simulation of the ProDisc-L disc replacement using adaptive finite element analysis. J Neurosurg Spine 2007;7(2):165-73.

121. Daly KJ, Ross ER, Norris H, McCollum CN. Vascular complications of prosthetic inter-vertebral discs. Eur Spine J 2006;15 Suppl 5:644-9.

122. Gloria A, Causa F, De Santis R, Netti PA, Ambrosio L. Dynamic-mechanical properties of a novel composite intervertebral disc prosthesis. J Mater Sci Mater Med 2007;18(11):2159-65.

123. Sakai D, Mochida J, Iwashina T, Hiyama A, Omi H, Imai M, Nakai T, Ando K, Hotta T. Regenerative effects of transplanting mesenchymal stem cells embedded in atelocollagen to the degenerated intervertebral disc. Biomaterials 2006;27(3):335-45.

124. Heuer F, Ulrich S, Claes L, Wilke HJ. Biomechanical evaluation of conventional anulus fibrosus closure methods required for nucleus replacement. Laboratory investigation. J Neurosurg Spine 2008;9(3):307-13.

125. Neidlinger-Wilke C, Wurtz K, Liedert A, Schmidt C, Borm W, Ignatius A, Wilke HJ, Claes L. A three-dimensional collagen matrix as a suitable culture system for the comparison of cyclic strain and hydrostatic pressure effects on intervertebral disc cells. J Neurosurg Spine 2005;2(4):457-65.

126. Leung VY, Chan D, Cheung KM. Regeneration of intervertebral disc by mesenchymal stem cells: potentials, limitations, and future direction. Eur Spine J 2006;15 Suppl 3:S406-13.

127. Caplan AI. Mesenchymal stem cells. J Orthop Res 1991;9(5):641-50.

128. Deans RJ, Moseley AB. Mesenchymal stem cells: biology and potential clinical uses. Exp Hematol 2000;28(8):875-84.

129. Rendal-Vazquez ME, Maneiro-Pampin E, Rodriguez-Cabarcos M, Fernandez-Mallo O, Lopez de Ullibarri I, Andion-Nunez C, Blanco FJ. Effect of cryopreservation on human articular chondrocyte viability, proliferation, and collagen expression. Cryobiology 2001;42(1):2-10.

130. Meisel HJ, Ganey T, Hutton WC, Libera J, Minkus Y, Alasevic O. Clinical experience in cell-based therapeutics: intervention and outcome. Eur Spine J 2006;15 Suppl 3:S397-405.

131. Bertram H, Kroeber M, Wang H, Unglaub F, Guehring T, Carstens C, Richter W. Matrix-assisted cell transfer for intervertebral disc cell therapy. Biochem Biophys Res Commun 2005;331(4):1185-92.

132. Hunziker EB. Articular cartilage repair: basic science and clinical progress. A review of the current status and prospects. Osteoarthritis Cartilage 2002;10(6):432-63.

133. Masuda K, Oegema TR, Jr., An HS. Growth factors and treatment of intervertebral disc degeneration. Spine (Phila Pa 1976) 2004;29(23):2757-69.

134. Osada R, Ohshima H, Ishihara H, Yudoh K, Sakai K, Matsui H, Tsuji H. Autocrine/paracrine mechanism of insulin-like growth factor-1 secretion, and the effect of insulin-like growth factor-1 on proteoglycan synthesis in bovine intervertebral discs. J Orthop Res 1996;14(5):690-9.

135. Gruber HE, Norton HJ, Hanley EN, Jr. Anti-apoptotic effects of IGF-1 and PDGF on human intervertebral disc cells in vitro. Spine (Phila Pa 1976) 2000;25(17):2153-7.

136. Guerne PA, Sublet A, Lotz M. Growth factor responsiveness of human articular chondrocytes: distinct profiles in primary chondrocytes, subcultured chondrocytes, and fibroblasts. J Cell Physiol 1994;158(3):476-84.

137. Alini M, Li W, Markovic P, Aebi M, Spiro RC, Roughley PJ. The potential and limitations of a cell-seeded collagen/hyaluronan scaffold to engineer an intervertebral disc-like matrix. Spine (Phila Pa 1976) 2003;28(5):446-54; discussion 453.

138. Thompson JP, Oegema TR, Jr., Bradford DS. Stimulation of mature canine intervertebral disc by growth factors. Spine (Phila Pa 1976) 1991;16(3):253-60.

139. Pattison ST, Melrose J, Ghosh P, Taylor TK. Regulation of gelatinase-A (MMP-2) production by ovine intervertebral disc nucleus pulposus cells grown in alginate bead culture by Transforming Growth Factor-beta(1)and insulin like growth factor-I. Cell Biol Int 2001;25(7):679-89.

140. Chen P, Vukicevic S, Sampath TK, Luyten FP. Bovine articular chondrocytes do not undergo hypertrophy when cultured in the presence of serum and osteogenic protein-1. Biochem Biophys Res Commun 1993;197(3):1253-9.

141. Masuda K, Takegami K, An H, Kumano F, Chiba K, Andersson GB, Schmid T, Thonar E. Recombinant osteogenic protein-1 upregulates extracellular matrix metabolism by rabbit annulus fibrosus and nucleus pulposus cells cultured in alginate beads. J Orthop Res 2003;21(5):922-30.

142. Zhang Y, An HS, Song S, Toofanfard M, Masuda K, Andersson GB, Thonar EJ. Growth factor osteogenic protein-1: differing effects on cells from three distinct zones in the bovine intervertebral disc. Am J Phys Med Rehabil 2004;83(7):515-21.

143. An HS, Takegami K, Kamada H, Nguyen CM, Thonar EJ, Singh K, Andersson GB, Masuda K. Intradiscal administration of osteogenic protein-1 increases intervertebral disc height and proteoglycan content in the nucleus pulposus in normal adolescent rabbits. Spine (Phila Pa 1976) 2005;30(1):25-31; discussion 31-2.

144. Masuda K, Imai Y, Okuma M, Muehleman C, Nakagawa K, Akeda K, Thonar E, Andersson G, An HS. Osteogenic protein-1 injection into a degenerated disc induces the restoration of disc height and structural changes in the rabbit anular puncture model. Spine (Phila Pa 1976) 2006;31(7):742-54.

145. Liu J, Roughley PJ, Mort JS. Identification of human intervertebral disc stromelysin and its involvement in matrix degradation. J Orthop Res 1991;9(4):568-75.

146. Igarashi T, Kikuchi S, Shubayev V, Myers RR. 2000 Volvo Award winner in basic science studies: Exogenous tumor necrosis factor-alpha mimics nucleus pulposus-induced neuropathology. Molecular, histologic, and behavioral comparisons in rats. Spine (Phila Pa 1976) 2000;25(23):2975-80.

147. Le Maitre CL, Freemont AJ, Hoyland JA. The role of interleukin-1 in the pathogenesis of human intervertebral disc degeneration. Arthritis Res Ther 2005;7(4):R732-45.

148. Takegami K, Thonar EJ, An HS, Kamada H, Masuda K. Osteogenic protein-1 enhances matrix replenishment by intervertebral disc cells previously exposed to interleukin-1. Spine 2002;27(12):1318-25.

149. Tolonen J, Gronblad M, Virri J, Seitsalo S, Rytomaa T, Karaharju E. Basic fibroblast growth factor immunoreactivity in blood vessels and cells of disc herniations. Spine (Phila Pa 1976) 1995;20(3):271-6.

150. Walsh AJ, Bradford DS, Lotz JC. In vivo growth factor treatment of degenerated intervertebral discs. Spine (Phila Pa 1976) 2004;29(2):156-63.

151. Lee SJ. Cytokine delivery and tissue engineering. Yonsei Med J 2000;41(6):704-19.

152. Nagae M, Ikeda T, Mikami Y, Hase H, Ozawa H, Matsuda K, Sakamoto H, Tabata Y, Kawata M, Kubo T. Intervertebral disc regeneration using platelet-rich plasma and biodegradable gelatin hydrogel microspheres. Tissue Eng 2007;13(1):147-58.

153. Eppley BL, Woodell JE, Higgins J. Platelet quantification and growth factor analysis from platelet-rich plasma: implications for wound healing. Plast Reconstr Surg 2004;114(6):1502-8.

154. Halloran DO, Grad S, Stoddart M, Dockery P, Alini M, Pandit AS. An injectable cross-linked scaffold for nucleus pulposus regeneration. Biomaterials 2008;29(4):438-47.

155. FDA Briefing.

156. Wilke HJ, Heuer F, Neidlinger-Wilke C, Claes L. Is a collagen scaffold for a tissue engineered nucleus replacement capable of restoring disc height and stability in an animal model? Eur Spine J 2006;15 Suppl 3:S433-8.

157. Ochi M, Uchio Y, Tobita M, Kuriwaka M. Current concepts in tissue engineering technique for repair of cartilage defect. Artif Organs 2001;25(3):172-9.

158. Sato M, Asazuma T, Ishihara M, Kikuchi T, Kikuchi M, Fujikawa K. An experimental study of the regeneration of the intervertebral disc with an allograft of cultured annulus fibrosus cells using a tissue-engineering method. Spine (Phila Pa 1976) 2003;28(6):548-53.

159. Abbushi A, Endres M, Cabraja M, Kroppenstedt SN, Thomale UW, Sittinger M, Hegewald AA, Morawietz L, Lemke AJ, Bansemer VG and others. Regeneration of intervertebral disc tissue by resorbable cell-free polyglycolic acid-based implants in a rabbit model of disc degeneration. Spine (Phila Pa 1976) 2008;33(14):1527-32.

160. Hegewald AA, Enz A, Endres M, Sittinger M, Woiciechowsky C, Thome C, Kaps C. Engineering of polymer-based grafts with cells derived from human nucleus pulposus tissue of the lumbar spine. J Tissue Eng Regen Med 2010.

161. Revell PA, Damien E, Di Silvio L, Gurav N, Longinotti C, Ambrosio L. Tissue engineered intervertebral disc repair in the pig using injectable polymers. J Mater Sci Mater Med 2007;18(2):303-8.

162. Mwale F, Iordanova M, Demers CN, Steffen T, Roughley P, Antoniou J. Biological evaluation of chitosan salts cross-linked to genipin as a cell scaffold for disk tissue engineering. Tissue Eng 2005;11(1-2):130-40.

163. Qiu Y, Zhang N, Kang Q, An Y, Wen X. Chemically modified light-curable chitosans with enhanced potential for bone tissue repair. J Biomed Mater Res A 2009;89(3):772-9.

164. Nishida K, Kang JD, Gilbertson LG, Moon SH, Suh JK, Vogt MT, Robbins PD, Evans CH. Modulation of the biologic activity of the rabbit intervertebral disc by gene therapy: an in vivo study of adenovirus-mediated transfer of the human transforming growth factor beta 1 encoding gene. Spine (Phila Pa 1976) 1999;24(23):2419-25.

165. Bumgardner JD, Wiser R, Gerard PD, Bergin P, Chestnutt B, Marin M, Ramsey V, Elder SH, Gilbert JA. Chitosan: potential use as a bioactive coating for orthopaedic and craniofacial/dental implants. J Biomater Sci Polym Ed 2003;14(5):423-38.

166. Nettles DL, Elder SH, Gilbert JA. Potential use of chitosan as a cell scaffold material for cartilage tissue engineering. Tissue Eng 2002;8(6):1009-16.

167. Saldanha KJ, Piper SL, Ainslie KM, Kim HT, Majumdar S. Magnetic resonance imaging of iron oxide labelled stem cells: applications to tissue engineering based regeneration of the intervertebral disc. Eur Cell Mater 2008;16:17-25.

168. Thomas J, Gomes K, Lowman A, Marcolongo M. The effect of dehydration history on PVA/PVP hydrogels for nucleus pulposus replacement. J Biomed Mater Res B Appl Biomater 2004;69(2):135-40.

169. Liu Y, Webb K, Kirker KR, Bernshaw NJ, Tresco PA, Gray SD, Prestwich GD. Composite articular cartilage engineered on a chondrocyte-seeded aliphatic polyurethane sponge. Tissue Eng 2004;10(7-8):1084-92.

170. Guilak F, Sah R, Setton LA. Physical regulation of cartilage metabolism. In: Mow VC, Hayes WC, editors. Basic orthopaedic biomechanics. Philadelphia: Lippincott-Raven Publishers; 1997. p 179-207.

171. Kim SH, Yoon SJ, Choi B, Ha HJ, Rhee JM, Kim MS, Yang YS, Lee HB, Khang G. Evaluation of Various Types of Scaffold for Tissue Engineered Intervertebral Disc. In: Fisher JP, editor. Tissue Engineering, Advances in Experimental Medicine and Biology: Springer; 2007. p 167-81.

172. Lee SJ, Khang G, Lee YM, Lee HB. Interaction of human chondrocytes and NIH/3T3 fibroblasts on chloric acid-treated biodegradable polymer surfaces. J Biomater Sci Polym Ed 2002;13(2):197-212.

173. Brown RQ, Mount A, Burg KJ. Evaluation of polymer scaffolds to be used in a composite injectable system for intervertebral disc tissue engineering. J Biomed Mater Res A 2005;74(1):32-9.

174. Hodde JP, Record RD, Liang HA, Badylak SF. Vascular endothelial growth factor in porcine-derived extracellular matrix. Endothelium 2001;8(1):11-24.

175. Voytik-Harbin SL, Brightman AO, Kraine MR, Waisner B, Badylak SF. Identification of extractable growth factors from small intestinal submucosa. J Cell Biochem 1997;67(4):478-91.

176. Le Visage C, Yang SH, Kadakia L, Sieber AN, Kostuik JP, Leong KW. Small intestinal submucosa as a potential bioscaffold for intervertebral disc regeneration. Spine (Phila Pa 1976) 2006;31(21):2423-30; discussion 2431.

177. Record RD, Hillegonds D, Simmons C, Tullius R, Rickey FA, Elmore D, Badylak SF. In vivo degradation of 14C-labeled small intestinal submucosa (SIS) when used for urinary bladder repair. Biomaterials 2001;22(19):2653-9.

178. Badylak S, Liang A, Record R, Tullius R, Hodde J. Endothelial cell adherence to small intestinal submucosa: an acellular bioscaffold. Biomaterials 1999;20(23-24):2257-63.

179. Helen W, Merry CL, Blaker JJ, Gough JE. Three-dimensional culture of annulus fibrosus cells within PDLLA/Bioglass composite foam scaffolds: assessment of cell attachment, proliferation and extracellular matrix production. Biomaterials 2007;28(11):2010-20.

180. Wan Y, Feng G, Shen FH, Laurencin CT, Li X. Biphasic scaffold for annulus fibrosus tissue regeneration. Biomaterials 2008;29(6):643-52.

181. Nerurkar NL, Elliott DM, Mauck RL. Mechanics of oriented electrospun nanofibrous scaffolds for annulus fibrosus tissue engineering. J Orthop Res 2007;25(8):1018-28.

182. Takahata M, Kotani Y, Abumi K, Shikinami Y, Kadosawa T, Kaneda K, Minami A. Bone ingrowth fixation of artificial intervertebral disc consisting of bioceramic-coated three-dimensional fabric. Spine 2003;28(7):637-44; discussion 644.

183. Kotani Y, Abumi K, Shikinami Y, Takada T, Kadoya K, Shimamoto N, Ito M, Kadosawa T, Fujinaga T, Kaneda K. Artificial intervertebral disc replacement using bioactive three-dimensional fabric: design, development, and preliminary animal study. Spine 2002;27(9):929-35; discussion 935-6.

184. Husson JL, Korge A, Polard JL, Nydegger T, Kneubuhler S, Mayer HM. A memory coiling spiral as nucleus pulposus prosthesis: concept, specifications, bench testing, and first clinical results. J Spinal Disord Tech 2003;16(4):405-11.

185. Mizuno H, Roy AK, Zaporojan V, Vacanti CA, Ueda M, Bonassar LJ. Biomechanical and biochemical characterization of composite tissue-engineered intervertebral discs. Biomaterials 2006;27(3):362-70.

186. Mizuno H, Roy AK, Vacanti CA, Kojima K, Ueda M, Bonassar LJ. Tissue-engineered composites of anulus fibrosus and nucleus pulposus for intervertebral disc replacement. Spine (Phila Pa 1976) 2004;29(12):1290-7; discussion 1297-8.

187. Endres M, Abbushi A, Thomale UW, Cabraja M, Kroppenstedt SN, Morawietz L, Casalis PA, Zenclussen ML, Lemke AJ, Horn P and others. Intervertebral disc regeneration after implantation of a cell-free bioresorbable implant in a rabbit disc degeneration model. Biomaterials 2010;31(22):5836-41.

188. Vernon B, Tirelli N, Bachi T, Haldimann D, Hubbell JA. Water-borne, in situ crosslinked biomaterials from phase-segregated precursors. J Biomed Mater Res A 2003;64(3):447-56.

189. Masuda K, Lotz JC. New challenges for intervertebral disc treatment using regenerative medicine. Tissue Eng Part B Rev;16(1):147-58.

190. Lotz JC, Colliou OK, Chin JR, Duncan NA, Liebenberg E. Compression-induced degeneration of the intervertebral disc: an in vivo mouse model and finite-element study. Spine (Phila Pa 1976) 1998;23(23):2493-506.

191. Hutton WC, Toribatake Y, Elmer WA, Ganey TM, Tomita K, Whitesides TE. The effect of compressive force applied to the intervertebral disc in vivo. A study of proteoglycans and collagen. Spine (Phila Pa 1976) 1998;23(23):2524-37.

192. Sah RL, Ratcliffe A. Translational models for musculoskeletal tissue engineering and regenerative medicine. Tissue Eng Part B Rev;16(1):1-3.

193. Hoogendoorn RJ, Helder MN, Kroeze RJ, Bank RA, Smit TH, Wuisman PI. Reproducible long-term disc degeneration in a large animal model. Spine (Phila Pa 1976) 2008;33(9):949-54.

194. Henriksson HB, Svanvik T, Jonsson M, Hagman M, Horn M, Lindahl A, Brisby H. Transplantation of human mesenchymal stems cells into intervertebral discs in a xenogeneic porcine model. Spine (Phila Pa 1976) 2009;34(2):141-8.

195. White AA, 3rd. Clinical biomechanics of cervical spine implants. Spine 1989;14(10):1040-5.

196. Rand N, Juliao S, Spengler D. Static Hydrostatic Loading Induces Apoptosis in Human Intervertebral Disc Cells. 2000; Orlando, FL.

197. Humzah MD, Soames RW. Human intervertebral disc: structure and function. Anat Rec 1988;220(4):337-56.

198. Meakin JR. Replacing the nucleus pulposus of the intervertebral disk: prediction of suitable properties of a replacement material using finite element analysis. J Mater Sci Mater Med 2001;12(3):207-13.

199. Gilbertson L, Ahn SH, Teng PN, Studer RK, Niyibizi C, Kang JD. The effects of recombinant human bone morphogenetic protein-2, recombinant human bone morphogenetic protein-12, and adenoviral bone morphogenetic protein-12 on matrix synthesis in human annulus fibrosis and nucleus pulposus cells. Spine J 2008;8(3):449-56.

200. Sittinger M, Hutmacher DW, Risbud MV. Current strategies for cell delivery in cartilage and bone regeneration. Curr Opin Biotechnol 2004;15(5):411-8.

CHAPTER 3

3. FABRICATION OF A BIOMIMETIC ELASTIC INTERVERTEBRAL DISC SCAFFOLD USING ADDITIVE MANUFACTURING

3.1 Introduction

Over 80% of the adult population is affected by low back pain at some point in their lives. Surgical procedures are performed on roughly 5% of the population to alleviate this pain, amounting to nearly $90 billion in annual healthcare costs [1]. Degeneration of the intervertebral disc (IVD) causes compression of the spinal nerves and adjacent vertebrae, proving to be a primary cause of low back pain. The exact causes of IVD degeneration are unknown, but it is thought that natural aging, excessive mechanical compression, and biological or genetic factors each play a significant role in the degenerative process [2-5]. Current methods to alleviate the pain caused by a degenerated disc include spinal fusion and artificial disc replacement. Spinal fusion does not restore disc function and may cause further degeneration of adjacent IVDs by altering the biomechanics of the spine [6]. Artificial IVD replacements have recently started to gather interest, with two IVD implants currently approved for use in the United States [7,8]. These implants help replace the degenerated disc and restore some motion; however, they cannot sustain compressive forces due to their lack of elasticity. Additionally, current implants may produce wear debris and cause stress shielding on the vertebrae, resulting in further disc degeneration and eventually implant failure [9]. Tissue engineered IVD scaffolds may offer advantages over current approaches, including preservation of disc

height and natural motion while encouraging formation of natural tissue. Additionally, an artificially engineered elastic polymeric disc offers a solution to the problems encountered with current disc replacements as it would be capable of supporting compressive forces on the spine without permanent deformation.

Many researchers have attempted to fabricate an IVD scaffold, but none have completely satisfied critical requirements for both reproducing morphological and mechanical properties of native IVD tissue [10-12]. However, creating a tissue engineered IVD has proven difficult, as its structure is highly unique, containing a highly aligned and lamellar annulus fibrosus (AF). Overall, the IVD is avascular with a bean shaped structure [13]. The AF is a collagen-rich fibrous structure containing between 15-25 multilayered, oriented concentric layers (lamellae) [14]. This lamellar architecture helps support the biomechanics of the disc by preventing excessive tensile force from bursting the inner IVD while supporting compressive forces on the spine [15]. Cells within the AF are highly oriented and parallel to the lamellar collagen fibers [16]. To our best knowledge, no researchers have replicated the microstructure of the AF when designing a tissue engineered construct. Because it is vital that a tissue engineered structure closely mimics the native morphology of the disc, a scaffold with a similar structure to the native AF, containing concentric lamellar layers, would prove to be a significant advancement compared to current tissue engineering strategies. Furthermore, the development of an IVD scaffold with mechanical properties similar to those of native tissue are rarely investigated. Therefore, a tissue engineered IVD construct that better emulates mechanical properties of the native disc will prove advantageous in the future.

A lamellar disc scaffold formed from elastomeric polymers would offer a high compliance and allow restoration of natural three-dimensional spinal motions. A lamellar construct mimics the natural histological structure found in the outer region of natural IVDs and allows a greater surface area for cell adhesion, alignment, and growth. Currently, many different techniques have been used to create an IVD scaffold [12,17-20]. However, none have been able to fabricate a lamellar structure mimicking the natural IVD histology. To this end, we created an additive manufacturing technique that combines ultra-fine pipettes for liquid polymer extrusion and a freezing stage for the solidification of the scaffolds. This scaffold fabrication method permits the use of many different polymers and is suitable for creating scaffolds with different three-dimensional configurations. This paper will primarily focus on the use of a biodegradable and elastic polyurethane (PU) for the application of IVD tissue regeneration, as polyurethane exhibits elastic properties similar to natural IVD tissue, and has shown to encourage cartilage growth in previous studies [21].

3.2 Materials and Methods

3.2.1 Scaffold Fabrication

A custom-built computer aided manufacturing device integrated with a freezing stage was used for this study as shown in figure 3.1. Microsoft Visual Basic was used to program the device for three-dimensional scaffold designs. Scaffolds were designed by manually programming the device to resemble the native IVD tissue structure as seen in

the literature [22]. The nozzle tip was made from a calibrated fire-pulled glass injection pipette to allow high resolution printing. Specifically, 5 μL glass capillary tubes (Drummond wiretrol, Drummond Scientific Company, Broomall, PA) were heated and pulled on a micropipette puller (Narishige PC-10, Japan) to have a well-controlled inner diameter varying between 5 μm and 50 μm.

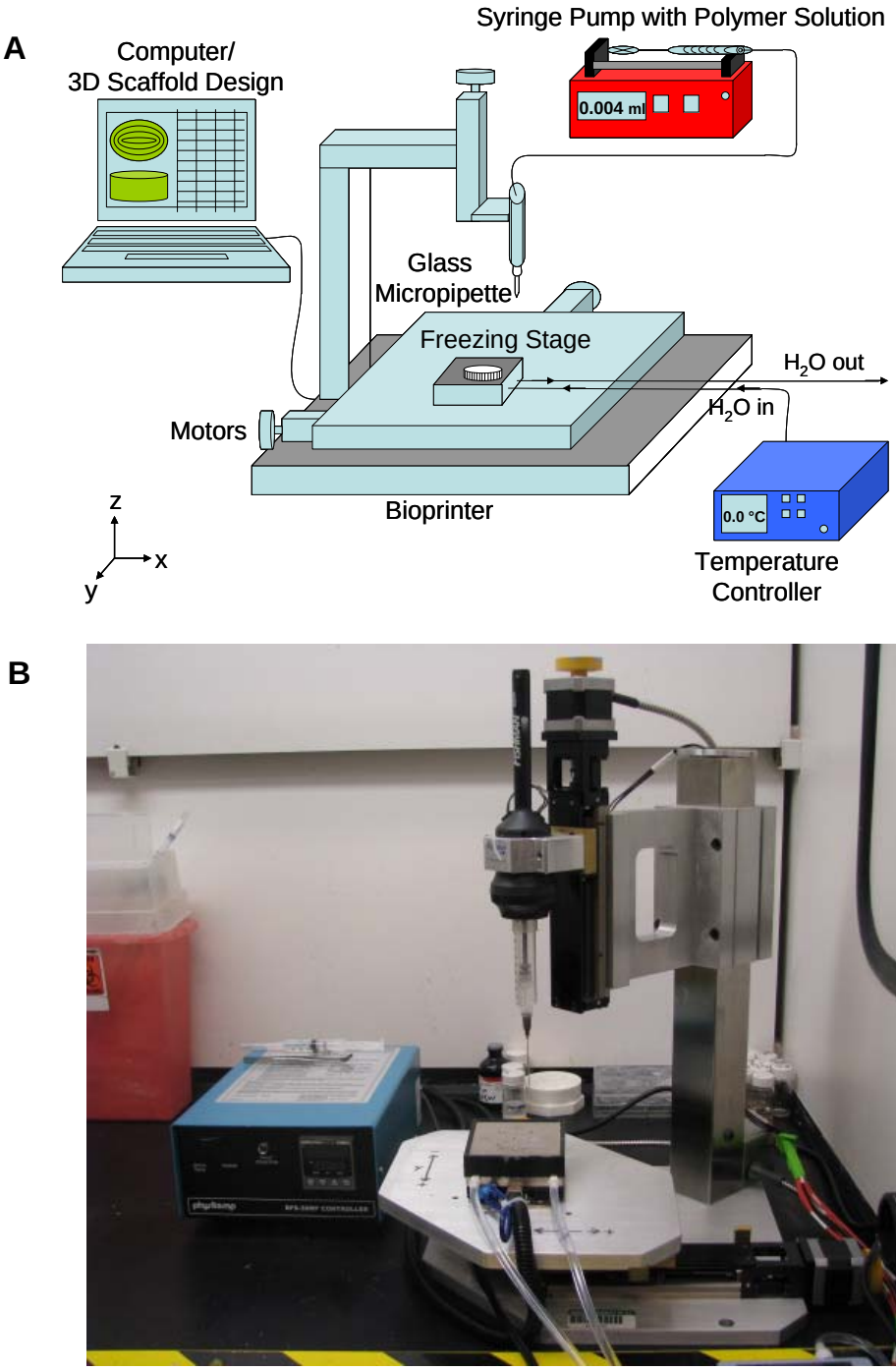

Figure 3. 1: Schematic (A) and image (B) of the apparatus using CAD, a temperature controlled freezing stage, and micropipettes. The device allowed for control of the X-Y-Z axes down to micron level resolution, while separately controlling the polymer solution extrusion rate.

Degradable lysine diisocyanate (LDI, Kyowa Hakko Kogyo Co., Japan) and polycaprolactone diol (PCL, Sigma-Aldrich, USA) based polyurethane was synthesized and purified similar to techniques used by others [23,24]. Briefly, 1:1 molar ratios of hard segment LDI and soft segment PCL were added dropwise into dimethylformamide (DMF, Sigma) and stirred for 3 hours. The resulting polyurethane was then dissolved again in DMF at a concentration of 15% w/v under nitrogen gas flow protection and stirred overnight. This polymer solution was extruded out of a syringe through an ultra-fine glass injection pipette. Polymer solution was fed at a flow rate of 0.005 ml/min onto a glass collection plate placed on the freezing stage (maintained at -4° C). The micropipette tip was positioned approximately 30 μm above the collecting substrate. The freezing stage maintained the scaffold resolution by increasing the polymer solution viscosity below its freezing point and causing the polymer to harden in place as it was extruded out of the pipette tip. Briefly, the scaffold material is solidified through temperature convection from the cold stage to the point where the material is extruded out of the pipette tip. When the temperature is finely controlled, the polymer solution will solidify upon extrusion after reaching its freezing point and allow the structure to support subsequent layer by layer deposition. Thus, the device and freezing stage can precisely control the extrusion and resolution of the polymer, therefore allowing the creation of custom designed scaffolds. The approximate build time for each IVD scaffold layer was approximately 3 minutes. After the printing of each layer, the micropipette was raised 20-40 μm in the z-direction and the computer program continued to build the next layer of the structure. After the printing procedure was done, solidified scaffolds were

removed from the freezing stage and freeze-dried for 24 hours to extract the solvent. Large ice crystal formation on the freezing stage was avoided, by operating in a low humidity environment, because it alters the physical properties of the extruded polymer, thereby affecting polymer shape.

3.2.2 Mechanical Properties of Scaffolds

Mechanical testing was used to characterize the compressive properties of the scaffolds using unconfined compression experiments. Scaffolds (5.75 mm in diameter × 2 mm in height) were compressed at a rate of 1 mm · min^{-1} using a DMA Q800 system (TA Instruments, Delaware, U.S.A.) and stopped at roughly 50% strain (n=4). Engineering stress and strain were recorded and evaluated. The compressive tests were performed on hydrated samples at room temperature. Dynamic compression tests were completed on the hydrated samples at room temperature at 0.008 Hz up to a compressive strain of 65%. Tests were not completed past 65% compressive strain, as previous studies have shown that the IVD only experiences roughly 15% compressive strain, and compressive testing to 65% ensured the scaffold would perform well under extreme conditions [25]. Dynamic shear testing was also performed on the scaffolds similarly to previous studies on the IVD [26]. Dynamic shear properties were measured for 12 samples each at 3 compressive strains (15%, 30%, and 45%) using an AR G2 dynamic rheometer (TA Instruments). Briefly, each sample was subjected to a shear strain of 1.5% at oscillation frequencies ranging from 0.05 Hz to 1.05 Hz in 0.05 Hz intervals, similar to previous dynamic testing conditions on IVDs [27]. These frequencies were chosen as they

are comparable to normal physiologic loading rates in the IVD [28]. Dynamic shear properties were measured at 3 levels of compressive strain because the disc is always under some degree of compressive force, usually around 15%. Other levels of compressive strains, e.g., 30% and 45%, were also tested to account for severe loading circumstances.

3.2.3 In vitro cell culture experiments

Scaffolds used for cell culture were sterilized with 70% ethanol for 30 minutes and then rinsed 3 times with sterile PBS for 2 hours per rinse. Bovine IVD cells were seeded on the scaffolds at a density of $1x10^5$ cells. RPMI 1640 Media with 10% FBS and 1% antibiotic/antimycotic solution was changed every other day throughout the study. Cells were cultured on the scaffolds for up to 19 days. An alamarBlue® assay to measure cell proliferation and viability (Invitrogen, Carlsbad, CA) was performed on every other day from day 1 to day 19 to examine the growth and cytocompatibility of IVD cells on printed elastic PU scaffolds versus a flat surface control. Briefly, cells were cultured in an alamarBlue® and media mixture at a ratio of 1:40, for 4 hours, after which the media was removed and absorbance at 570 nm and 600 nm was measured using spectrophotometry.

3.2.4 Morphological Study

Scanning electron microscopy (SEM, Hitachi TM-1000) was used to visualize the morphology of the printed scaffold. All fluorescent and light microscope images were

taken using a Leica TCS SP5 AOBS Confocal Microscope (Leica Microsystems Inc., Exton, PA, U.S.A.). For fluorescent staining, cells were fixed with 4% paraformaldehyde after 3 weeks of culture, and phalloidin 488 and DAPI were used to stain the actin filaments and the nuclei of the chondrocytes within the scaffolds, respectively. The morphology of the IVD cells was observed to determine if cells were spread out and attached to the 3-D scaffolds.

3.2.5 Statistical Analysis

One-way ANOVA was performed on the values of G'(storage shear modulus) and G* (complex shear modulus) across the frequency range 0.05-1.05 Hz with a least significant difference (LSD) post hoc comparison set at $p<0.05$ using SPSS 17 statistical software (Chicago, USA). The results of the alamarBlue® assay comparing PU scaffolds with control samples were also analyzed using the methods described above.

3.3 Results

3.3.1 Scaffold Fabrication

The method presented in this paper uses a freezing stage coupled with a custom-built additive manufacturing apparatus allowing for the creation of scaffolds with multiple layers and lamellar structures using solid freeform fabrication through the extrusion of polymer solutions onto a temperature controlled stage. The freezing stage aided in the solidification of the structure at the time polymer solution was extruded out of the ultra-

fine pipettes through convection of the cold temperatures from the stage to the extruded polymer solution. Ultra-fine pipettes allowed for fabrication of scaffolds with similar structure to native IVD tissue with the high resolution and reproducibility necessary for controlling the scaffold microstructure. Figure 3.2 shows SEM images of the scaffold, confirms the 3-D structure, and the ability of the scaffold to mimic native lamellar IVD structure.

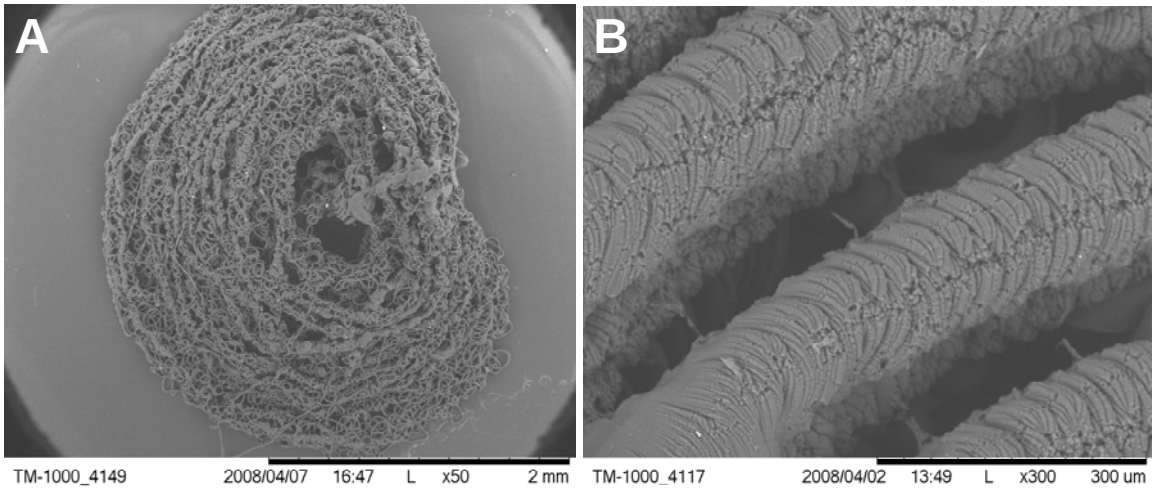

Figure 3. 2: SEM images of a custom designed and layered PU 3-D scaffold structure mimicking the natural shape of the IVD and showing a lamellar structure (A), multiple layers of PU stacked in a 3-D structure, proving accuracy and effectiveness of the bioprinter, micropipettes, and freezing stage to maintain high resolution in three dimensions (B).

3.3.2 Mechanical Properties of Scaffolds

Elastic properties were determined with mechanical analysis of the scaffolds in compression and shear. The average compressive stress-strain curve is shown in figure 3.3A. The scaffolds showed a J-shaped stress-strain curve, observed in soft tissues similar to the IVD. The initial compressive storage modulus (E') in the toe region was 45.4 ± 5.6

KPa (mean ± the standard error of the mean), while the compressive modulus (E') of the linear region was 350 ± 19.6 KPa. These values correspond to similar tests carried out on native IVD tissue [28,29]. The shape of the curve indicates that the scaffolds significantly stiffen under large strains (greater than 40%). Elastic hysteresis was observed in the scaffold during dynamic compression (figure 3.3B). Scaffolds did not show permanent deformation after 5 cycles of compressive loading up to 65% strain, which is significantly more strain than native IVD tissue typically undergoes during loading, proving the scaffolds can handle deformation well [25]. Aside from basic compressive testing, compressive shear testing to 1.5% strain was also carried out as the native IVD undergoes shear deformations [26]. During compressive shear tests, compression at 15%, 30%, and 45% strain were used, as compressive strains of around 15% are similar to normal physiologic compressive strains [25,30]. The storage shear modulus (G') represents the elastic stored energy of the scaffold material. The dynamic shear modulus (G*) is comprised of both G' and G" (energy lost as heat) and can provide important information as a material property. The printed PU IVD scaffolds displayed significant elastic responses, during shear tests, in which G* was primarily governed by G'. One-way ANOVA was performed across each frequency for G*, G', and G'' with compressive strain serving as the comparison factor. All of the dynamic shear properties were dependent both on the frequency and the compressive strain. Increases in compressive strain resulted in increases for G*, G', and G''. Increasing the frequency also increased the compressive dynamic shear properties, but this was not found to be significant. The compressive strain effect was found to be significant for G*, G', and G'' ($p<0.05$) as

shown in Table 3.1. Since the material displayed primarily elastic behavior, the trends for G'' are not shown in figure 3.4 due to the minor contributions to G*. During shear testing, all recorded frequencies between 0.05-1.05 Hz were analyzed against the compressive strains and showed significant differences between all strains with p-values all below 0.02. At a frequency of 1.0 Hz, compressive dynamic shear moduli were 57 ± 23.7 KPa, 97 ± 15.2 KPa, and 135± 12.6 KPa for 15%, 30%, and 45% compressive strains, respectively. At a frequency of 1.0 Hz, compressive storage shear moduli were 56.7 ± 23.7 KPa, 96.5 ± 15.2 KPa, and 134± 12.4 KPa at 15%, 30%, and 45% compressive strains, respectively. Figure 3.4 validates that energy is primarily stored by the material during deformation, as G' and G* are highly similar, proving the material has significant elastic behavior. Furthermore, our results were very similar to other compressive shear studies performed on native tissue [26].

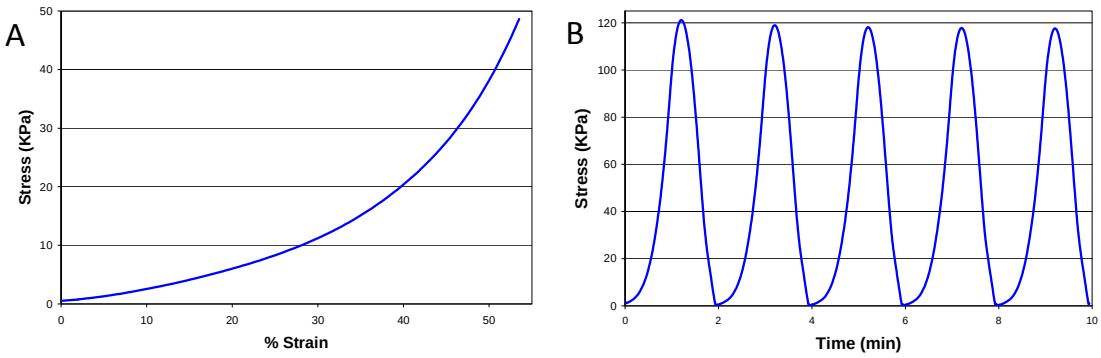

Figure 3. 3: (A) Stress-strain curve showing average behavior of printed PU IVD scaffolds. Scaffolds exhibited elastic behavior, showing a J-shaped stress-strain curve typically observed in soft tissues like the IVD. (B) Representative dynamic compressive testing on PU IVD scaffolds which exhibited elastic hysteresis, and did not show permanent deformation after multiple cycles of dynamic compressive loading.

Table 3. 1: Statistical analysis for Dynamic Shear Moduli at 1 Hz between Compressive Strains of 15%, 30%, and 45% (n=12).

Variation		Mean (KPa)	The standard error of the mean (KPa)	Significance
Storage Modulus (G')	15%	56.65	23.74	p<0.05
	30%	96.5	15.16	
	45%	133.9	12.55	
Loss Modulus (G'')	15%	6.51	1.97	p<0.05
	30%	9.55	1.27	
	45%	13.09	1.63	
Dynamic Modulus (G*)	15%	57.03	23.77	p<0.05
	30%	96.96	15.2	
	45%	134.55	12.62	

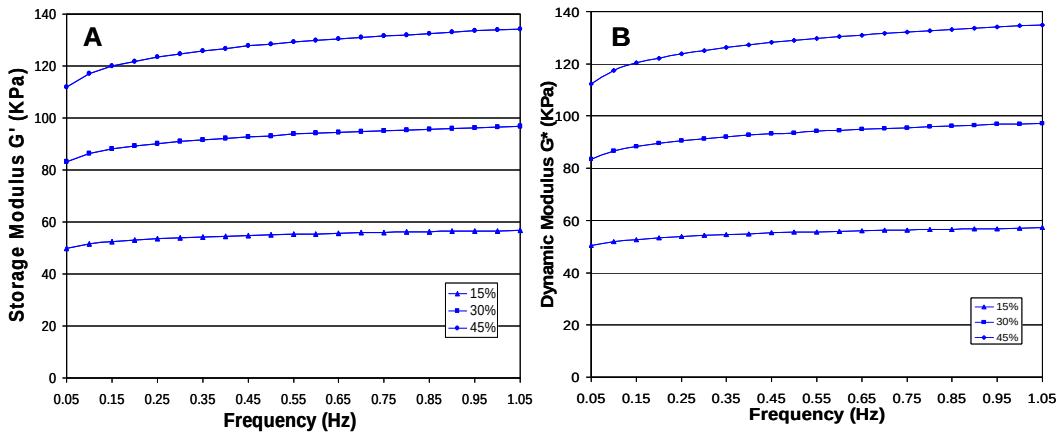

Figure 3. 4: Mean values of the storage modulus G' (A), and the dynamic shear modulus G* (B) at a fixed shear strain of 1.5% over the frequency range of 0.05-1.05 Hz. Samples were tested at compressive strains of 15%, 30%, and 45%, and storage shear moduli was found to significantly increase with increasing strain.

3.3.3 In vitro evaluation

The scaffold presented a structure which promoted IVD cell attachment and growth on the elastic lamellar scaffolds as shown in figure 3.5. Chondrocytes aligned along the concentric lamellae proving the ability of the scaffold to promote a desired cell response, as cells in the native IVD are highly aligned along the lamellae. The elastic materials used to create the scaffold were found to be biocompatible and promoted cellular proliferation. An alamarBlue® assay was used to determine cell viability on the scaffold constructs by measuring metabolic activity of the cells. After 19 days in cell culture the cells proved to remain more viable on the PU scaffold constructs compared to the 2D culture (figures 3.5 & 3.6). The data presented shows the average of 12 samples ± standard error of the mean. There was no negative effect on cell viability of the printed IVD scaffold as compared to the tissue culture polystyrene. Additionally, scaffold degradation did not affect cell viability or proliferation since the material we developed has a degradation profile for 5-6 months. Table 3.2 shows that on days 13, 17, and 19 increased cell proliferation was observed on the PU scaffolds which was significantly different from the control wells ($p<0.05$). It should be noted that cell proliferation decreased after day 15. This is probably due to the fact that the cells had reached confluence. In some of the control wells, the confluent cells contracted into ball like structures, possibly limiting the presence of adherent cells on substrates.

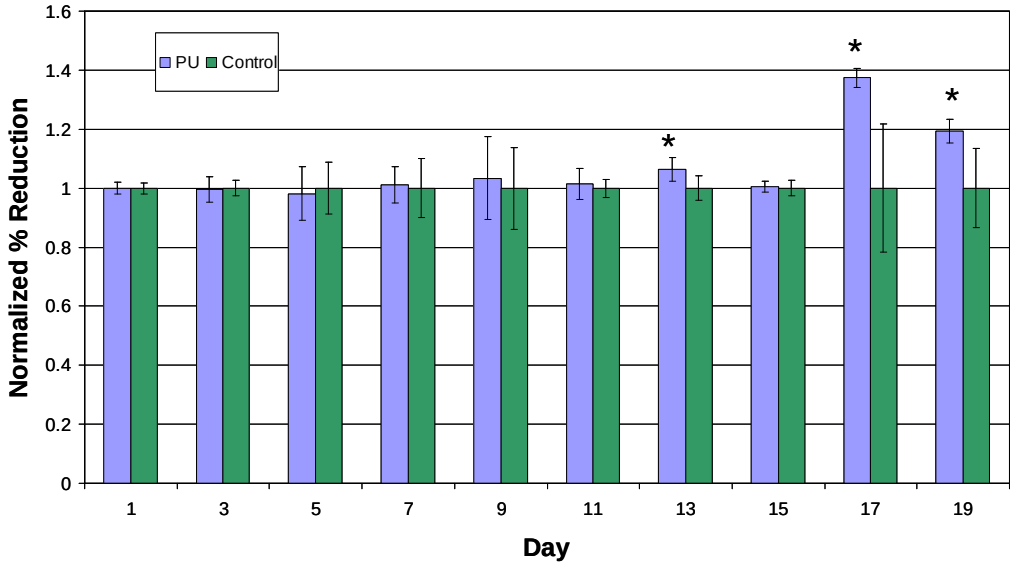

Figure 3. 5: Normalized % reduction graph using AlamarBlue cell metabolic assay showing cytocompatibility of PU scaffolds (n=12) compared to the control (n=12). Average of control wells was normalized to 1, and the PU scaffolds were compared at each day (Annotation '*' indicates samples were statistically significant, p<0.05).

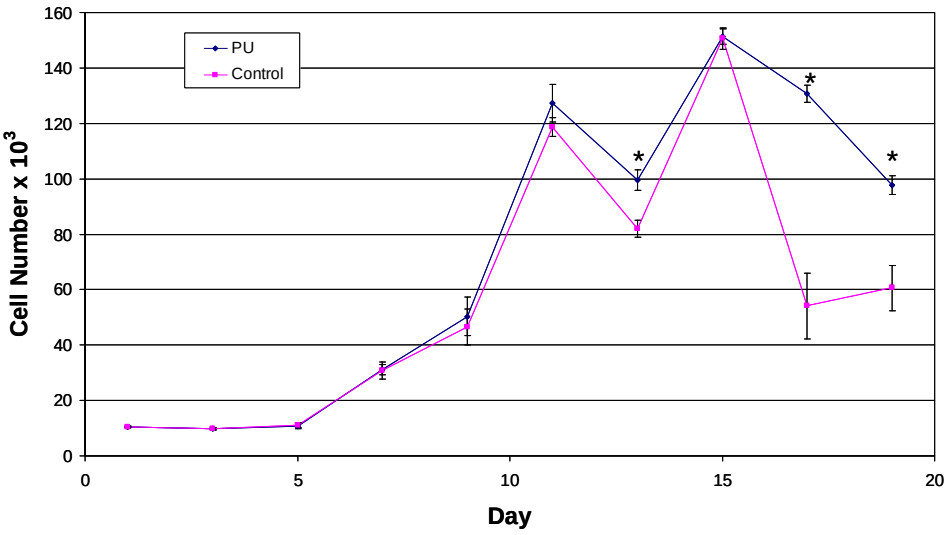

Figure 3. 6: Chondrocyte viability measured using metabolic AlamarBlue assay. Comparable proliferation and viability of chondrocytes were found on printed PU IVD scaffolds and tissue culture polystyrene wells (Annotation '*' indicates samples were statistically significant, p<0.05).

Table 3. 2: Statistical analysis for Normalized % Reduction of AlamarBlue Metabolic Cell Assay for Cytotoxicity (n=12).

Variation		Mean (%)	Standard Deviation (%)	Significance
Day 13	**PU**	106.39	3.97	p<0.05
	Control	100	4.19	
Day 17	**PU**	137.45	3.23	p<0.05
	Control	100	1.85	
Day 19	**PU**	119.45	4.05	p<0.05
	Control	100	13.41	

3.3.4 Morphological Study

Using our device, elastic polymers were deposited onto a freezing stage using extrusion to form lamellar structures mimicking the natural structure of IVD tissue as shown in figure 3.7. Polymer extrusion can be controlled precisely up to a micron level resolution. Figure 3.2 shows that concentric layers were created with spacing ranging from 20µm to 200µm for the accommodation of cells while allowing room for extracellular matrix proteins to be secreted. Additionally, cells preferentially aligned along the scaffold structure, showing comparable morphology to native IVD cell alignment within the concentric lamellae (figure 3.7) [22,31].

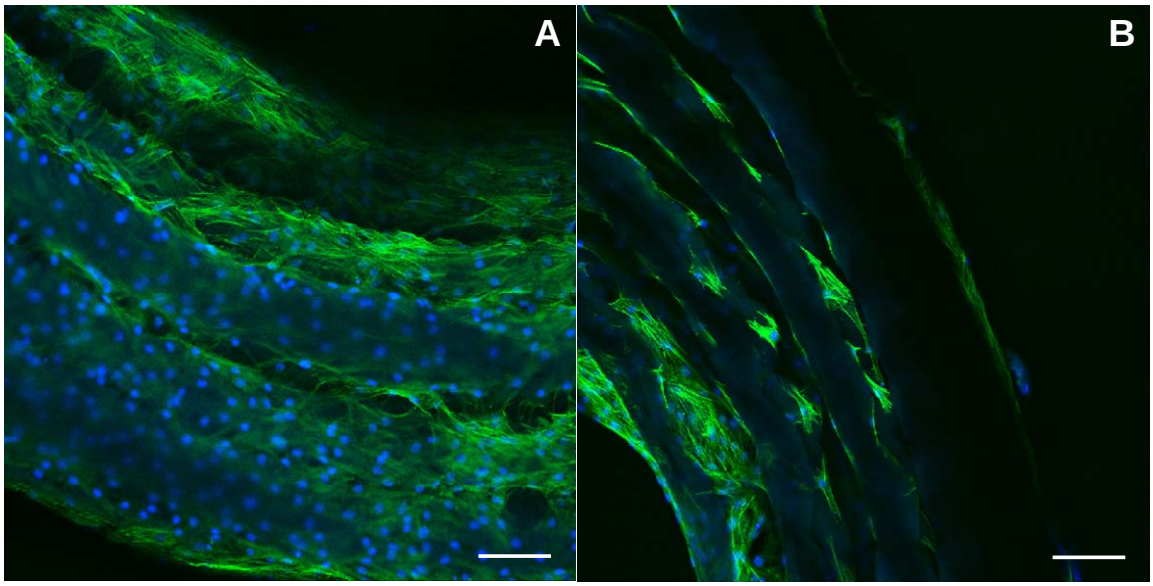

Figure 3. 7: Top view of the scaffold showing viable cells across the entire lamellar structure, with cells attaching to the entire scaffold (A), inside view of 3-D scaffold, proving cell infiltration into the inner lamellae (B). It can be seen that spacing can be accurately controlled to allow the migration of cells into the lamellae. Cells within the lamellae also aligned with the scaffold. (Scale bar = 100 µm).

3.4 Discussion

The bioprinting apparatus described permitted the use of multiple solution based polymers and showed the capacity to use both natural and synthetic materials. The freezing stage allowed for fast solidification of the polymer solution and could maintain temperatures from -40 °C to room temperature, allowing the rate at which the polymer solidified to be precisely controlled. The method used in this paper proved the capability to control both micro and macrostructure of material constructs using computer aided design. For comparison, the compressive storage moduli of the scaffolds appears to be sufficient for the repair of the outer region of the IVD as our experimental values (350

KPa) are within the range of 220-540 KPa previously reported in the literature for native IVD tissue [29]. However, compressive loads were on the low spectrum of physiologic values. We expect that when cells grow into the scaffold and will produce extracellular matrix to further improve the compressive loading capability. The scaffold created provides elastic properties while mimicking the natural shape and morphology of the IVD, as the outer region of the scaffold consists of layered, elastic PU forming concentric lamellae.

The scaffolds fabricated using this technique exhibited elastic properties which may help increase natural motion while also absorbing loads within the spine. Dynamic shear mechanical data was specifically analyzed at 1 Hz because this value is similar to frequencies observed during common everyday activities. Although frequencies may increase up to 10 Hz, this is highly uncommon [28,32]. Dynamic viscoelastic analysis of the scaffolds proved the elastic nature of the degradable PU. For comparison, the experimental values of G' (56.7 KPa) and G* (57 KPa) were slightly larger than the reported native IVD tissue values of 5.8 and 7.4 KPa, respectively [26]. However, the experimental value of G" (6.5 KPa) was almost identical to the reported value of 5.2 KPa [26]. This analysis leads to the interpretation that the material used here is slightly more elastic than the native IVD tissue. The cyclic compressive shear moduli of the material increased with compressive strain and also frequency, proving the effectiveness of the scaffold to respond to large loads. An increase in stiffness under large stresses is a common feature of the IVD, possibly preserving disc structure under larger loads to help maintain cell viability. The primary effect of G' during shear testing indicates that the

governing component of this scaffold material is the elastic portion. Values of the loss tangent (tan delta) were not significantly different between compressive strains, indicating that the ratio of stored energy to dissipated energy remained relatively constant at increased strain (data not shown).

Many previous studies have attempted to fabricate a suitable IVD scaffold, but none have accounted for the complex lamellar structure of the annulus fibrosus in the outer IVD region. This study uses a specialized biofabrication method to create scaffolds with very similar structure and overall shape of native IVD tissue. This study also highlights the importance scaffold microstructure plays in guiding cell behavior through cell-matrix contact. Chondrocytes seeded onto the scaffolds directly infiltrated into the lamellae. Eventually, the cells began to elongate along the layers of the scaffold. After 19 days in culture, the chondrocytes form an aligned cell structure similar to that observed in native IVD. Throughout this culture period, the scaffolding material did not yet begin to degrade. Results from cytotoxicity and cell viability assays indicate that this material is non-toxic and serves as an excellent scaffold choice for further investigations into IVD regeneration. In another study to evaluate the degradation of our LDI-based PU, we found that the degradation products are not toxic to cells. This study serves as proof that the future of IVD tissue engineering will rely on the ability and successes of researchers to properly design and fabricate scaffolds that satisfy the requirements of matching native tissue properties with the engineered materials.

3.5 Conclusion

This is the first study to use a freezing stage to control the resolution of a three dimensional additive manufacturing device for the fabrication of an IVD scaffold. An advantage of this technique is the ability to successfully reproduce large quantities of tissue scaffolds. By combining ultra-fine micropipettes and a freezing stage, the resolution of the apparatus can be greatly improved. The use of the freezing stage effectively allows a high resolution design down to the micron level. With the freezing stage, structure of the scaffold can be controlled precisely allowing for control over cell morphology. Multiple facets were investigated prior to the creation of the scaffold including: motor speed, polymer extrusion rate, polymer concentration, and freezing stage temperature. The spacing between the subsequent layers of the printed elastic scaffolds is mimetic to the natural IVD and the spacing allows room for cell attachment while providing space for ECM deposition within the scaffold and ultimately creating a favorable structure to promote IVD regeneration. The biodegradable PU scaffolds exhibited superb elastic properties under compression, proving the construct to be an ideal material for IVD tissue regeneration. Furthermore, during compressive shear testing at physiological frequencies, the scaffolding constructs behaved similarly to native IVD tissue, proving their effectiveness to emulate native IVD biomechanics. Future studies will be carried out over a longer time period to determine how scaffold degradation affects both cell viability and mechanical properties.

3.6 References

1. Luo X, Pietrobon R, Sun SX, Liu GG, Hey L. Estimates and patterns of direct health care expenditures among individuals with back pain in the United States. Spine 2004;29(1):79-86.

2. Boos N, Weissbach S, Rohrbach H, Weiler C, Spratt KF, Nerlich AG. Classification of age-related changes in lumbar intervertebral discs: 2002 Volvo Award in basic science. Spine (Phila Pa 1976) 2002;27(23):2631-44.

3. Masuda K, An HS. Prevention of disc degeneration with growth factors. Eur Spine J 2006;15 Suppl 3:S422-32.

4. An HS, Thonar EJ, Masuda K. Biological repair of intervertebral disc. Spine (Phila Pa 1976) 2003;28(15 Suppl):S86-92.

5. Fazzalari NL, Costi JJ, Hearn TC, Fraser RD, Vernon-Roberts B, Hutchinson J, Manthey BA, Parkinson IH, Sinclair C. Mechanical and pathologic consequences of induced concentric anular tears in an ovine model. Spine (Phila Pa 1976) 2001;26(23):2575-81.

6. Cowan JA, Jr., Dimick JB, Wainess R, Upchurch GR, Jr., Chandler WF, La Marca F. Changes in the utilization of spinal fusion in the United States. Neurosurgery 2006;59(1):15-20; discussion 15-20.

7. Huang RC, Girardi FP, Cammisa FP, Jr., Lim MR, Tropiano P, Marnay T. Correlation between range of motion and outcome after lumbar total disc replacement: 8.6-year follow-up. Spine 2005;30(12):1407-11.

8. McAfee PC, Cunningham B, Holsapple G, Adams K, Blumenthal S, Guyer RD, Dmietriev A, Maxwell JH, Regan JJ, Isaza J. A prospective, randomized, multicenter Food and Drug Administration investigational device exemption study of lumbar total disc replacement with the CHARITE artificial disc versus lumbar fusion: part II: evaluation of radiographic outcomes and correlation of surgical technique accuracy with clinical outcomes. Spine 2005;30(14):1576-83; discussion E388-90.

9. Shuff C, An HS. Artificial disc replacement: the new solution for discogenic low back pain? Am J Orthop 2005;34(1):8-12.

10. Alini M, Li W, Markovic P, Aebi M, Spiro RC, Roughley PJ. The potential and limitations of a cell-seeded collagen/hyaluronan scaffold to engineer an intervertebral disc-like matrix. Spine (Phila Pa 1976) 2003;28(5):446-54; discussion 453.

11. Mwale F, Iordanova M, Demers CN, Steffen T, Roughley P, Antoniou J. Biological evaluation of chitosan salts cross-linked to genipin as a cell scaffold for disk tissue engineering. Tissue Eng 2005;11(1-2):130-40.

12. Wan Y, Feng G, Shen FH, Laurencin CT, Li X. Biphasic scaffold for annulus fibrosus tissue regeneration. Biomaterials 2008;29(6):643-52.

13. Yao H, Gu WY. Physical signals and solute transport in human intervertebral disc during compressive stress relaxation: 3D finite element analysis. Biorheology 2006;43(3-4):323-35.

14. Hukins DW. Tissue engineering: a live disc. Nat Mater 2005;4(12):881-2.

15. Wan Y, Feng G, Shen FH, Balian G, Laurencin CT, Li X. Novel biodegradable poly(1,8-octanediol malate) for annulus fibrosus regeneration. Macromol Biosci 2007;7(11):1217-24.

16. Melrose J, Smith SM, Appleyard RC, Little CB. Aggrecan, versican and type VI collagen are components of annular translamellar crossbridges in the intervertebral disc. Eur Spine J 2008;17(2):314-24.

17. Ruan DK, Xin H, Zhang C, Wang C, Xu C, Li C, He Q. Experimental intervertebral disc regeneration with tissue-engineered composite in a canine model. Tissue Eng Part A;16(7):2381-9.

18. Zhang C, Ruan D, Zhang R. [In vitro studies on tissue engineered intervertebral disc]. Zhongguo Xiu Fu Chong Jian Wai Ke Za Zhi 2007;21(5):478-81.

19. Nesti LJ, Li WJ, Shanti RM, Jiang YJ, Jackson W, Freedman BA, Kuklo TR, Giuliani JR, Tuan RS. Intervertebral disc tissue engineering using a novel hyaluronic acid-nanofibrous scaffold (HANFS) amalgam. Tissue Eng Part A 2008;14(9):1527-37.

20. Yang X, Li X. Nucleus pulposus tissue engineering: a brief review. Eur Spine J 2009;18(11):1564-72.

21. Grad S, Kupcsik L, Gorna K, Gogolewski S, Alini M. The use of biodegradable polyurethane scaffolds for cartilage tissue engineering: potential and limitations. Biomaterials 2003;24(28):5163-71.

22. Setton LA, Bonassar L, Masuda K. Regeneration and Replacement of the Intervertebral Disc: Elsevier; 2007.

23. Zhang C, Zhang N, Wen X. Synthesis and characterization of biocompatible, degradable, light-curable, polyurethane-based elastic hydrogels. J Biomed Mater Res A 2007;82(3):637-50.

24. Base Asplund JO, Bowden T, Mathisen T, Hilborn J. Variable hard segment length in poly(urethane urea) through excess of diisocyanate and vapor phase addition of water. Macromolecules 2006;39:4380-85.

25. Joshi A, Fussell G, Thomas J, Hsuan A, Lowman A, Karduna A, Vresilovic E, Marcolongo M. Functional compressive mechanics of a PVA/PVP nucleus pulposus replacement. Biomaterials 2006;27(2):176-84.

26. Iatridis JC, Setton LA, Weidenbaum M, Mow VC. The viscoelastic behavior of the non-degenerate human lumbar nucleus pulposus in shear. J Biomech 1997;30(10):1005-13.

27. Yao H, Justiz MA, Flagler D, Gu WY. Effects of swelling pressure and hydraulic permeability on dynamic compressive behavior of lumbar annulus fibrosus. Ann Biomed Eng 2002;30(10):1234-41.

28. Iatridis JC, Setton LA, Foster RJ, Rawlins BA, Weidenbaum M, Mow VC. Degeneration affects the anisotropic and nonlinear behaviors of human anulus fibrosus in compression. J Biomech 1998;31(6):535-44.

29. Best BA, Guilak F, Setton LA, Zhu W, Saed-Nejad F, Ratcliffe A, Weidenbaum M, Mow VC. Compressive mechanical properties of the human anulus fibrosus and their relationship to biochemical composition. Spine (Phila Pa 1976) 1994;19(2):212-21.

30. White AA, 3rd. Clinical biomechanics of cervical spine implants. Spine (Phila Pa 1976) 1989;14(10):1040-5.

31. Guerin HAL, Elliot DM. Structure and Properties of Soft Tissues in the Spine. In: Kurtz SM, Edidin, A. A., editor. Spine Technology Handbook: Elsevier; 2006.

32. Krag MH, Pflaster DS, Johnson CC, Haugh LD, Pope MH. Effect of denucleation and degeneration grade on intervertebral disc stress relaxation. Trans Orthop Res Soc 1993;18(207).

CHAPTER 4

4. FABRICATION OF AN ELASTIC LAMELLAR SCAFFOLD USING RAPID PROTOTYPING FOR INTERVERTEBRAL DISC REGENERATION

4.1 Introduction

Low back pain, which affects over 80% of the adult population at some point in their lives, accounts for 5% of all surgical procedures, amounting to nearly $90 billion in annual costs [1]. One primary cause of low back pain is the degeneration of the intervertebral disc (IVD), which results in the compression of the spinal nerves and adjacent vertebrae [2]. Exact causes of degeneration are unknown, but it is thought that natural aging, biological and genetic factors, and mechanical stimuli may play a significant role in the degenerative process [3-6]. Conventional methods to alleviate this pain include spinal fusion and artificial disc replacement, neither of which restore natural kinematics within the spinal column [7-11]. As an alternative to these conventional approaches, tissue engineered IVD constructs offer the advantage of biointegration while preserving the essential attributes of natural motion and disc space restoration. The use of elastic polymeric artificial discs to mimic the mechanical properties of the native IVD offer a solution to some of the problems encountered with current disc replacements.

The IVD is the soft and tough fibrocartilage disc that is sandwiched between adjacent vertebrae in the spine. This tissue functions as: 1) a ligament that holds the vertebrae of the spine together; 2) a shock absorber; and 3) a "pivot point" that allows the spine to bend, rotate, and twist. The IVD is composed of three structures: the nucleus

pulposus (NP), the water-rich gelatinous center that primarily bears the pressure; the annulus fibrosus (AF), the collagen-rich fibrous structure of 15~25 concentric sheets of collagen (lamellae) that confines the pressurized nucleus; and the vertebral end-plates (VEP), which are cartilaginous plates that are interwoven into the annulus at the disc-vertebrae interface and supply nutrients to the disc [12]. Chondrocyte-like disc cells reside in all three of these structures. The disc is kidney shaped and avascular, making natural regeneration difficult [13].

The current study focuses on the fabrication of structures that precisely mimic every facet of the AF, as the complex tissue architecture of this region has posed great challenges to researchers. This is most likely due to their inability to closely match the biological function, microstructure, and mechanical properties of the intricate AF. This region is a lamellar structure composed of collagen type I and II fibers, which maintain the tensile properties and prevent mechanical bulging of the disc, while also providing support for cell guidance and proteoglycan synthesis [14]. Cells within the AF are oriented in alignment with the lamellar collagen fibers [15]. It has been shown that cell alignment can be guided in accordance with a scaffold, as aligned substrates have been shown to influence cell morphology [16,17]. This is highly important for an IVD scaffold, in order to allow chondrocytes to spread out, align, and organize their cytoskeletons similar as in the native tissue [18,19]. In addition, aligned cells usually generate highly organized ECM in the direction of cell orientation [18,20]. This increase in cell orientation and ECM production on aligned substrates has also been shown to significantly increase the mechanical strength of the scaffolds [21]. From this data, it can be seen that a tissue engineered scaffold that

closely mimics the native architecture of the disc as closely as possible, which contains highly ordered lamellar layers, would demonstrate a major advancement compared to current IVD scaffold fabrication methods.

Few scaffold fabrication techniques have allowed for the reproducibility and spatial control over IVD scaffold design that rapid prototyping permits. However, electrospun nanofibers and other materials have been created to mimic the AF [22,23]. These scaffolds do not have the ability to be fabricated in a spatially controlled manner. Furthermore, few researchers have investigated the fabrication of IVD scaffolds with similar mechanical properties to the native disc. The mechanical integrity of the IVD is very important because it aids in maintaining spinal column height. The elastic nature of the IVD also allows the disc to absorb large compressive loads without permanent deformation. Therefore, we aim to reproduce an elastic IVD scaffolding material that better mimics natural IVD morphology and biomechanics.

The scaffold fabrication technology presented here uses a freezing stage coupled with a custom-made rapid prototyping apparatus to fabricate scaffolds that mimic the native IVD microstructures with high reproducibility. Additionally, this rapid prototyping setup enables the creation of patient specific scaffolds to make the technique more clinically relevant. The device extrudes polymer solution onto a freezing stage to create scaffolds through a layer-by-layer process, also termed "additive manufacturing" [24-27]. The freezing stage increases the polymer viscosity and solidifies the solution as it is extruded out of ultra-fine micropipettes, allowing the device to maintain a high resolution. In this study, a degradable chitosan/gelatin (Chs/Gtn) solution was used to

create an IVD scaffold that provides elastic properties, and promotes IVD cell adhesion and proliferation in alignment with the lamellar region. In addition to mechanical properties, the scaffold was designed in CAD to mimic the native AF, forming concentric lamellae in a kidney-like shape. Currently, we are not aware of any research claiming to have replicated IVD shape, microstructure, and the mechanical properties of the AF when fabricating an IVD scaffold or construct.

There is a great need for the development of tissue engineered scaffolds that simulate the natural 3-D morphology and microenvironment of targeted tissues. Many researchers have investigated tissue engineering applications to fabricate IVD scaffolds. However, the majority of studies on IVD tissue regeneration fail to simultaneously account for both biomechanical properties and natural tissue morphology, both of which are imperative for the success of an IVD scaffold [28-30]. The close correlation between the biological function and the molecular composition of the disc structures strongly suggests that a major task of IVD regeneration is to create scaffolds that precisely reproduce the structural and biological functions of disc structure. In this study, we aim to fabricate IVD scaffolds with the similar microstructures and mechanical properties as the native IVD tissue, and prove that tissue regeneration of the IVD is possible.

4.2 Materials and Methods

4.2.1 Rapid Prototyping Device

A rapid prototyping instrument was developed in our lab in order to fit the specific needs of this study (Figure 4.1). The motion controlling hardware and software were specially designed to fabricate scaffolds that mimic the AF region of the IVD. Microsoft Visual Basic was used to program the controlling software and control the motors and dispensers. AutoCAD was used to design the scaffolds mimicking the patterns of IVD lamellae. Micropipettes with 25 μm inner diameter were used as printing tips. A freezing stage (model BFS-30MP, Physitemp Inc., Clifton, NJ) with a finely tuned temperature control was used for fast freezing of the dispensed polymer solution into 3-D structures through layer-by-layer fabrication.

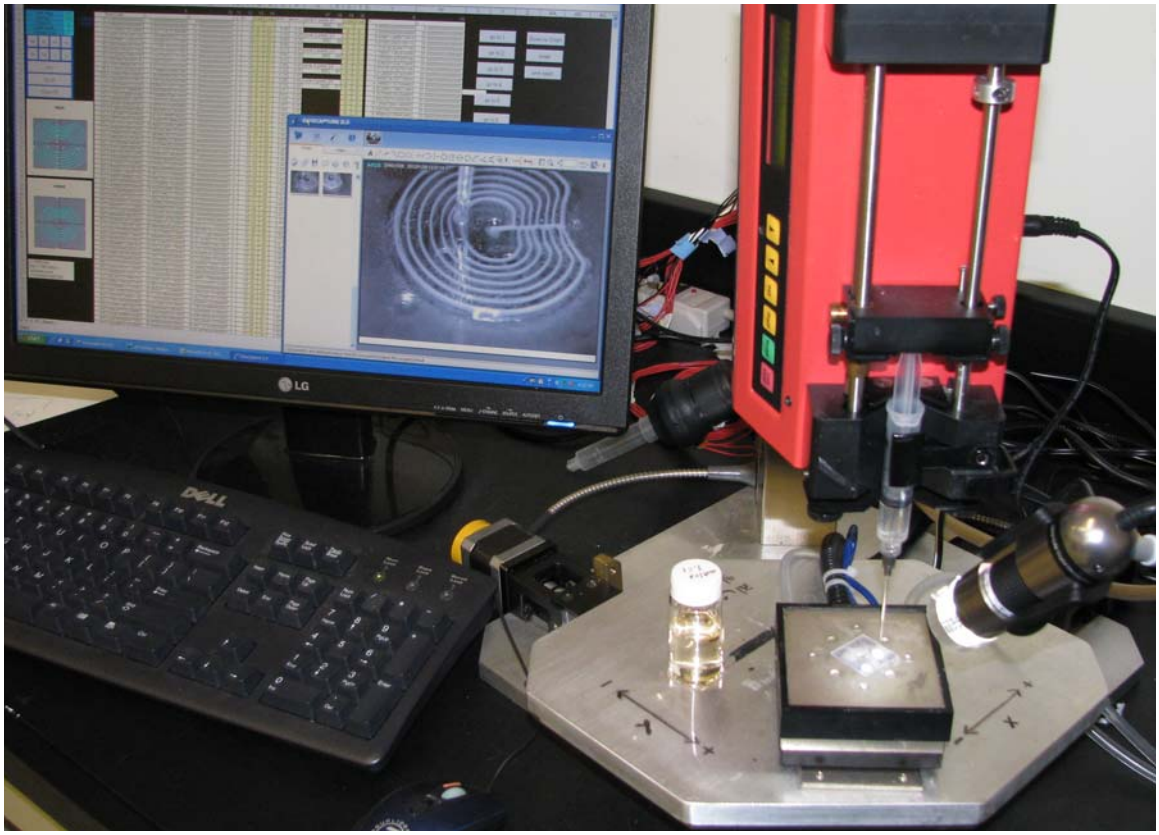

Figure 4. 1: The home made computer-controlled rapid prototyping apparatus with temperature-controlled stage for 3-D IVD scaffold printing.

4.2.2 Polymer Synthesis

Light curable, biodegradable, and biocompatible chitosan/gelatin (Chs/GEL) materials were created using a method developed in our lab for cartilage tissue regeneration [31]. Briefly, 5% gelatin was dissolved in dimethyl sulfoxide (DMSO) and 1% Irgacure 2959 (obtained from Ciba Specialty Chemicals) was dissolved separately in DMSO. 75 mg of methacrylate modified photocurable chitosan was mixed with 0.5 mg of Irgacure solution and added to 1.05 g of the gelatin/DMSO solution and dissolved for

10 minutes. The resulting solution was then used to fabricate the IVD scaffolds using the homemade bioprinter.

4.2.3 Scaffold Fabrication

Scaffolds were designed to replicate the natural IVD shape and histological morphology, as detailed in the literature (Figure 4.2) [32]. The polymer solution was dispensed using a syringe pump (Kent Scientific, Torrington, CT) at a flow rate of 0.005 ml/min. The polymer solution was fed through a glass micropipette tip and deposited on the freezing stage, which was set at 0° C. The approximate build time for each scaffold layer was around 5 minutes. After printing a layer, the micropipette was raised 50 μm in the z-direction and continued to lay the next layer. After finishing printing the whole structure, the freezing stage was powered off and ultraviolet light was exposed to the printed structure for 10 minutes to further solidify the scaffolds. The scaffolds were then frozen again and subjected to freeze-drying for 24 hours to extract the solvent. After lyopholization, scaffolds were rinsed with phosphate buffered saline (PBS) 3 times and then sterilized in 70% ethanol for 30 minutes, followed by 3 more rinses in sterile PBS.

4.2.4 Isolation and Culture of Chondrocytes on the 3-D Scaffolds

The IVDs of 4 to 5 month old calves were surgically removed and digested in order to isolate the IVD chondrocytes. The primary bovine IVD chondrocytes were cultured to passage 2 and then seeded on the scaffolds at a density of 1.25×10^4

cells/scaffold to examine their growth on the printed constructs. The IVD constructs were incubated at 37 °C and 5% CO_2 for 10 days before fixing in 4% paraformaldehyde and staining with AlexaFluor 488 Phalloidin (Invitrogen, Carlsbad, CA), for the actin filaments, and DAPI (Invitrogen, Carlsbad, CA), for the cell nuclei.

4.2.5 Visualization

Scanning Electron Microscopy (SEM, Hitachi TM-1000, Tokyo, Japan) was used to visualize the morphology of the fabricated scaffold. All microscope images of fluorescently labeled cells were taken using a Leica TCS SP5 AOBS Confocal Microscope (Leica Microsystems Inc., Exton, PA). The morphology of the cells was observed to determine if cells were attached, spread out, and aligned on the 3-D scaffolds. Images were then compared to native IVD tissue structures from the literature.

4.2.6 Mechanical Testing

Mechanical properties of the scaffolds were characterized using unconfined compression tests on hydrated samples at room temperature. IVD scaffolds (5.75 mm x 1.75 mm, diameter x height) were compressed at a rate of 1 mm/minute using a Dynamic Mechanical Analysis (DMA) Q800 system (TA Instruments, New Castle, DE) and discontinued at 45% strain. As previous studies have shown the IVD to experience roughly only about 15% compressive strain [33-35], compression to 45% accounted for loading of the scaffolds under extreme conditions. Afterwards, the engineering stress and

strain were evaluated while the compressive elastic modulus was calculated from the data of the stress-strain curves. Additionally, unconfined dynamic compression tests were completed for 7 cycles at a rate of 1 mm/minute over the range of 30-45% compressive strain. These strains were used as they simulate strains that are slightly larger than normal physiological loads, which prove the ability of the material to recover under abnormal conditions [36,37]. Dynamic experiments were also performed on the scaffolds, similar to previous studies [37]. Dynamic confined compression was used to compare the behavior of the scaffold material with native human IVD tissue at physiological frequencies. Briefly, 5 mm diameter hydrated samples were compressed to 10% strain and then dynamically compressed with amplitude of 1 μm using a frequency sweep ranging from 0.25 Hz to 5 Hz. This compressive strain and frequency range both simulate normal physiologic loading conditions within the IVD [33,38,39]. The values of G' (storage moduli), G'' (loss moduli), G* (complex moduli), and tan δ (phase angle) were all recorded and analyzed. All samples were tested in triplicate and represented as average ± standard deviation. The load cell readings were recorded on a computer and analyzed with TA Universal Analysis 2000 Software (TA Instruments, New Castle, DE).

4.2.7 Statistical Analysis

One-way ANOVA was performed on the values of G', G'', G*, and tan δ across the frequency range of 0.25 Hz to 5 Hz to compare the IVD scaffolds with the native human IVD tissues. A least significant difference (LSD) post hoc comparison set at

$p<0.05$ was used. SPSS V17 software (Chicago, USA) was used to perform the statistic analysis.

4.3 Results

4.3.1 Scaffold fabrication

Using the customized 3-D bioprinter (Figure 4.1), elastic Chs/Gtn polymers were fabricated into lamellar structures mimicking the natural shape (Figure 4.2A) and microstructure (Figure 4.2B) of the IVD. The video for the high resolution IVD scaffold printing process can be viewed from the supplemental materials section. The custom micropipettes enabled the fabrication of scaffolds with high resolution and concentric layers, having a thickness of 50-100 μm, with spacing of 100-200 μm for the accommodation of cells (Figure 4.3 & 4.4) [40-42]. The freezing stage allowed for fast solidification of the polymer solution and maintained the polymer solution viscosity, making it ideal for scaffold shape retention. In figure 4.3 and 4.4, it can be observed that cells lined along the scaffold patterns and migrated into the voids between the concentric lamellae, demonstrating the efficacy of this scaffold in mimicking the structure of the ECM and guiding the cellular organization of the native IVD. This is confirmed by comparing the structure of our fabricated scaffolds (Figure 4.4 A&B) with native IVD tissues (Figure 4.4C).

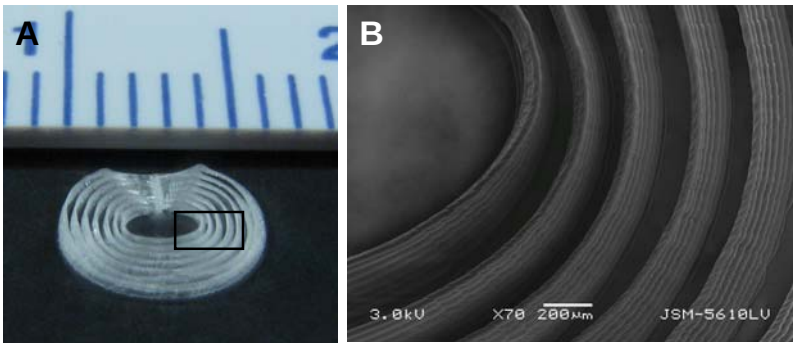

Figure 4. 2: Top-view image of the multilayered IVD scaffold, showing that the structure mimics the kidney shape and the organization of the concentric lamellar microstructures of the natural IVD (A). High magnification SEM image of the Chs/Gtn scaffold lamellae stacked in multiple layers, proving the efficacy of this technique to create layered structures in 3-D while accurately controlling spacing between layers, similar to native tissue (B).

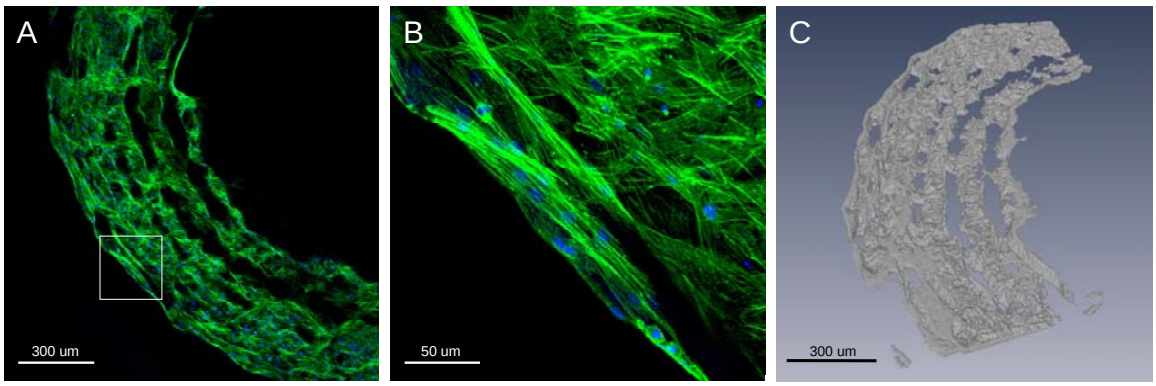

Figure 4. 3: Cells aligned along the 3-D Chs/Gtn IVD scaffold structure (A), higher magnification image showing cell elongation and alignment along lamellar scaffold (B). Actin filaments and nuclei stained in green and blue, respectively. 3-D rendering of cells on scaffold from Figure 4.3A (C). Cells and actin cytoskeleton are shown in grey, while the scaffold is where the empty lamellar channels are located.

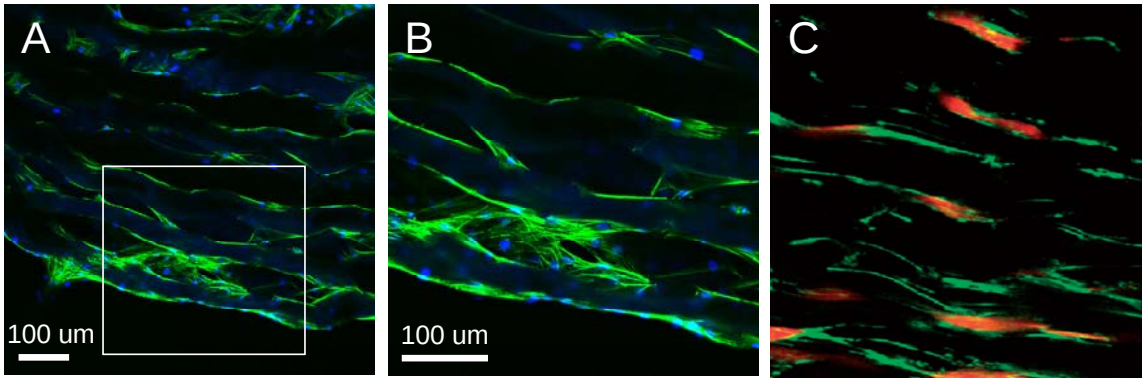

Figure 4. 4: Top view of the 3-D scaffold showing aligned IVD chondrocytes inside the scaffold, demonstrating cell infiltration into the inner lamellae (A), higher magnification image of cells aligned along lamellae (B), and cells in natural IVD tissue for comparison (C). Actin filaments are stained green (A-C), while nuclei are stained blue (A,B), and orange (C). [32]

4.3.2 Culture of Chondrocytes on the 3-D Scaffolds

The fabricated constructs resembled the native IVD architecture and shape, containing a highly ordered outer AF region, while emulating the elastic nature of the native IVD. Cells grew well on all of the scaffolds, confirming preliminary results demonstrating excellent biocompatibility [31]. Bovine IVD cells attached, migrated, and spread uniformly on and within the lamellar scaffolds, while proliferating in three dimensions (Figure 4.3 & 4.4). The designed 3-D scaffold increased the surface area of the construct allowing cells to attach and conform to the native tissue architecture. The cells became elongated and became layered in a concentric fashion similar to the native AF (Figure 4.3 & 4.4). This preferential cell alignment exhibited comparable cell morphology to the lamellae of native IVD tissue (Figure 4.3C) [32,43].

4.3.3 Biomechanical Analysis

The average compressive elastic modulus for the toe region, at <5% strain, was 0.101 ± 0.03 MPa, while the average elastic modulus for the elastic region, at >15% strain, was 0.31 ± 0.018 MPa (n=7). A representative stress-strain curve of the scaffold can be seen in Figure 4.5. There was no evidence that sustained compressive forces negatively affected scaffold thickness, as no permanent deformation occurred in samples compressed to 45% strain. This larger strain, compared to the typical 15% compressive strain that the IVD normally experiences, was used to validate the efficacy of the Chs/Gtn scaffolds in maintaining its ability to support extreme or abnormal loading [33-35]. The IVD, like other soft tissues, exhibits a J-shaped stress-strain curve similar to the curve shown in Figure 4.5, representing the Chs/Gtn scaffolds. Elastic hysteresis of the scaffolding material was observed after dynamic compressive loading, as seen in Figure 4.6. After 3 cycles of preconditioning, repeatable cycles were achieved where the material showed elastic properties. Scaffolds demonstrated the ability to resist fatigue over time, therefore proving an excellent choice as a disc replacement material. These results confirm that the elastic scaffold has ideal properties to absorb forces and recover without experiencing significant deformation. The Chs/Gtn scaffolds and native tissue were tested using dynamic physiological frequencies around 1 Hz across a range from 0.25 to 5 Hz (Figure 4.7). Specifically, G', G'', G*, and tan δ were analyzed for both samples, and the results indicated that the scaffolding material behaved very similar to native human IVD tissues. As seen in figure 4.7, energy is primarily stored by the material during deformation, as G'

and G* values between the scaffold and tissue are very similar, demonstrating that native IVD tissue and the scaffolding material are significantly governed by elastic properties. No significant difference was seen between the mechanical properties of the native tissue and scaffolds (Table 4.1), indicating that the scaffolds are suitable for use as an IVD replacement.

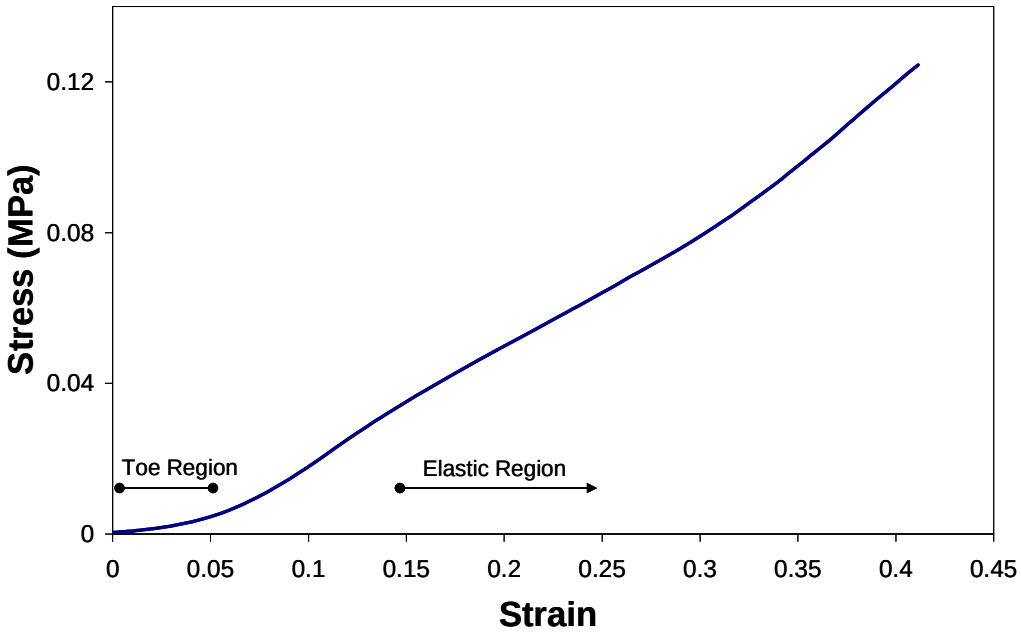

Figure 4. 5: Representative compressive stress-strain curve showing a J-shaped curve of the Chs/Gtn IVD scaffold with an initial toe region followed by a linear elastic region.

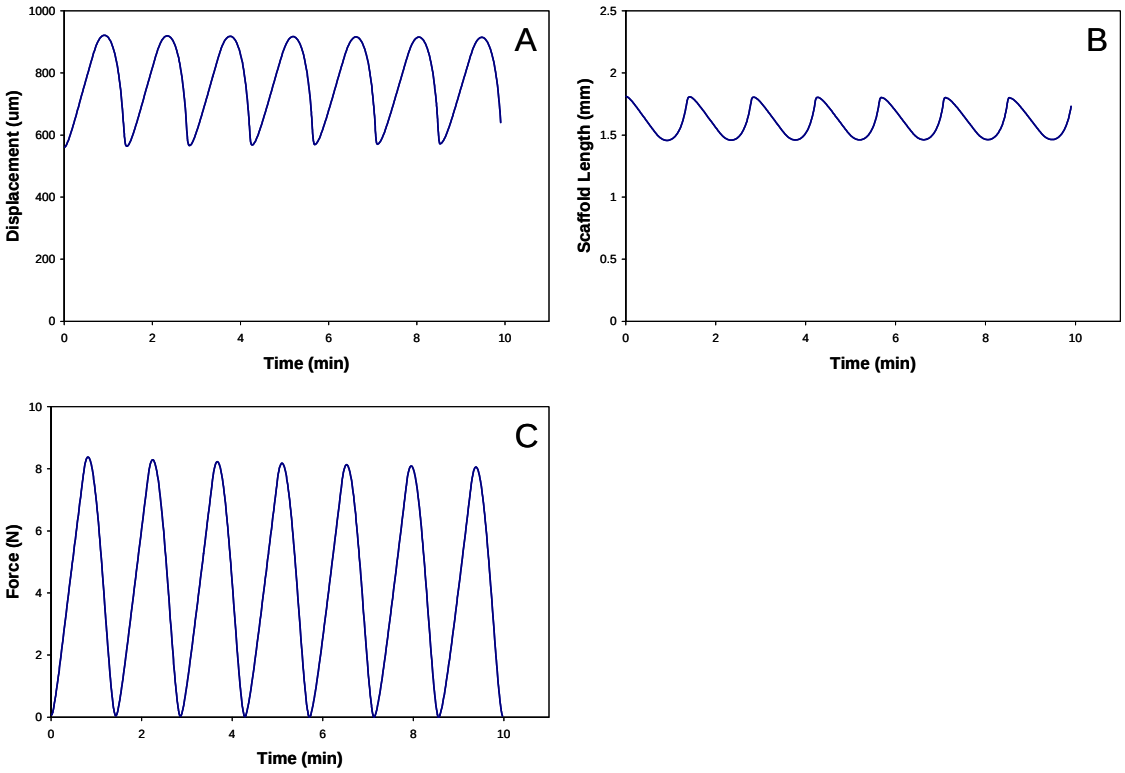

Figure 4. 6: Representative dynamic compressive loading curve of the Chs/Gtn IVD scaffold. For the displacement of 30% to 45% (A), scaffold size was not altered after compressing (B), and the scaffolds were able to maintain constant forces, proving that the Chs/Gtn material is maintaining its elastic integrity (C).

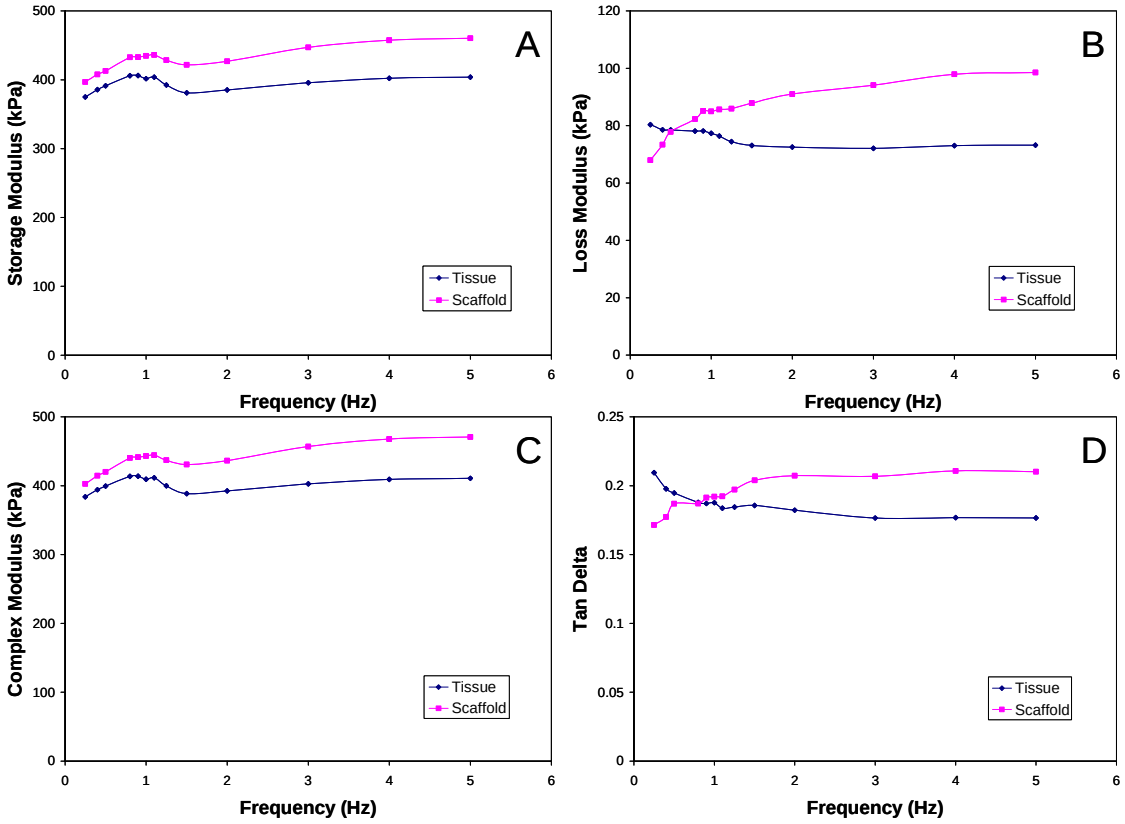

Figure 4. 7: Graphs showing very similar average G' (A), G'' (B), G* (C), and tan δ (D) of human IVD tissues and IVD scaffolds (n=7). Samples were tested across a dynamic frequency range from 0.25 to 5 Hz.

Table 4. 1: At a physiological frequency of 1 Hz, there was no significant difference in mechanical properties (G', G'', G*, and tan δ) between the scaffolds and the native IVD tissues. Data is shown as average ± standard deviation.

	Storage Modulus (kPa)	**Loss Modulus (kPa)**	**Complex Modulus (kPa)**	**Tangent Delta**
Tissues (n=7)	401.6 ± 191.8	77.3 ± 45.1	409.3 ± 196.1	0.188 ± 0.055
Scaffolds (n=7)	434.8 ± 214.5	85 ± 45.9	443 ± 219.3	0.192 ± 0.016

4.4 Discussion

One hurdle in the field of regenerative medicine is to create a method to fabricate tissue scaffolds that can be translated clinically for a variety of patients. The rapid prototyping technology developed here incorporates a customized scaffold design, enabling the creation of patient-specific tissue engineered constructs. Current disc replacement strategies do not account for biological growth or integration when compared to the native IVD. Furthermore, previous scaffold fabrication methods aimed at overcoming the shortcomings of spinal fusion and the current disc replacements fail to address the importance of replicating scaffold microstructure and biomechanics. Therefore, a rapid prototyping approach was developed in which 3-D scaffolds with morphological, biological, and mechanical properties similar to those of native IVDs could be produced. This method provides a way for 3-D scaffold formation through layer-by-layer fabrication in a reproducible and cost effective manner.

A lamellar disc scaffold formed from elastomers would offer much better compliance and may allow the restoration of natural three dimensional spinal motions compared to current disc replacement options. The novel scaffold with lamellar structures closely mimics the histological structure found in the AF portion of native IVDs. Lamellar structures also allow a greater surface area for cell adhesion and growth. Currently, many different techniques have been used to fabricate scaffolds for IVD regeneration; however, few have been able to fabricate the complex lamellar structure that is unique to natural IVD architecture. The ability of our bioprinted scaffold to mimic the lamellar pattern, thickness, as well as the spacing between the lamellae within the

native IVD, corresponds with data supported by the literature for both the layer thickness as well as the interlamellar spacing [40-42]. Furthermore, this study shows the ability to guide cell organization on a scaffold mimicking IVD microstructure by controlling scaffold microstructures. To this end, we used a bioprinting-based rapid prototyping technique that combines ultra-fine micropipettes for liquid extrusion and a freezing stage for the fast solidification of the biomimetic scaffolds. As the polymer solutions solidify rapidly, the scaffold becomes self supporting and supports the addition of new layers and the creation of 3-D structures. This method is highly valuable as it allows for the use of many different polymer solutions and can reproducibly create scaffolds with varying 3-D configurations and definitive microstructures.

The scaffolds created mimic the native IVD structure while promoting cell attachment and viability. Chondrocytes attached and aligned in the direction of the outer lamellae, similar as in the native structure of the IVD. When mimicking the highly organized native IVD, it is important that the lamellar IVD scaffold transforms cells into an aligned configuration. This aligned configuration will translate into the production of ECM in alignment with the fabricated scaffold as evidenced by other studies using oriented substrates to increase matrix deposition [18,19,44]. Scaffold images show a structure in which cells could attach, proliferate, and create ECM necessary for maintaining IVD function [45-47]. Space for aggrecan production is extremely important in the IVD as their hydrophilic properties help the disc material retain water and remain healthy and functional. In addition, cellular synthesis of aligned matrix within the material will further increase the mechanical properties of the scaffold [21].

The 3-D elastic Chs/Gtn scaffold showed superb deformability while having the ability to be press fitted in between the vertebrae. Large compressive stresses can be achieved without the polymer scaffold material failing. Furthermore, the compressive moduli of the scaffold correlates with properties of normal IVD tissue reported in the literature, proving the efficacy of our scaffolds in satisfying native disc biomechanics requirements [39,48,49]. Dynamic testing proved that the scaffolds could handle large deformations, accounting for extreme physiologic circumstances. Additionally, the material remained elastic under higher physiological frequencies. Dynamic mechanical data was specifically analyzed at 1 Hz because this value is similar to frequencies experienced in humans during common everyday activities [50]. These dynamic loading tests validated these scaffolds as suitable IVD disc replacements, as both the native tissue and scaffolding material had similar properties as well as were both governed by the storage modulus (G').

The IVD has a limited potential to regenerate because it is avascular, making IVD degeneration a difficult therapeutic target and a challenging task for tissue engineering. Current surgical remedies to solve the problem of disc degeneration do not address the need for a regenerative therapeutic based material design. An elastic, degradable polymer based scaffold that is biocompatible and can preserve natural 3-D kinematics within the spine is needed. The novel biomaterial scaffold design discussed in this paper mimics the AF architecture of the native IVD by successfully reproducing the lamellar nature of the disc. Furthermore, this scaffold is advantageous over other IVD therapies as it replicates natural IVD tissue biomechanical properties. The technique described utilizes a method

that may help regenerate the unique IVD structure for future applications by matching native tissue structure and biomechanics. Also, as this method of rapid prototyping does not use high temperatures, it allows for drug encapsulation and has the ability to use a broad variety of biomaterials, making it an ideal candidate for a wide variety of future applications.

4.5 Conclusion

The development of a computer-aided tissue engineering platform for IVD regeneration is a challenging task. This study focused on using a rapid prototyping technique to fabricate IVD scaffolds with similar microstructures and biomechanics to the native IVD tissues. It was determined that the fabricated scaffolds, in combination with IVD cells, may be suitable to promote IVD tissue regeneration as they encouraged cell morphology and arrangement similar to native IVD tissues. In addition, the lamellar scaffold design and materials exhibited the necessary mechanical properties to match natural IVD biomechanics.

4.6 References

1. Luo X, Pietrobon R, Sun SX, Liu GG, Hey L. Estimates and patterns of direct health care expenditures among individuals with back pain in the United States. Spine 2004;29(1):79-86.

2. Whatley BR. Intervertebral disc (IVD): Structure, degeneration, repair, and regeneration. Mater. Sci. Eng., C 2012;32(2):61-77.

3. An HS, Thonar EJ, Masuda K. Biological repair of intervertebral disc. Spine (Phila Pa 1976) 2003;28(15 Suppl):S86-92.

4. Boos N, Weissbach S, Rohrbach H, Weiler C, Spratt KF, Nerlich AG. Classification of age-related changes in lumbar intervertebral discs: 2002 Volvo Award in basic science. Spine (Phila Pa 1976) 2002;27(23):2631-44.

5. Fazzalari NL, Costi JJ, Hearn TC, Fraser RD, Vernon-Roberts B, Hutchinson J, Manthey BA, Parkinson IH, Sinclair C. Mechanical and pathologic consequences of induced concentric anular tears in an ovine model. Spine (Phila Pa 1976) 2001;26(23):2575-81.

6. Masuda K, An HS. Prevention of disc degeneration with growth factors. Eur Spine J 2006;15 Suppl 3:S422-32.

7. Huang RC, Girardi FP, Cammisa FP, Jr., Lim MR, Tropiano P, Marnay T. Correlation between range of motion and outcome after lumbar total disc replacement: 8.6-year follow-up. Spine 2005;30(12):1407-11.

8. McAfee PC, Cunningham B, Holsapple G, Adams K, Blumenthal S, Guyer RD, Dmietriev A, Maxwell JH, Regan JJ, Isaza J. A prospective, randomized, multicenter Food and Drug Administration investigational device exemption study of lumbar total disc replacement with the CHARITE artificial disc versus lumbar fusion: part II: evaluation of radiographic outcomes and correlation of surgical technique accuracy with clinical outcomes. Spine 2005;30(14):1576-83; discussion E388-90.

9. Palepu V, Kodigudla M, Goel VK. Biomechanics of disc degeneration. Adv Orthop 2012:1-17.

10. Erkan S, Rivera Y, Wu C, Mehbod AA, Transfeldt EE. Biomechanical comparison of a two-level Maverick disc replacement with a hybrid one-level disc replacement and one-level anterior lumbar interbody fusion. Spine J 2009;9(10):830-5.

11. Kafer W, Clessienne CB, Daxle M, Kocak T, Reichel H, Cakir B. Posterior component impingement after lumbar total disc replacement: a radiographic analysis of 66 ProDisc-L prostheses in 56 patients. Spine (Phila Pa 1976) 2008;33(22):2444-9.
12. Hukins DW. Tissue engineering: a live disc. Nat Mater 2005;4(12):881-2.

13. Yao H, Gu WY. Physical signals and solute transport in human intervertebral disc during compressive stress relaxation: 3D finite element analysis. Biorheology 2006;43(3-4):323-35.

14. Wan Y, Feng G, Shen FH, Balian G, Laurencin CT, Li X. Novel biodegradable poly(1,8-octanediol malate) for annulus fibrosus regeneration. Macromol Biosci 2007;7(11):1217-24.

15. Melrose J, Smith SM, Appleyard RC, Little CB. Aggrecan, versican and type VI collagen are components of annular translamellar crossbridges in the intervertebral disc. Eur Spine J 2008;17(2):314-24.

16. Huang ZM, Zhang YZ, Kotaki M, Ramakrishna S. A review on polymer nanofibers by electrospinning and their applications in nanocomposites. Composites Sci Technol 2003(63):2223-53.

17. Li D, Xia Y. Electrospinning of nanofibers: reinventing the wheel? Advanced Materials 2004;16(14):1151-70.

18. Li WJ, Danielson KG, Alexander PG, Tuan RS. Biological response of chondrocytes cultured in three-dimensional nanofibrous poly(epsilon-caprolactone) scaffolds. J Biomed Mater Res A 2003;67(4):1105-14.

19. Li WJ, Jiang YJ, Tuan RS. Chondrocyte phenotype in engineered fibrous matrix is regulated by fiber size. Tissue Eng 2006;12(7):1775-85.

20. Aviss KJ, Gough JE, Downes S. Aligned electrospun polymer fibres for skeletal muscle regeneration. Eur Cell Mater;19:193-204.

21. Baker BM, Mauck RL. The effect of nanofiber alignment on the maturation of engineered meniscus constructs. Biomaterials 2007;28(11):1967-77.

22. Chang G, Kim HJ, Kaplan D, Vunjak-Novakovic G, Kandel RA. Porous silk scaffolds can be used for tissue engineering annulus fibrosus. Eur Spine J 2007;16(11):1848-57.

23. Nesti LJ, Li WJ, Shanti RM, Jiang YJ, Jackson W, Freedman BA, Kuklo TR, Giuliani JR, Tuan RS. Intervertebral disc tissue engineering using a novel hyaluronic acid-nanofibrous scaffold (HANFS) amalgam. Tissue Eng Part A 2008;14(9):1527-37.

24. Liu X, Ma PX. Polymeric scaffolds for bone tissue engineering. Ann Biomed Eng 2004;32(3):477-86.

25. Marga F, Jakab K, Khatiwala C, Shepherd B, Dorfman S, Hubbard B, Colbert S, Gabor F. Toward engineering functional organ modules by additive manufacturing. Biofabrication 2012;4(2):022001.

26. Sun W, Forgacs G. The 2010 International Conference on Biofabrication (BF2010) special issue. Biofabrication 2011;3(3):030201.

27. Zein I, Hutmacher DW, Tan KC, Teoh SH. Fused deposition modeling of novel scaffold architectures for tissue engineering applications. Biomaterials 2002;23(4):1169-85.

28. Alini M, Li W, Markovic P, Aebi M, Spiro RC, Roughley PJ. The potential and limitations of a cell-seeded collagen/hyaluronan scaffold to engineer an intervertebral disc-like matrix. Spine (Phila Pa 1976) 2003;28(5):446-54; discussion 453.

29. Mwale F, Iordanova M, Demers CN, Steffen T, Roughley P, Antoniou J. Biological evaluation of chitosan salts cross-linked to genipin as a cell scaffold for disk tissue engineering. Tissue Eng 2005;11(1-2):130-40.

30. Wan Y, Feng G, Shen FH, Laurencin CT, Li X. Biphasic scaffold for annulus fibrosus tissue regeneration. Biomaterials 2008;29(6):643-52.

31. Wen X, Qiu Y, Vanden Berg-Foels WS; Regeneration of tissue without cell transplantation. US Patent Application # 20120100185 A1. 2012.

32. Setton LA, Bonassar L, Masuda K. Regeneration and Replacement of the Intervertebral Disc: Elsevier; 2007.

33. Joshi A, Fussell G, Thomas J, Hsuan A, Lowman A, Karduna A, Vresilovic E, Marcolongo M. Functional compressive mechanics of a PVA/PVP nucleus pulposus replacement. Biomaterials 2006;27(2):176-84.

34. White AA, 3rd. Clinical biomechanics of cervical spine implants. Spine (Phila Pa 1976) 1989;14(10):1040-5.

35. Wuertz K, Godburn K, MacLean JJ, Barbir A, Donnelly JS, Roughley PJ, Alini M, Iatridis JC. In vivo remodeling of intervertebral discs in response to short- and long-term dynamic compression. J Orthop Res 2009;27(9):1235-42.

36. Hansson TH, Keller TS, Spengler DM. Mechanical behavior of the human lumbar spine. II. Fatigue strength during dynamic compressive loading. J Orthop Res 1987;5(4):479-87.

37. Korecki CL, MacLean JJ, Iatridis JC. Dynamic compression effects on intervertebral disc mechanics and biology. Spine (Phila Pa 1976) 2008;33(13):1403-9.

38. Yao H, Justiz MA, Flagler D, Gu WY. Effects of swelling pressure and hydraulic permeability on dynamic compressive behavior of lumbar annulus fibrosus. Ann Biomed Eng 2002;30(10):1234-41.

39. Iatridis JC, Setton LA, Foster RJ, Rawlins BA, Weidenbaum M, Mow VC. Degeneration affects the anisotropic and nonlinear behaviors of human anulus fibrosus in compression. J Biomech 1998;31(6):535-44.

40. Cassidy JJ, Hiltner A, Baer E. Hierarchical structure of the intervertebral disc. Connect Tissue Res 1989;23(1):75-88.

41. Marchand F, Ahmed AM. Investigation of the laminate structure of lumbar disc anulus fibrosus. Spine 1990;15(5):402-10.

42. Tsuji H, Hirano N, Ohshima H, Ishihara H, Terahata N, Motoe T. Structural variation of the anterior and posterior anulus fibrosus in the development of human lumbar intervertebral disc. A risk factor for intervertebral disc rupture. Spine 1993;18(2):204-10.

43. Guerin HAL, Elliot DM. Structure and Properties of Soft Tissues in the Spine. In: Kurtz SM, Edidin, A. A., editor. Spine Technology Handbook: Elsevier; 2006.

44. Moffat KL, Kwei AS, Spalazzi JP, Doty SB, Levine WN, Lu HH. Novel nanofiber-based scaffold for rotator cuff repair and augmentation. Tissue Eng Part A 2009;15(1):115-26.

45. Ohshima H, Tsuji H, Hirano N, Ishihara H, Katoh Y, Yamada H. Water diffusion pathway, swelling pressure, and biomechanical properties of the intervertebral disc during compression load. Spine 1989;14(11):1234-44.

46. Urban JP, McMullin JF. Swelling pressure of the inervertebral disc: influence of proteoglycan and collagen contents. Biorheology 1985;22(2):145-57.

47. Urban JP, McMullin JF. Swelling pressure of the lumbar intervertebral discs: influence of age, spinal level, composition, and degeneration. Spine 1988;13(2):179-87.

48. Best BA, Guilak F, Setton LA, Zhu W, Saed-Nejad F, Ratcliffe A, Weidenbaum M, Mow VC. Compressive mechanical properties of the human anulus fibrosus and their relationship to biochemical composition. Spine (Phila Pa 1976) 1994;19(2):212-21.

49. Wilke HJ, Neef P, Caimi M, Hoogland T, Claes LE. New in vivo measurements of pressures in the intervertebral disc in daily life. Spine (Phila Pa 1976) 1999;24(8):755-62.

50. Lotz JC, Hsieh AH, Walsh AL, Palmer EI, Chin JR. Mechanobiology of the intervertebral disc. Biochem Soc Trans 2002;30(Pt 6):853-8.

CHAPTER 5

5. FULLY CELLULARIZED 3-D TISSUE ENGINEERED CONSTRUCTS FOR INTERVERTEBRAL DISC (IVD) REGENERATION

5.1 Introduction

Currently an understudied aspect within the tissue engineering realm, research focusing on intervertebral disc (IVD) degeneration and treatments, has fallen short in their aims to improve patients' quality of life. The degenerated IVD, which causes intense low back pain, has been implicated in significant economic strain throughout the world.[1] Clinical attempts to alleviate this pain, such as discectomy, spinal fusion, and disc replacements, are far from satisfactory as they focus only on the alleviation of some symptoms, while failing to address the underlying causes of disc degeneration. To improve upon conventional clinical strategies, some researchers have begun to investigate unique approaches towards slowing IVD degeneration or promoting IVD tissue regeneration. In the long term, the most ideal approach should involve the regeneration of IVD tissue. Some current strategies focused towards regenerating IVD tissue have proven successful in promoting the synthesis of extracellular matrix (ECM) proteins similar to those present in the native tissue.[2,3] However, current attempts towards regenerating IVD tissue do not accurately mimic the IVD histological microstructure, specifically the organized lamellar structure within the outer region of the IVD.

In order to successfully regenerate IVD tissue, there is a pressing need to fabricate tissue engineered scaffolds with a similar histological architecture of native IVD tissue. This is of vital importance, as it is widely known that cells respond to their physical environment.[4] A scaffold with a controlled microstructure has the ability to guide and control cellular orientation and morphology.[5] This is especially important for scaffolds aimed at regenerating the outer annulus fibrosus (AF) region of the IVD, as it is highly organized and possesses a concentric lamellar structure.[6] Therefore, a scaffold which can mimic the native lamellar orientation of the native AF region would be able to control cellular alignment and morphology in accordance with the scaffold structure. Furthermore, studies have shown that ECM synthesis is controlled by cellular morphology.[7,8] ECM composition as well as its structure, have been demonstrated to be affected by cell behavior on a tissue scaffold. Therefore, a biomimetic IVD scaffold should control cellular structure and promote synthesis of ECM with similar orientation and composition. This ultimately promotes the formation of a tissue structure with similar characteristics to that of native IVD tissue.

To further expand upon the ability to mimic native ECM tissue histology, a strategy to create fully cellularized IVD scaffolds would prove to be favorable for tissue regeneration. The ability to successfully retain seeded cells within a scaffold plays a critical role in encouraging the formation of a 3-D tissue.[9] Cellularized structures are important due to the fact that they provide a necessary platform to promote the formation of functionalized, living tissue. Currently, the attempts that have been made to create a cellularized IVD tissue structure have focused primarily on bioreactor systems, magnetic

seeding, or stacking of singular layered cell-biomaterial constructs.[9-11] However, few other platforms have been investigated to encourage cellular infiltration within a tissue scaffold. Therefore, a major task in promoting tissue regeneration is the ability to couple functional cells within biomaterial scaffolds. A cellularized structure promotes the living functionality of the biomaterial scaffold for tissue regeneration. Furthermore, it is likely that cellularized scaffolds will improve tissue formation, as cellularizing a tissue engineered scaffold in 3-D is required to form 3-D tissues.[12,13] Many advances have been made in creating cellularized tissue scaffolds.[14,15] Further, the ability of cells to be seeded within a scaffold is vital for the creation of 3-D tissue constructs.[9] 3-D cellularization better emulates the native tissue environment, promoting regenerated tissue and synthesized matrix more similar to native tissue.[16,17] In this study, we describe a biofabrication strategy to aid in the rapid formation of a 3-D cellularized tissue engineered construct. A home-made computer-controlled scaffold bioprinter were used to fabricate a 3-D scaffold fully mimicking the outer region of native IVD tissue. Multicellular chondrocyte spheroids were formed robotically using our home-made multicellular spheroid maker and then patterned robotically within the lamellar voids of the fabricated IVD scaffold structures. Spheroids were used as they have previously shown to increase ECM content when compared to singular cells.[19] This allowed the rapid cellularization of the scaffolding construct. The 3-D multicellular spheroids began to attach and spread within the scaffold lamellae while exhibiting a similar cellular morphology as in the natural tissue. Additionally, synthesized ECM composition and

structure within the 3-D cellularized IVD scaffold proved similar to that of the native tissue.

To address the current issues faced with IVD tissue engineering, we have developed a unique biofabrication strategy to accurately mimic the histological hierarchy as well as the biomechanics of native IVD tissue.[18] This technique offers the advantage of computer aided design (CAD), allowing precise control over the shape, as well as the defined microstructure, of the biomimetic IVD scaffolds. Using this biofabrication strategy, it was shown that the lamellar IVD tissue histology could be simulated with the biomimetic scaffolds. Further, this approach enables high resolution fabrication of reproducible scaffolding constructs using a variety of polymeric biomaterials. To take advantage of the automated process, custom-made robotics were used to fabricate 3-D multicellular spheroids. These multicellular spheroids were patterned into the void lamellar regions of the biomimetic IVD scaffold to create a functional cellularized tissue structure. It was found that the 3-D cellularized scaffold emulated native IVD cellular structure as well as ECM matrix composition and structure. Ultimately, a strategy similar to the one described here may be used to create a tissue engineered IVD structure that may be directly implanted into patients to restore natural IVD tissue function.

5.2 Materials and Methods

5.2.1 Scaffold Fabrication

Scaffolds were fabricated using a home-made computer-controlled bioprinter. Medical grade polyurethane (PU) was dissolved in DMF at a concentration of 15%. The solution was then extruded using a 3-D biofabrication device where the scaffold was designed using AutoCAD (Figure 5.1A). Specifically, the polymer solution was extruded out through a micropipette-based needle (50 μm diameter) and onto a computer- and temperature-controlled collecting stage. As the polymer solution was extruded through the tip, the solution viscosity drastically increased and it solidified instantly, as the temperature-controlled stage was set below the freezing point of the polymer solution, at -5° C.

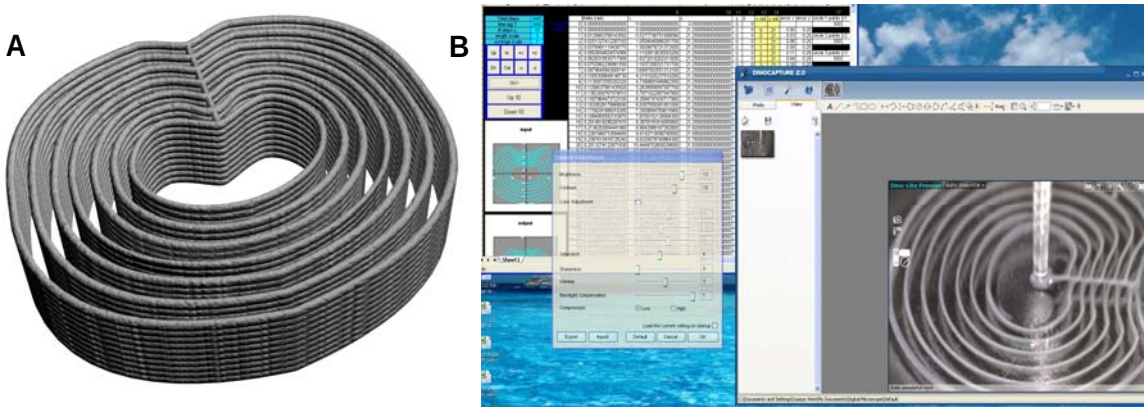

Figure 5. 1: CAD design of the multilayered scaffold mimicking the overall shape and morphology of the native IVD tissue (A). Software interface was developed to allow the designed scaffolds to be printed and monitored during the printing process in real-time (B).

5.2.2 Scaffold Characterization

The dimensions and morphology of the printed scaffolds were analyzed using a JEOL LV-5610 scanning electron microscope (SEM) (JEOL Electronics Inc., Tokyo, Japan). Specifically, the scaffolds lamellar layers and spacing were verified to match the lamellae size and spacing of native human IVD tissue. Once this was confirmed, the size of the spacing between the lamellar layers was assessed.

5.2.3 Multicellular Spheroid Fabrication

In order to develop a truly 3-D, fully cellularized structure for IVD formation, we used multicellular spheroids as building blocks to seed into the scaffolds. Using the data obtained from the SEM, it was determined that multicellular spheroids would need to be fabricated within a very specific size range in order to fit within the lamellae. Bovine chondrocytes were used to create multicellular spheroids with uniform size using a home-made spheroid maker. The process can be seen in figure 5.2. Briefly, a computer-operated device was used to stamp molten 2% agarose PBS solution until the mold had hardened. Cell suspensions were added into the agarose molds, and incubated at 37 °C and 5% CO_2 for 48 hours. Cell spheroids were then gathered for positioning into the scaffold.

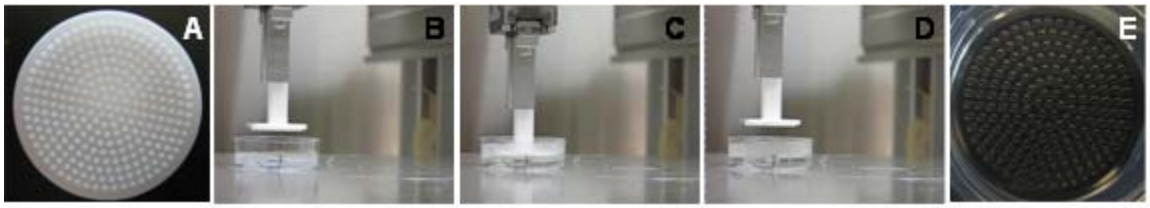

Figure 5. 2: (A) Plastic male-mold used to fabricate agarose microwells, (B-D) automated robotic stamping of agarose gel by the plastic male-mold, and thus (E) robotically produced agarose microwells.

5.2.4 Scaffold Cellularization

To seed the scaffolds, multicellular spheroids were pipetted into the prefabricated scaffolds using a custom-made computer-controlled robotic positioning system. The chondrocyte spheroids were placed into the void lamellar scaffold spacing using precise positioning. A schematic of this process can be seen in figure 5.3. To compare the ability of spheroids to increase 3-D tissue formation, single cells were also seeded into the scaffolds as a control at the same cell number. The scaffolds were cultured for 4 weeks to create fully cellularized IVD scaffolding constructs. Media was changed and collected throughout the culture period for further biochemical analysis of secreted ECM. An inverted microscope (Olympus Co., Tokyo, Japan) was used to monitor cell growth on the scaffolds.

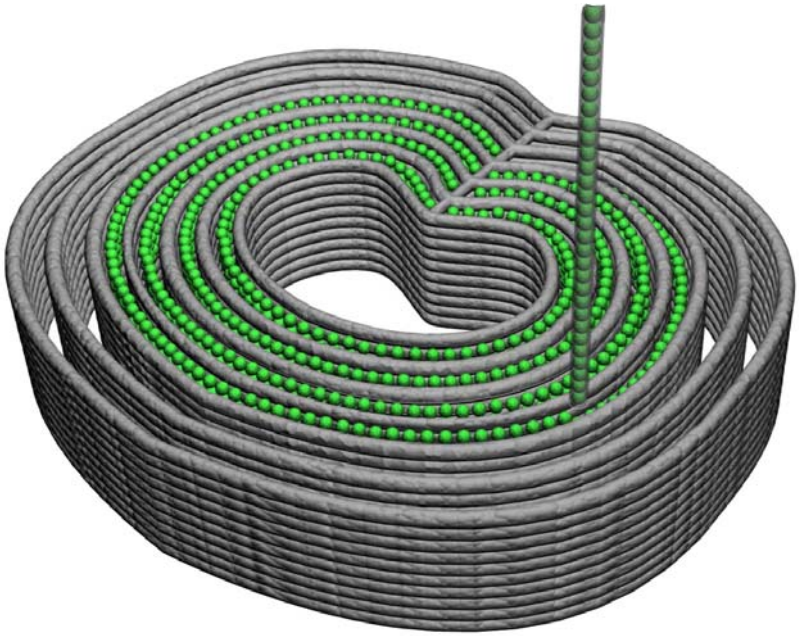

Figure 5. 3: Schematic of spheroid deposition within IVD scaffold lamellae.

5.2.5 Biochemical Analysis

After 4 weeks in culture, the IVD tissue scaffolds were evaluated to determine the ECM content of the constructs. Additionally, the molecules solubilized in the media supernatant were collected throughout the study to determine the amount of specific ECM released. All colorometric assays were analyzed using a Synergy H1 Hybrid plate reader (Biotek, Winooski, VT, USA). To determine the amount of ECM retained within the scaffolds, the samples were digested: in a papain solution [20] overnight at 60 °C for sulfated-glycosaminoglycan (sGAG) and hydroxyproline quantification, or in pepsin and elastase digest for 7 days at 4 °C for collagen I and II quantification. In order to normalize the amount of newly formed ECM components, DNA content was quantified. The analyzed sGAG, hydroxyproline, and collagen types I & II quantities (μg) were

normalized by the average total DNA content (μg) to enable comparison between sample groups. Additionally, the hydroxyproline content was normalized to sGAG to compare sample groups with values similar to native cartilage tissue. The scaffolds seeded with 3-D multicellular spheroids (experimental group) were compared to scaffolds seeded with single cells (control).

5.2.5.1 DNA Quantification

In order to normalize the biochemical data between each test group, the DNA content within each scaffold group was analyzed using a DNA Quantitation Flourescent Assay Kit (Sigma-Aldrich, St.Louis, MO, USA).[21] Briefly, 25 μL of cell digest solution in papain was combined with 200 μL of Hoeschst dye (2 μg/mL). Standard curves were created using calf thymus DNA. Fluorescence was read at 360 nm excitation and 460 nm emission.

5.2.5.2 sGAG Synthesis

Cellular production of sGAGs was analyzed using 1,9-Dimethyl-Methylene Blue (DMMB) salt (Sigma-Aldrich), similarly to techniques used by others.[22] Briefly, 16 mg of DMMB was dissolved in 1 L of distilled water containing 3.04 g glycine, and 2.37 g NaCl and stirred overnight. This was followed by the addition of 95 mL of 0.1 M HCl to give a pH of 3.0. The solution was stored at room temperature and away from light. 50 μL samples of cell digest solution in papain were then transferred into a flat bottom 96

well plate (Greiner Bio-One, Frickenhausen, Germany) containing 200 µL of DMMB reagent per well. The absorbance was read at 525 nm. Standard curves were created using chondroitin sulfate from shark cartilage (Sigma-Aldrich) with a linear concentration ranging from 0-100 µg/mL.

5.2.5.3 Hydroxyproline Formation

The total amount of collagen was analyzed using a hydroxyproline assay kit (Sigma-Aldrich), as hydroxyproline has been previously defined as a marker for overall collagen production.[23,24] Briefly, 100 µL samples of cell digest solution in papain were hydrolyzed in the presence of 12 M HCl at 120 °C for 3 hours followed by evaporation of the samples. Samples were reacted with Chloramine T for 5 minutes followed by an incubation with 4-(Dimethylamino)benzaldehyde (DMAB)for 90 minutes. Standard curves were created using the provided hydroxyproline standard. The absorbance was then read at 560 nm.

5.2.5.4 Collagen Types I & II Synthesis

After evaluating hydroxyproline content, additional biochemical analysis was needed to determine and quantify which types of collagen were present. Specifically, collagen types I & II were chosen for an enzyme-linked immunosorbent assay (ELISA) analysis as they are the most prevalent collagens in the IVD. Chondrex ELISAs for both collagen types I & II (Chondrex, Inc., Redmond, WA, USA) were used and the relevant

protocols were followed. Briefly, capture antibodies were added to 96 well plates overnight, followed by a 2 hour incubation of the pepsin and elastase digested samples. Detection antibodies were then added for 2 hours followed by the addition of streptavidin peroxidase for 1 hour. Then, the OPD chromagen was added for 30 minutes followed by the addition of 2N sulfuric acid to stop the reaction. Collagen samples were compared against collagen standards and absorbance was read at 490 nm for both collagen types I & II.

5.2.6 Immunohistochemistry

Cellularized constructs were fluorescently analyzed to evaluate the presence and structure of collagen types I & II, and to visualize the cell nuclei. Nuclei were stained with DAPI (blue), while collagens were stained using secondary antibodies (collagen type I: green, collagen type II: red). Briefly, cellularized constructs were fixed in 4% paraformaldehyde and blocked using 4% goat serum. Rabbit anti-bovine collagen type I polyclonal antibody (Millipore, Bedford, MA, USA) was added overnight followed by rinsing three times and the addition of Cy2-conjugated goat anti-rabbit IgG (Jackson ImmnoResearch, West Grove, PA, USA) and subsequent washing. This was repeated for the mouse anti-collagen type II monoclonal primary antibody (Millipore) and the Cy3-conjugated goat anti-mouse IgG (Jackson ImmnoResearch) followed by washing. DAPI (Invitrogen, Carlsbad, CA, USA) was then used similarly to fluorescently label cell nuclei within the scaffold constructs. Samples were observed using a Fluoview-FV1000

laser scanning confocal microscope (Olympus) to qualitatively analyze 3-D cellularization of the scaffolds and subsequent ECM formation.

5.2.7 Statistical Analysis

Data were expressed as mean ± standard error of mean. An independent-sample *t*-test was performed on all biochemical analyses to compare the two IVD scaffold groups: 1) control scaffolds seeded with single cells, 2) experimental scaffolds seeded with multicellular spheroids. Significance was determined at $p<0.05$. SPSS V17 software (Chicago, IL, USA) was used to perform the statistic analysis.

5.3 Results

5.3.1 Scaffold Structure

Utilizing our layer-by-layer and temperature controlled biofabrication strategy, reproducible multilayered 3-D scaffolds mimicking native IVD structures were easily fabricated. The overall shape and structure of the native IVD was extensively studied in order to design biomimetic scaffolds with similar properties using AutoCAD. A unique concentric lamellar structure was created, with each layer having a thickness of 50 μm and the spacing between each concentric lamellae at 175 μm. This structure can be observed in the SEM image in figure 5.4, where the uniform and layered structure is highly apparent.

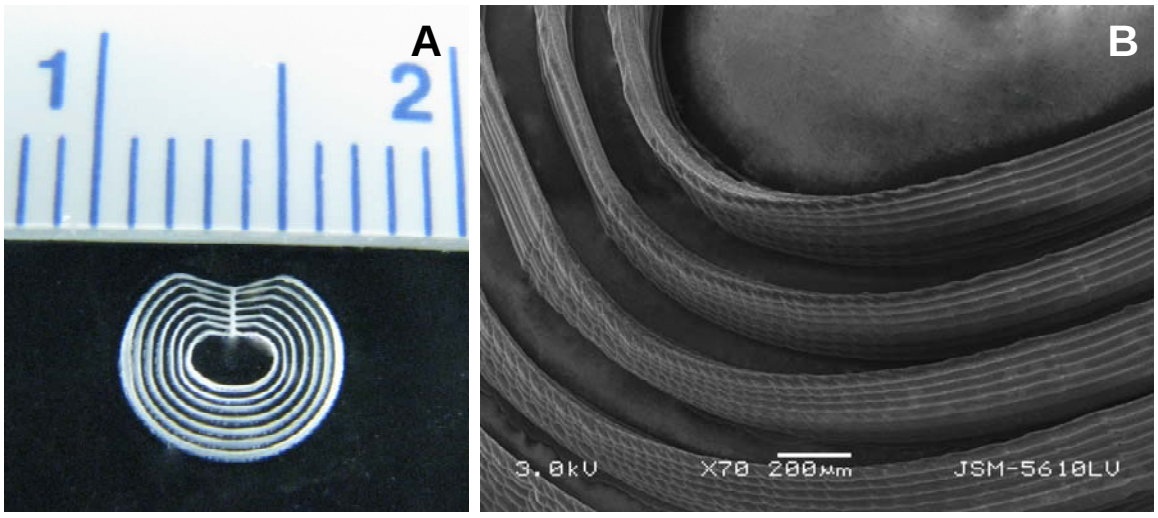

Figure 5. 4: Overall image showing scaffold size and shape (A). SEM image showing multilayered scaffold structure with highly uniform and concentric lamellar layers mimicking native IVD structure (B).

5.3.2 Spheroid Properties

Using the robotic spheroid maker, highly uniform spheroids were fabricated with precise diameters of 125 µm using cell seeding densities of 1.3 x 10^4 cells/agarose mold (Figure 5.5). This size proved optimal as it enabled the spheroids to be easily extruded into the lamellar voids of the scaffolds, which were slightly larger than the spheroid diameter.

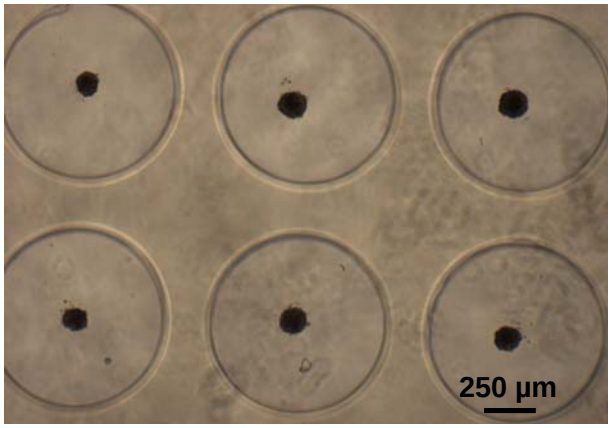

Figure 5. 5: Multicellular chondrocyte spheroids in culture within microwells, demonstrating a highly uniform diameter of 125 µm.

5.3.3 Scaffold Cellularization

After seeding, spheroids appeared to fully integrate within the scaffold lamellae. The multicellular spheroids began to fuse days after initial seeding. After 1 week, the spheroids are fused and fully integrated with the scaffolds and formed 3-D tissues. The single cells attached to the scaffolds and covered the entire structure, however, they failed to fully cellularize the lamellar voids as compared to the multicellular spheroids. In the case of both the single cells and the multicellular spheroids, the cells within the lamellar voids oriented themselves in alignment with the lamellar scaffold structure.

5.3.4 Biochemical Analysis

The production of ECM by the tissue engineered constructs was identified by evaluating the amount of sGAG, hydroxyproline, and collagen types I & II in each sample after 4 weeks. A summary of the synthesized ECM composition retained within

the scaffolds can be seen in Table 1. Additionally, a summary of ECM released within the media supernatant is given in Table 2. The data is normalized to mean DNA content.

Table 5. 1: Synthesized ECM within Scaffold after 4 weeks (Mean ± Standard Error of Mean). *p<0.05

	GAG (µg) / DNA (µg)	**Hydroxyproline (µg) / DNA (µg)**	**GAG (µg) / Hydroxyproline (µg)**	**Col I (µg) / DNA (µg)**	**Col II (µg) / DNA (µg)**
Spheroids	119.8 ± 2.7*	8.4 ± 1.1*	11.9 ± 1.4*	4.6 ± 0.9*	3.8 ± 0.1*
Single Cells	54.4 ± 3.6	5.5 ± 0.4	8.3 ± 0.6	1.6 ± 0.2	1.8 ± 0.1

Table 5. 2: Synthesized ECM Released in Supernatant after 4 weeks (Mean ± Standard Error of Mean). *p<0.05

	GAG (µg) / DNA (µg)	**Col I (µg) / DNA (µg)**	**Col II (µg) / DNA (µg)**
Spheroids	141.4 ± 11.1*	3.74 ± 1.0*	2.6 ± 0.3*
Single Cells	108.9 ± 6.0	1.0 ± 0.3	1.1 ± 0.1

5.3.4.1 sGAG Synthesis

The amount of sGAG (spheroids 119.8 ± 2.7 µg/µg, versus single 54.4 ± 3.6 µg/µg) retained within the construct was significantly greater in the scaffolds seeded with multicellular spheroids compared to the single cell controls, as shown in Figure 5.6A (n=7 per group, $p<0.05$). Additionally, as shown in Figure 5.7A, the quantity of sGAG (spheroids 141.4 ± 11.1 µg/µg, versus single 108.9 ± 6.0 µg/µg) released into the supernatant was also significantly greater in the scaffolds seeded with multicellular spheroids compared to the single cell controls (n=7 per group, $p<0.05$).

5.3.4.2 Hydroxyproline Formation

Hydroxyproline (spheroids 8.4 ± 1.1 μg/μg, versus single 5.5 ± 0.4 μg/μg) quantity was significantly greater in the scaffolds seeded with spheroids versus the single cells as seen in Figure 5.6B (n=7 per group, $p<0.05$). Additionally, the GAG/hydroxyproline ratio (spheroids 11.9 ± 1.4 μg/μg, versus single 8.3 ± 0.6 μg/μg) was also significantly greater in the scaffolds seeded with multicellular spheroids as seen in Table 1 (n = 7 per group, $p<0.05$).

5.3.4.3 Collagen Types I & II Synthesis

The amount of collagen type I (spheroids 4.6 ± 0.9 μg/μg, versus single 1.6 ± 0.2 μg/μg) retained within the construct was significantly larger in the scaffolds seeded with spheroids versus the single cell control as seen in Figure 5.6C (n = 7 per group, $p<0.05$). Similarly, as shown in Figure 5.6D, the amount of collagen type II (spheroids 3.8 ± 0.1 μg/μg, versus single 1.8 ± 0.1 μg/μg) preserved within the scaffold was significantly larger in the experimental group with multicellular spheroid seeded scaffolds (n = 7 per group, $p<0.05$). Figure 5.7B shows that the quantity of collagen type I (spheroids 3.74 ± 1.0 μg/μg, versus single 1.0 ± 0.3 μg/μg) released into the supernatant was significantly greater in the scaffolds seeded with spheroids versus the single cell control (n = 7 per group, $p<0.05$). This was also observed for the amount of collagen type II (spheroids 2.6 ± 0.3 μg/μg, versus single 1.1 ± 0.1 μg/μg) released into the media was significantly larger in the experimental group with multicellular spheroid seeded scaffolds compared to the single cell controls as shown in Figure 5.7C (n = 7 per group, $p<0.05$).

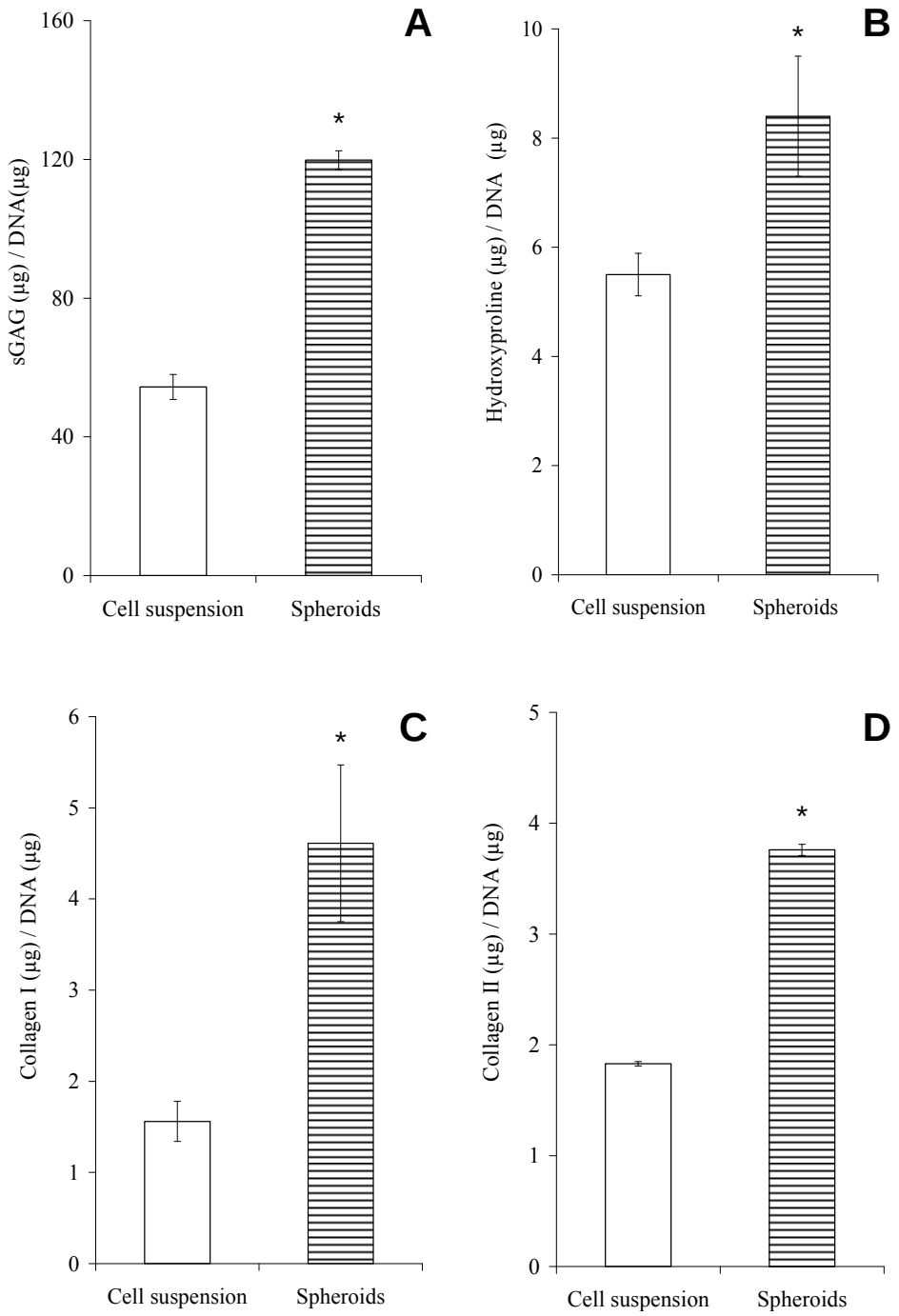

Figure 5. 6: Results from biochemical analysis of ECM within the scaffolds cellularized with cell suspension and spheroids after 4 weeks. Statistical analysis comparing groups showed significant differences for all study groups (n =7 for each group, *p<0.05). The sGAG (A), hydroxyproline (B), collagen type I (C), and collagen type II (D) content was all significantly greater in the scaffolds cellularized with sperhoids than with the same number of cells seeded in the format of cell suspension.

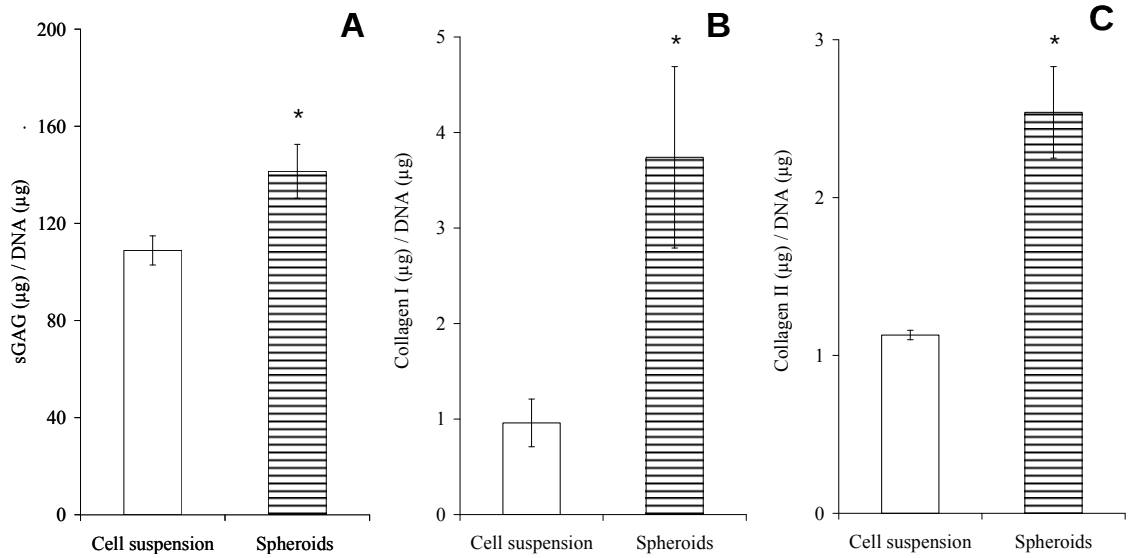

Figure 5. 7: Results from biochemical analysis of ECM released from scaffolds cellularized with cell suspension and spheroids over 4 weeks. Statistical analysis comparing groups showed significant differences for all study groups (n =7 for each group, *p<0.05). The sGAG (A), collagen type I (B), and collagen type II (C) release was all significantly greater in the scaffolds cellularized with sperhoids than with the same number of cells seeded in a single cell suspension.

5.3.5 Immunohistochemistry

Image analysis provided qualitative evidence that the synthesized collagenous ECM was fully integrated within the voids of the lamellar structure in a similar fashion to native IVD tissue. Further, cells as well as ECM, were organized in a 3-D configuration. The cell suspension (control) seeded into the biomimetic scaffolds synthesized some collagenous ECM, but cells only attached to the scaffold surface and failed to synthesize enough ECM to fill in the lamellar void (Figure 5.8A-D). A side projection view showing that the seeded cells in suspension attached to the scaffold surface and secreted

extracellular molecules, but failed to secrete biomolecules occupying the lamellar void space as the matrix only accumulated on the scaffold surface as shown in figure 5.8E-H. On the other hand, the multicellular spheroids fully infiltrated the scaffold lamellae and grew in a 3-D fashion that enabled the creation of a completely cellularized IVD construct. Further, staining of collagenous ECM within the lamellae appeared to be much greater in the scaffolds seeded with spheroids versus single cells, as synthesized matrix can be seen throughout the entire lamellar voids (Figure 5.8I-L). A side projection view proving that the multicellular spheroids fully cellularized the lamellar void and synthesized a 3-D collagenous matrix throughout the construct can be seen in figure 5.8M-P.

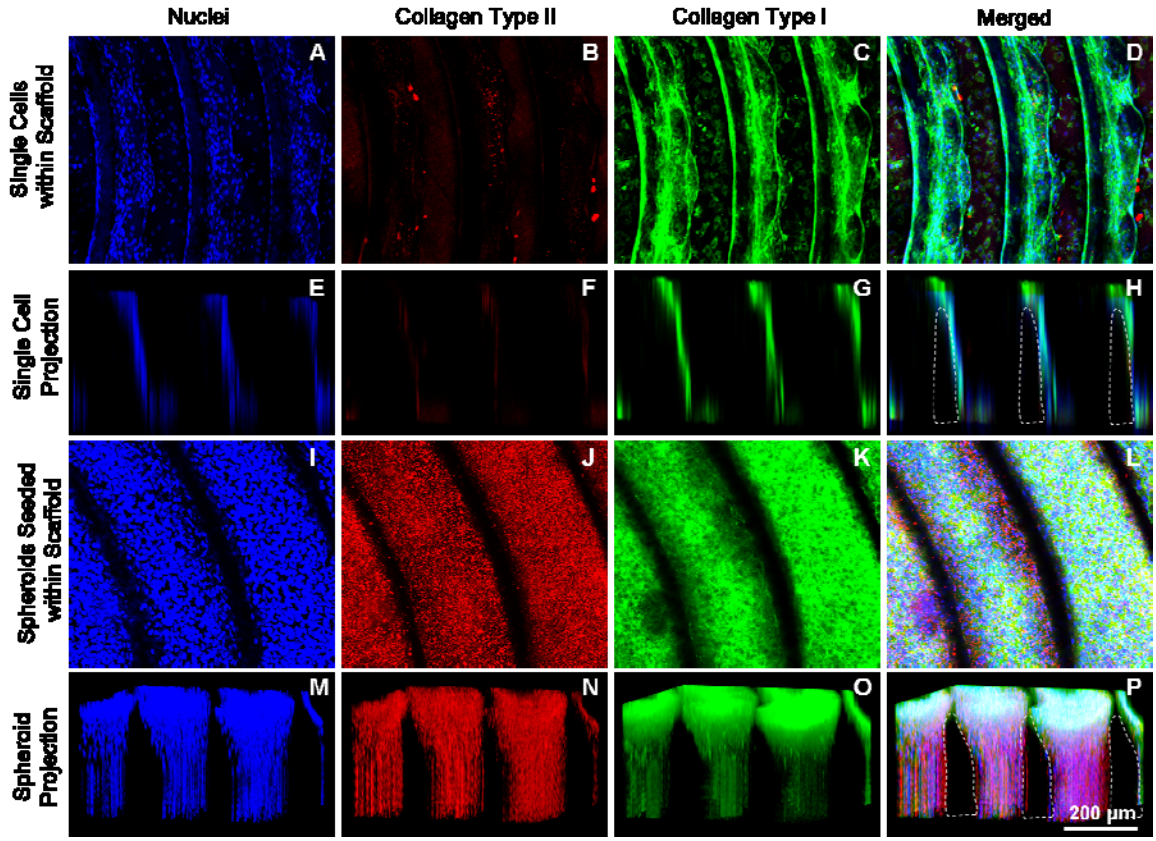

Figure 5. 8: Fluorescent images showing chondrocyte growth and ECM synthesis in the scaffolds. An overview of the cell suspension controls seeded onto the scaffold after 4 weeks can be seen in: (A) nuclei, (B) collagen type II, (C) collagen type I, and (D) merged image. A side projection view of the single cells on the scaffold shows that the cells were superficially adhered to the scaffold surface and did not cellularize the lamellar region while only producing ECM along the scaffold surface: (E) nuclei, (F) collagen type II, (G) collagen type I, and (H) merged image.
In comparison, an overview of the spheroids seeded onto the scaffold shows that the entire construct is cellularized with large quantities of ECM produced : (I) nuclei, (J) collagen type II, (K) collagen type I, and (L) merged image. A side projection view of the spheroids within the scaffold further validates that the spheroids have cellularized the lamellar void and have produced ECM in a 3-D manner: (M) nuclei, (N) collagen type II, (O) collagen type I, and (P) merged image. The dotted zone in (H) and (P) shows the lamellar scaffold structure.

5.4 Discussion

The field of tissue engineering aims to regenerate living tissue that possesses a similar structure and function to the natural healthy tissue, with the ultimate goal of replacing the targeted diseased tissue. Tissue engineering often utilizes scaffolds as a template to guide cell growth and tissue formation. The structure of tissue engineered scaffolds is important as it not only dictates the mechanical integrity of the construct, but also guides cell behavior and function as well as new ECM organization. For these reasons, it is important for the scaffold structure to closely mimic the native tissue architecture in order to successfully regenerate the native tissue. The corresponding structure will control cell behavior, and ultimately cellular function. Due to current limitations in achieving a cell-based functional scaffold that simulates the native tissue, an approach was developed to provide a fully cellularized-construct for IVD tissue regeneration.

First, biomimetic IVD scaffolds were fabricated using a novel biofabrication approach that allowed for the creation of a scaffold with an overall morphology and microstructure which strongly resembles the architecture of the native IVD tissue. Advantages of our scaffold over other methods currently being investigated is the use of an organized lamellar structure, which is more similar to native collagen fibril structure present in the IVD.[25] Our fabricated scaffold had the ability to mimic the structure, layer thickness, and interlamellar spacing of the native human IVD, as similar values have been reported in the literature for these characteristics.[26-28] As discussed above, by closely mimicking this structure we believe we will be able to more effectively

regenerate a tissue construct that is highly similar to native IVD tissue, which has been identified as a major challenge in tissue engineering the IVD.[29] Further, the interlamellar spacing provided by our scaffolds will allow for cell infiltration and ECM organization.

The novel biofabrication approach discussed above, along with a robotic seeding strategy, allowed for the ability to organize cell density and distribution within the tissue scaffold, directly controlling the capacity to form 3-D tissue engineered constructs. Typically, after seeding cells onto a 3-D scaffold, it is difficult for cells to further fill up the whole volume of the scaffold and the cells end up adhering only to the scaffold surface.[20,30] This results in a tissue engineered scaffold that is not entirely or homogenously cellularized due to the decreased cell content within the void regions. Furthermore, the majority of studies involving cell-biomaterial constructs use single cells or cell suspensions where cells are only able to adhere to the surface of the scaffold material and pore walls. Therefore, these seeding techniques are not able to actually cellularize the whole pores or voids themselves within the constructs. A major issue with the use of single cells in these applications is a low cell retention within the constructs.[31] To circumvent these issues, 3-D multicellular spheroids were fabricated to have a slightly smaller diameter than the lamellar voids of the fabricated IVD scaffolds. The chondrocyte spheroids were then deposited into the lamellar voids where they attached to the scaffold lamellae and aligned along the structures in a 3-D fashion similar as in the native tissue. Single cells were seeded onto the IVD scaffold as controls. It was found that this unique strategy of incorporating spheroids within the scaffold provides an efficient and quick 3-D cellularization of the construct, which has been described as a

major challenge.[9] Further, after initial seeding, cell spheroids began to fuse together followed by cellular adhesion to the scaffold. Eventually, the spheroids formed a 3-D cell layer which was entirely homogenous, avoiding challenges met by others attempting to cellularize 3-D scaffolds.[32] Furthermore, the spheroids synthesized ECM throughout the scaffold voids, comparable to the matrix formed within the natural IVD, while the cell seeded by suspension only produced matrix on the scaffold surface.

Multicellular spheroids showed excellent ingrowth within the lamellar voids of the IVD scaffolds, which led to a more uniform distribution of cells within the 3-D structure. Further, it appears that these spheroids encouraged organized tissue formation, with the production of ECM such as collagens and GAGs, within the lamellar spacing of the scaffold. As expected, larger values for retained ECM components were obtained with the cellular spheroids as they aided in the preservation of more ECM components. This is similar to what others have observed.[33,34] Specifically, the values we observed for GAG content within the spheroid cellularized scaffold are within values reported by others for native cartilage tissues and also tissue engineered constructs.[33,35-40] Additionally, our data regarding the GAG/Hydroxyproline ratio correlates well with other studies involving cartilage and IVD tissue, with values between 2:1 and 27:1.[41] Based on the observed hydroxyproline levels, indicative of overall collagen content, and further biochemical analysis of specific collagen types, it is evident that collagen types I & II are the major constituents of the collagenous ECM within the IVD constructs. Further, the collagen content within our structures is also similar to what others have reported for tissue engineered constructs.[42] Our results showed similar amounts of collagen types I &

II, though, there were larger overall quantities of collagen type I as compared to collagen type II. This ratio is similar to that seen in the AF region of the IVD tissue, which this scaffold aims to replace.[43]

We believe that the reason the scaffolding constructs seeded with spheroids retained more matrix is because they provided a 3-D platform for cell growth while promoting the synthesis and entrapment of matrix more similar to that of native tissue. As seen in the results, there was not only a significant increase in the amount of ECM production within the scaffolds cellularized with spheroids, but also a significant increase in the amount of ECM released into the supernatant. We believe that the scaffolds seeded with spheroids produced and released more ECM due to the 3-D cell morphology of the spheroids within the scaffold lamellae, which better mimics the native tissue atmosphere. The 3-D cellular and matrix interactions provided by the spheroids more closely emulates the native tissue environment.[44] However, the increase in matrix production in the spheroid cellularized scaffolds may be due to the fact that a more hypoxic environment was created, as nutrient diffusion to the cells within the spheroids may be decreased. Many studies have shown an increase in ECM synthesis (GAGs and collagens) when chondrocytes are placed in a hypoxic environment, more similar to that of native IVD tissue.[45-49]

Upon further examination of the 3-D tissue engineered constructs, immunostaining showed uniform cell distributions throughout the entire thickness of the spheroid cellularized scaffolds when compared with the single cell scaffolds. Subsequently, ECM deposition was also found throughout the scaffold thickness in the

spheroid seeded scaffolds. Collagen type I staining appeared to mimic the scaffold, especially in the scaffold cellularized with spheroids, perhaps proving that the ECM was indeed mimicking the scaffold structure. Further, collagen type II showed up throughout the voids within the lamellar scaffold. These results show that multicellular spheroids better integrate within the IVD scaffold than cells from suspension and synthesize functional tissue in a similar fashion to native IVD tissue.

5.6 Conclusion

This study is the first of its kind attempting to fabricate a fully cellularized 3-D tissue construct for IVD tissue regeneration. The purpose of this study was to create a unique IVD scaffold which provided the ability to create a homogenous cell distribution throughout the structure. This improved upon current cell seeding methods by creating a fully cellularized scaffold environment with similar matrix compositions to that of native IVD tissue. The techniques described in this paper are not limited to an IVD scaffold, and have the ability to be applied to various tissue scaffold technologies. It is our hope that in the future this approach could be used, in certain applications, to replace conventional 2-D culture methods by providing a more native 3-D physiological environment for cells.

5.7 References

1. Luo X, Pietrobon R, Sun SX, Liu GG, Hey L. Estimates and patterns of direct health care expenditures among individuals with back pain in the United States. Spine (Phila Pa 1976) 2004;29(1):79-86.

2. Nesti LJ, Li WJ, Shanti RM, Jiang YJ, Jackson W, Freedman BA, Kuklo TR, Giuliani JR, Tuan RS. Intervertebral disc tissue engineering using a novel hyaluronic acid-nanofibrous scaffold (HANFS) amalgam. Tissue Eng Part A 2008;14(9):1527-37.

3. Wan Y, Feng G, Shen FH, Laurencin CT, Li X. Biphasic scaffold for annulus fibrosus tissue regeneration. Biomaterials 2008;29(6):643-52.

4. Grinnell F. Fibroblast biology in three-dimensional collagen matrices. Trends Cell Biol 2003;13(5):264-9.

5. Mauck RL, Baker BM, Nerurkar NL, Burdick JA, Li WJ, Tuan RS, Elliott DM. Engineering on the straight and narrow: the mechanics of nanofibrous assemblies for fiber-reinforced tissue regeneration. Tissue Eng Part B Rev 2009;15(2):171-93.

6. Roberts S, Evans H, Trivedi J, Menage J. Histology and pathology of the human intervertebral disc. J Bone Joint Surg Am 2006;88 Suppl 2:10-4.

7. Davis GE, Senger DR. Endothelial extracellular matrix: biosynthesis, remodeling, and functions during vascular morphogenesis and neovessel stabilization. Circ Res 2005;97(11):1093-107.

8. Wang Y, Kim UJ, Blasioli DJ, Kim HJ, Kaplan DL. In vitro cartilage tissue engineering with 3D porous aqueous-derived silk scaffolds and mesenchymal stem cells. Biomaterials 2005;26(34):7082-94.

9. Anil Kumar PR, Varma HK, Kumary TV. Cell patch seeding and functional analysis of cellularized scaffolds for tissue engineering. Biomed Mater 2007;2(1):48-54.

10. Martin I, Wendt D, Heberer M. The role of bioreactors in tissue engineering. Trends Biotechnol 2004;22(2):80-6.

11. Shimizu K, Ito A, Honda H. Enhanced cell-seeding into 3D porous scaffolds by use of magnetite nanoparticles. J Biomed Mater Res B Appl Biomater 2006;77(2):265-72.

12. Ju YM, Choi JS, Atala A, Yoo JJ, Lee SJ. Bilayered scaffold for engineering cellularized blood vessels. Biomaterials 2010;31(15):4313-21.

13. Langer R, Vacanti JP. Tissue engineering. Science 1993;260(5110):920-6.

14. Sikavitsas VI, Bancroft GN, Mikos AG. Formation of three-dimensional cell/polymer constructs for bone tissue engineering in a spinner flask and a rotating wall vessel bioreactor. J Biomed Mater Res 2002;62(1):136-48.

15. Sittinger M, Reitzel D, Dauner M, Hierlemann H, Hammer C, Kastenbauer E, Planck H, Burmester GR, Bujia J. Resorbable polyesters in cartilage engineering: affinity and biocompatibility of polymer fiber structures to chondrocytes. J Biomed Mater Res 1996;33(2):57-63.

16. Cimetta E, Flaibani M, Mella M, Serena E, Boldrin L, De Coppi P, Elvassore N. Enhancement of viability of muscle precursor cells on 3D scaffold in a perfusion bioreactor. Int J Artif Organs 2007;30(5):415-28.

17. Prestwich GD. Simplifying the extracellular matrix for 3-D cell culture and tissue engineering: a pragmatic approach. J Cell Biochem 2007;101(6):1370-83.

18. Whatley BR, Kuo J, Shuai C, Damon BJ, Wen X. Fabrication of a biomimetic elastic intervertebral disk scaffold using additive manufacturing. Biofabrication 2011;3(1):015004.

19. Lee YJ, Kong MH, Song KY, Lee KH, Heo SH. The Relation Between Sox9, TGF-B1, and Proteoglycan in Human Intervertebral Disc Cells. J. Korean Neurosurg Soc 2008;43:149-154.

20. Schmidt D, Mol A, Neuenschwander S, Breymann C, Gossi M, Zund G, Turina M, Hoerstrup SP. Living patches engineered from human umbilical cord derived fibroblasts and endothelial progenitor cells. Eur J Cardiothorac Surg 2005;27(5):795-800.

21. Kim YJ, Sah RL, Doong JY, Grodzinsky AJ. Fluorometric assay of DNA in cartilage explants using Hoechst 33258. Anal Biochem 1988;174(1):168-76.

22. Farndale RW, Buttle DJ, Barrett AJ. Improved quantitation and discrimination of sulphated glycosaminoglycans by use of dimethylmethylene blue. Biochim Biophys Acta 1986;883(2):173-7.

23. Stegemann H, Stalder K. Determination of hydroxyproline. Clin Chim Acta 1967;18(2):267-73.

24. Woessner JF, Jr. The determination of hydroxyproline in tissue and protein samples containing small proportions of this imino acid. Arch Biochem Biophys 1961;93:440-7.

25. Zhuang Y, Huang B, Li CQ, Liu LT, Pan Y, Zheng WJ, Luo G, Zhou Y. Construction of tissue-engineered composite intervertebral disc and preliminary morphological and biochemical evaluation. Biochem Biophys Res Commun 2011;407(2):327-32.
26. Cassidy JJ, Hiltner A, Baer E. Hierarchical structure of the intervertebral disc. Connect Tissue Res 1989;23(1):75-88.

27. Marchand F, Ahmed AM. Investigation of the laminate structure of lumbar disc anulus fibrosus. Spine (Phila Pa 1976) 1990;15(5):402-10.

28. Tsuji H, Hirano N, Ohshima H, Ishihara H, Terahata N, Motoe T. Structural variation of the anterior and posterior anulus fibrosus in the development of human lumbar intervertebral disc. A risk factor for intervertebral disc rupture. Spine (Phila Pa 1976) 1993;18(2):204-10.

29. Bowles RD, Gebhard HH, Hartl R, Bonassar LJ. Tissue-engineered intervertebral discs produce new matrix, maintain disc height, and restore biomechanical function to the rodent spine. Proc Natl Acad Sci U S A 2011;108(32):13106-11.

30. Endo S, Saito N, Misawa Y, Sohara Y. Late pericarditis secondary to pericardial patch implantation 25 years prior. Eur J Cardiothorac Surg 2001;20(5):1059-60.

31. Blan NR, Birla RK. Design and fabrication of heart muscle using scaffold-based tissue engineering. J Biomed Mater Res A 2008;86(1):195-208.

32. Sachlos E, Czernuszka JT. Making tissue engineering scaffolds work. Review: the application of solid freeform fabrication technology to the production of tissue engineering scaffolds. Eur Cell Mater 2003;5:29-39; discussion 39-40.

33. Hoemann CD. Molecular and biochemical assays of cartilage components. Methods Mol Med 2004;101:127-56.

34. Yu H, Grynpas M, Kandel RA. Composition of cartilagenous tissue with mineralized and non-mineralized zones formed in vitro. Biomaterials 1997;18(21):1425-31.

35. Ameer GA, Mahmood TA, Langer R. A biodegradable composite scaffold for cell transplantation. J Orthop Res 2002;20(1):16-9.

36. Elisseeff J, Anseth K, Sims D, McIntosh W, Randolph M, Yaremchuk M, Langer R. Transdermal photopolymerization of poly(ethylene oxide)-based injectable hydrogels for tissue-engineered cartilage. Plast Reconstr Surg 1999;104(4):1014-22.

37. Wu F, Dunkelman N, Peterson A, Davisson T, De La Torre R, Jain D. Bioreactor development for tissue-engineered cartilage. Ann N Y Acad Sci 1999;875:405-11.

38. Le Maitre CL, Freemont AJ, Hoyland JA. Expression of cartilage-derived morphogenetic protein in human intervertebral discs and its effect on matrix synthesis in degenerate human nucleus pulposus cells. Arthritis Res Ther 2009;11(5):R137.

39. Pan Y, Chu T, Dong S, Hao Y, Ren X, Wang J, Wang W, Li C, Zhang Z, Zhou Y. Cells scaffold complex for Intervertebral disc Anulus Fibrosus tissue engineering: in vitro culture and product analysis. Mol Biol Rep 2012;39(9):8581-94.

40. Hayes AJ, Ralphs JR. The response of foetal annulus fibrosus cells to growth factors: modulation of matrix synthesis by TGF-beta1 and IGF-1. Histochem Cell Biol 2011;136(2):163-75.

41. Mwale F, Roughley P, Antoniou J. Distinction between the extracellular matrix of the nucleus pulposus and hyaline cartilage: a requisite for tissue engineering of intervertebral disc. Eur Cell Mater 2004;8:58-63; discussion 63-4.

42. Chang G, Kim HJ, Kaplan D, Vunjak-Novakovic G, Kandel RA. Porous silk scaffolds can be used for tissue engineering annulus fibrosus. Eur Spine J 2007;16(11):1848-57.

43. Mizuno H, Roy AK, Vacanti CA, Kojima K, Ueda M, Bonassar LJ. Tissue-engineered composites of anulus fibrosus and nucleus pulposus for intervertebral disc replacement. Spine (Phila Pa 1976) 2004;29(12):1290-7; discussion 1297-8.

44. Yamada KM, Cukierman E. Modeling tissue morphogenesis and cancer in 3D. Cell 2007;130(4):601-10.

45. Balguid A, Mol A, van Vlimmeren MA, Baaijens FP, Bouten CV. Hypoxia induces near-native mechanical properties in engineered heart valve tissue. Circulation 2009;119(2):290-7.

46. Elder BD, Athanasiou KA. Hydrostatic pressure in articular cartilage tissue engineering: from chondrocytes to tissue regeneration. Tissue Eng Part B Rev 2009;15(1):43-53.

47. Falanga V, Zhou L, Yufit T. Low oxygen tension stimulates collagen synthesis and COL1A1 transcription through the action of TGF-beta1. J Cell Physiol 2002;191(1):42-50.

48. Hirao M, Tamai N, Tsumaki N, Yoshikawa H, Myoui A. Oxygen tension regulates chondrocyte differentiation and function during endochondral ossification. J Biol Chem 2006;281(41):31079-92.

49. Wang DW, Fermor B, Gimble JM, Awad HA, Guilak F. Influence of oxygen on the proliferation and metabolism of adipose derived adult stem cells. J Cell Physiol 2005;204(1):184-91.

50. Korecki CL, Iatridis JC. Effects of Compression Loading, Injury, and Age on Intervertebral Disc Mechanica, Biology, and Metabolism Using Large Animal Organ and Cell Culture Systems: University of Vermont; 2008.

CHAPTER 6

6. OVERALL CONCLUSIONS AND FUTURE DIRECTIONS

6.1 Conclusions

The major impact of this work is in the development of a new technology useful in the biofabrication of tissue engineering scaffolds, especially for the fabrication of scaffolds for IVD tissue regeneration. This technology is based upon a custom-made additive manufacturing platform which enables the precise deposition of polymeric biomaterials to form structures with similar microstructures and mechanical properties to the targeted native tissue. Preliminary studies revealed the potential of the fabricated scaffold structures to improve upon current IVD scaffold fabrication technologies. Detailed conclusions are summarized below, by chapter.

Chapter 3: A novel technology was developed which utilized unique additive manufacturing techniques. This technology allowed for the extrusion of polymeric solutions into 3-D scaffold structures that more closely mimicked the morphology and structure of native IVD tissue. This was accomplished by extruding a polymeric solution through micropipettes onto a temperature-controlled collecting platform. By precisely controlling the temperature of the solution, the device enables the precise control of the polymeric deposition and allows the solution to be directly solidified due to the drastic decrease in temperature and subsequent increase in polymer solution viscosity. Evidence was provided for the ability of this biofabrication platform to utilize various

polymer solutions. Biocompatible and biodegradable polyurethane (PU) was used for this study. It was determined that the fabricated IVD scaffolds had a unique shape and microstructure, which was highly similar to the native tissue structure, and unlike any tissue scaffold developed to date. Further, scaffolds demonstrated favorable biocompatibility and mechanical properties, indicating that they could serve as an excellent approach for use in IVD tissue regeneration applications.

Chapter 4: Within this chapter, an extension of the previous study is presented. It was demonstrated that the custom-developed biofabrication strategy could be used with multiple polymeric solutions to broaden its impact on the ability to create clinically relevant scaffolds for IVD tissue regeneration. Specifically, an ultraviolet (UV) curable chitosan-gelatin (Chs/Gtn) material developed in our lab was extruded using the same fabrication method previously described. The scaffolds' overall shape and microstructure proved to mimic the native IVD tissue and histological ECM structure. Further, it was shown that the IVD scaffolds' lamellar size and spacing could be accurately controlled to fabricate biomimetic IVD scaffolds. Cellular behavior, specifically cell alignment in accordance with the scaffold, was analyzed and compared to native tissue. Results indicated that the scaffolds had the capability to control cellular morphology similar to that of native tissue. Additionally, the mechanical properties of the scaffold were evaluated. It was demonstrated that the scaffolds' elasticity as well as dynamic stability were highly similar to that of native IVD tissue.

Chapter 5: In this experiment, the biofabricated IVD scaffold structures were extensively evaluated *in vitro*. To further validate the advances in our scaffold fabrication process, the ability to create 3-D cellularized IVD scaffolds was thoroughly investigated. The unique aspects of biofabrication were fully utilized within this study, as 3-D multicellular spheroids were first created using a novel robotic approach, followed by their positioning within the biofabricated scaffolds' lamellae. The spheroids provided a 3-D platform for the cells to adhere and grow within the scaffold material. Further, the newly formed ECM was analyzed and proven to exhibit a highly similar structure and composition to native IVD tissue. This study shows the potential of biofabrication to provide unique solutions towards the creation of a 3-D cellularized structure for tissue regeneration.

6.2 Limitations & Challenges

Biomimetic IVD scaffolds for tissue regeneration were successfully created using novel biofabrication technologies presented in this dissertation. These scaffolds demonstrated very promising *in vitro* results. However, several challenges had to be overcome, with some still remaining, before having the ability to develop a more functional and clinically relevant engineered IVD scaffold for tissue regeneration. Some of these challenges are discussed and arranged by chapter below.

Chapter 3: A biofabrication method was presented revealing the ability to successfully create lamellar scaffolds for IVD tissue regeneration. The major challenge that had to be

overcome when fabricating the scaffolds was troubleshooting and optimizing the fabrication parameters of the custom-made device. We needed to investigate motor speeds, polymer solution viscosity, polymer extrusion rate, freezing temperature, and micropipette extrusion diameter. Once these parameters were determined, issues involving ambient humidity and solvent evaporation still arose as the scaffold fabrication process depends on precisely controlled conditions. During mechanical testing of the fabricated structures, it was determined that the mechanical properties of the PU scaffolds were far from ideal. Even though the elastic modulus was within the lower values reported for the human IVD, it is our belief that the scaffolds may need to be altered to improve their mechanical strength.

Chapter 4: Different polymeric solutions were utilized in this study to prove the ability of the biofabrication method to take advantage of the beneficial properties of various biomaterials. However, in order to ensure the effectiveness of using the new biomaterial solutions, the biofabrication parameters had to be optimized once again. Although the mechanical properties were significantly improved using the Chs/Gtn material compared to the PU used in chapter 3, there is still room for improvement of the mechanical stability of the structure in order to create a clinically relevant IVD tissue replacement.

Chapter 5: 3-D multicellular spheroids were used as building block to form a fully cellularized tissue structure. While the spheroids were easily positioned into the voids of the lamellar spacing and providing a feasible 3-D platform for 3-D tissue formation, the

cells were not able to migrate into the lamellar scaffold material due to the low porosity. We plan to advance the fabrication process by incorporating a porogen during the scaffold fabrication process so that cells can penetrate into the whole scaffold.

6.3 Future Goals

The ultimate goal of this project was to develop a unique biofabrication based technology for use in the creation of advanced functional scaffolds for IVD tissue regeneration. The immediate goals will be to address the challenges listed above while expanding upon the technologies developed here to improve the scaffolds. In the larger scheme, this biofabrication technology can be elaborated upon to fabricate better IVD scaffolds as well as other types of scaffold structures for various types of tissue in the body. Future plans and goals are summarized below.

One future objective is to advance the biofabrication platform to improve cellular response. The aim is to aid in the adhesion of the multicellular spheroids to each other, which may be accomplished by coating the spheroids in ECM protein or ECM-derived peptides, such as fibronectin, prior to extrusion within the scaffold lamellae. This would aid in cell fusion and create an entirely cellularized structure.

As for improving the tissue regeneration response to the biofabricated IVD strategy, we plan to control the differentiation of mesenchymal stem cells (MSCs) into IVD cell phenotypes by incorporating signaling molecules into and within the scaffold using nano-layer-by-layer (nanoLBL) technology as well as nanoparticle-based delivery. These techniques can be used to create a spatial and temporal release profile from the

IVD scaffold. Therefore, MSC differentiation can be regionally controlled using different combinations of biomolecules to produce specific cell lineages within the IVD. We have already discovered candidate signaling molecules to encourage stem cell migration and proliferation within the scaffold. *In vitro* studies analyzing the release kinetics of these molecules will then be performed. This will enable optimized differentiation cocktails to be created for each IVD region which support gene expression similar to native IVD tissue. The current challenges discussed above are being addressed to improve the biofabrication strategy.

Finally, the ultimate goal of this project is to assess *in vivo* growth of IVD tissue by using these signaling molecules in combination with the biomimetic IVD scaffold to recruit endogenous stem cells and control their proliferation and IVD phenotypic differentiation. With the proper combination of signaling molecules, the scaffolds will recruit endogenous stem cells and encourage proliferation, chondrogenic differentiation, and synthesis of ECM similar to that of native IVD tissue. Scaffolds will first be created with immobilized signaling molecules, followed by implantation and histological evaluation in subcutaneous rodent models. We also aim to assess the regenerated tissue by evaluating the mechanical properties and comparing those values to native IVD tissue.